UNIVERSITY OF TRENTO - Italy

International PhD Program in Biomolecular Sciences

XXVII Cycle

Translational control mechanisms in the p53 response network

Tutor

Alberto INGA

Laboratory of Transcriptional Networks

CIBIO, University of Trento

Ph.D. Thesis of

Sara ZACCARA

Laboratory of Transcriptional Networks, CIBIO, University of Trento

Academic Year 2013-2014

TABLE OF CONTENTS

1. OUTLINE OF THE THESIS

The sequence-specific transcription factor p53 is considered a master gene of cellular responses to homeostasis changes. It is also a prominent tumor suppressor gene with the title of "guardian of the genome". The increasing number of transcriptome analyses in cell lines treated with different agents activating p53, continues to add complexity to the vast transcriptional networks p53 regulates. To investigate mRNA translational control as an additional dimension of p53-directed gene expression responses, we performed *translatome* analyses upon its activation either by different agents or cellular contexts. Considered as a proxy for the proteome, the translatome allows us to characterize the translational status of each mRNA, independently from transcriptional modulations, and to evaluate the implications or correlations of changes in relative mRNA translation efficiencies with the phenotypic outcome.

We first performed treatment-specific translatome profiling in MCF7 cells upon Doxorubicin and Nutlin-3a treatments. Among translated genes, we detected the presence of translationally enhanced mRNAs with a virtually absent transcriptional modulation; those genes were enriched for apoptotic functions, suggesting that the apoptotic phenotype might be controlled not only at the transcriptional, but also at the translational level.

Seeking mechanisms underlying the mRNAs translational rate upon p53 activation, we identified the modulation of six RNA-binding proteins, where hnRNPD (AUF1) and CPEB4 are direct p53 targets, whereas SRSF1, DDX17, YBX1 and TARDBP are indirect targets, modulated at the translational level in a p53-dependent manner. In detail, we demonstrated the contribution of at least two p53-dependent translational mechanisms related to YBX1 translational repression, suggesting the presence of a controlled regulon at the crossroad of YBX1 mRNA translation.

Given our finding that apoptotic genes appear to be controlled by p53 also at the translational level, we decided to explore whether mRNAs translational control mechanisms are indeed an additional checkpoint to the phenotype. To this aim, we performed a cell-type specific translatome study upon Nutlin-3a treatment, a drug with evident therapeutic prospective. SJSA1, HCT116 and MCF7 cells were chosen as they exhibit different cellular responses to Nutlin-3A (cell cycle arrest, apoptosis, or both, respectively). Our preliminary data suggests that translational modulation can affect the complex process of cell fate choice upon p53 activation. Indeed, a lack of overlap among genes differentially modulated at the translational level was evident. Motif

search analysis at the 5'- and 3'-UTR of those genes highlighted the presence of different motifs in the three cell lines and the specific correlation of a C-rich motif with the apoptotic phenotype. Preliminary data on this motif will be presented and discussed.

Two independent projects will be presented as appendixes, both of them related to the general idea that more than one factor may determine the p53 response. Starting from the analysis of possible p53 interactions with other transcriptional co-factors, we investigated the cooperative interaction between p53 and NFκB. For the second project, combining data previously obtained by means of yeast-based p53 transactivation assays, we developed an algorithm, p53retriever, to scan DNA sequences and thus identify p53 response elements and classify them based on their transactivation potential.

2. INTRODUCTION

2.1. Restoring p53 activity

After 36 years from its discovery the TP53 gene still captures the scientific scenario because of its involvement in an high number of biological processes -metabolism, differentiation, motility, cell–cell communication- beyond the indisputable role as *tumor suppressor* [1]. Indeed, p53 protects from tumor development by controlling the genome and regulating the cell fate choice [2] [3]. Because of its critical functions, p53 is frequently mutated in around 50% of all malignant tumors. Nevertheless, the remaining half of cancers expresses wild-type p53, and its activation may offer a *"smart" therapeutic benefit* [4]. The possibility to manipulate p53 activation to promote tumor cell death is a very fascinating idea and is also one of the main points of this thesis.

That said, I will start with a brief overview of the main functions of p53 and of the mechanisms by which it is regulated.

a. p53's modus operandi

The concept that p53 can kill cancer cells is made even more appealing by the idea that p53 might selectively induce apoptosis in tumor cells, while causing only a reversible cell-cycle arrest phenotype in their normal counterparts; as we will see, however, this is an oversimplification of the complex and heterogeneous responses to p53 activation. Numerous studies have sought to reveal the molecular mechanisms that underlie the control of the response to p53 activation [3]; it is well established that p53 is a *sequence-specific transcription factor,* modulating the expression of an array of different genes in order to mediate its response [5][6].

Many factors influence the ability of p53 to function as a transcription factor:

- PROTEIN DOMAINS AND DNA BINDING AFFINITY:

First of all, the p53 binding affinity to target DNA sequences is crucial. Among p53 domains, the DNA-binding domain (DBD) localized in the core region, allows sequence-specific DNA binding. Virtually every residue in this ~200 amino acids domain has been found to be mutated in human tumors, with frequencies ranging from two fold higher for infrequent mutants to more than 1000 times for hot spot mutants, (UMD p53 database 2007_R1; http://p53.free. fr/) with respect to the ones in the other domains. Different p53 mutants in the same region display marked heterogeneity in terms of the

impact on structure and function; consequently, the transactivation capacity can be variably affected as well [7][8], *i.e.* next to p53 mutants exhibiting a complete loss of function, others retain partial function while others can exhibit gain of function.

At the same time, post-translational modifications may contribute to p53 binding affinity. For instance, the C-terminal phosphorylation of different residues are thought to enhance the sequence specific DNA binding ability of p53 by inducing a conformational change [9]. Similarly, other modifications like ubiquitination, acetylation, and sumoylation also affect its proteolytic turnover and sequence-specific DNA binding ability [10] [11].

- COFACTORS AND TRANSCRIPTION FACTORS:

Concerning the other domains, specific cofactors, some of which have tissue- or stress-specific expression, can bind to various regions of the p53 protein (mainly at the level of the transactivation domains, SH3-like domain and the basic domain at the C-terminus), and may thus contribute to p53 transactivation and binding selectivity [12][13]. For instance, ASPP1 and ASPP2 (apoptosis-stimulating proteins of p53 1 and 2) bind to p53 through their C-termini and stimulate the p53 apoptotic but not cell cycle arrest activity. Indeed, though the mechanism is still unclear, they can selectively stimulate the binding of p53 to the p53REs at the BAX promoter, but not to those in p21 or MDM2, thus preferentially promoting apoptosis [14] [15] . On the contrary, the hematopoietic zinc-finger factor HZF, facilitates p53 binding to the p53 responsive elements in p21 and 14-3-3σ genes, inhibits p53 binding to those in BAX, while having no effect on p53 binding to the MDM2 and HZF promoters [14] [11]. The potential for combined activation of transcription factors to generate transcriptional cooperation was recently explored by our group for p53 and the Estrogen Receptors [12] and, more recently, for p53 and NFκB (see ***Appendix a***).

- DNA TARGET SEQUENCE:

Features of the p53 binding-site, herein defined as response element (RE), play an important role in p53 DNA binding specificity as well as transcriptional specificity. Biochemical and functional studies have extensively characterized the p53 RE [16][5]: its canonical consensus, found mostly at the promoter of up-regulated p53 target genes, consists of two copies of the palindromic half-site RRRCWWGYYY separated by a spacer of 0–13nt, in which R = purine, W = adenine or thymine and Y = pyrimidine (**Figure 1**). This rather degenerate consensus sequence reflects the established observation that,

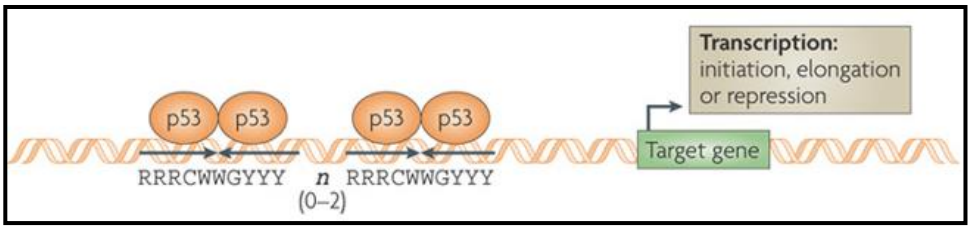

Figure 1: p53 is a transcription factor that recognize a response element on the promoter of its target genes [5].

virtually in all cases of validated p53 REs, an optimal consensus site is not found. This is because of mismatches in some cases resulting in partial binding sites referred to as non-canonical REs (see ***Appendix b***).

This observation has raised the hypothesis of a selection pressure to limit the intrinsic potential of p53 proteins to target binding sites, thereby allowing for modulation of p53-induced transcriptional changes by signal transduction pathways affecting p53 protein amount, DNA binding potential, quaternary structures and/or availability of multiple trans-factors [17]. For instance, p53 REs with lower DNA binding affinity appear to be more frequent in target genes involved in apoptosis. Additionally, cell cycle p53 REs are reported as more conserved than apoptotic p53 REs, suggesting that the cell cycle arrest program may have a more ancient root within the network [18] [14]. Genome-wide studies of p53 DNA binding *in-vivo* using chromatin immunoprecipitation (ChIP) in conjunction with hybridization (ChIP-chip) or followed by deep sequencing (ChIP-seq) contributed to refine the p53 consensus binding site and to predict a number of its target genes [16][6]. More recently, ChIP-exo approaches also allowed binding sites identification with a single base-pair resolution [19].

It must be noted that given the diversity of cell types and treatments being assayed, it is nearly impossible to define a common list of targets. For instance, a comparison of seven different p53 ChIP-seq experiments retrieved only 81 sites whose p53 occupancy is induced by each treatment [20].

b. Choosing to activate: main p53-regulators

As mentioned above, the tumor suppressor p53 is a potent anti-proliferative and pro-apoptotic protein that could harm normal cells if not properly regulated: this is why its level is accurately controlled in unstressed cells and MDM2 has a major role in this regulation [21][22]. In response

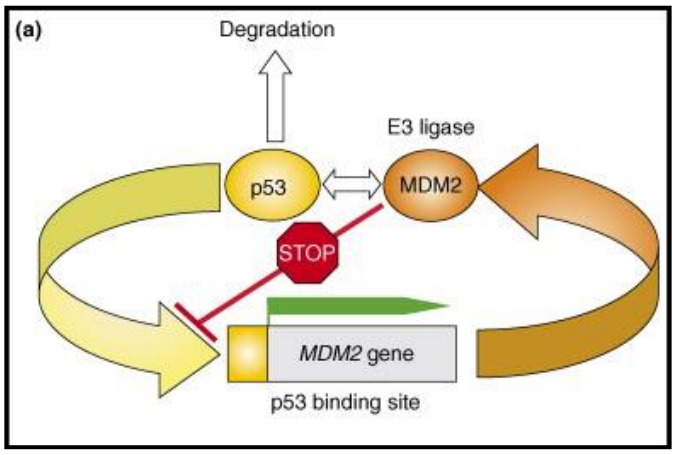

Figure 2: MDM2 is a main regulator of the p53 levels in normal condition. p53 actively transcribes MDM2. As its level rises, MDM2 binds and ubiquitinates p53 to inhibit p53 transcriptional activity and, thus, its own expression [23].

to various extra- and intra-cellular stresses, including but not limited to oncogene activation, DNA damage and hypoxia, different post-translational modifications such as phosphorylation and acetylation stabilize and activate p53. Regarding the main MDM2 regulator, p53 and MDM2 form an auto-regulatory feedback loop by which the two proteins mutually control their cellular levels (**Figure 2**). p53 binds to the promoter and regulates the expression of the MDM2 gene, one of its transcriptional targets; as the level of MDM2 rises, it binds and inactivates p53. MDM2 binds to the N-terminal transactivation domain of p53 and inhibits its transcription factor role. As an E3 ubiquitin ligase, MDM2 mono-ubiquitinates p53, promoting its enhanced nuclear export. MDM2 also poly-ubiquitinates p53 thus targeting it for proteasomal degradation. As a result, both p53 and MDM2 are kept at very low levels in unstressed cells [23]. Recently, three additional proteins, PIRH2, COP1 and ARF-BP1, have been discovered to bind p53 and act as p53 ubiquitin ligases. Currently, there is no evidence that any of these p53 ubiquitin ligases can substitute for MDM2 in the regulation of p53 stability. Furthermore, MDMX is a protein with high degree of homology to MDM2, especially in its N-terminal p53 binding domain; similarly to MDM2, MDMX binds to p53 with high affinity and effectively inhibits its transactivation properties. However, although MDMX possesses a RING domain, it is unable to ubiquitinate and to degrade p53. In contrast to MDM2, the MDMX (MDM4) gene is not transcriptionally regulated by p53, although a p53 bound RE has been mapped [24][25]. Overexpression of MDM2 or MDMX, achieved via different mechanisms such as gene amplification, increased transcription, enhanced mRNA stability and altered post-translational

modifications, leads to the inhibition of p53 in many cancer types, including sarcoma, glioma, melanoma and carcinoma [26].

c. Targeting p53

All these observations allow envisioning different strategies to restore p53 activity.

- **Un-specific p53 activation**

  Various chemotherapeutic drugs, commonly used in therapy, lead to p53 activation. Among them, Doxorubicin is a famous example. Through DNA intercalation, this drug inhibits topoisomerase II (leading to double strand breaks in the genome [27]) and DNA and RNA polymerases (causing replication and transcription arrest [28]). Even though it showed potent tumor-growth-inhibiting properties, Doxorubicin induces a plethora of cytotoxic effects, also in normal cells.

- **Specific p53 activation**

  More recently, new therapeutic approaches have been pursued with the development of small molecules able to induce p53 without significant genotoxic effects. Re-folding of p53 in tumors carrying point mutations in its gene, appears to be an attractive strategy; on the contrary, in tumors expressing wild-type p53, a promising approach is to block its major inhibitors, MDM2 and MDMX [29].

Given the relevance to this project, I will discuss the identification of a number of small molecules that relieve the inhibition of p53 caused by MDM2/X. The first discovered molecules were Nutlins (cis-imidasoline compounds, developed by Hoffman-Roche), followed by the development of spirooxindole compounds (MI series, including MI-63, MI-219), and benzodiazepinediones [23][30]. p53 reactivation by Nutlin-3A has been studied by a number of labs [6][31]; in different types of cancer cells Nutlin-3A was shown to bind MDM2 with nanomolar efficiency, activate p53 and suppress tumor growth, all without inducing the cytotoxic side effects associated with traditional chemotherapeutics. These studies provided the proof-of-concept of p53 rescue by MDM2 inhibition and a strong evidence for the feasibility of this strategy. Several phase I studies of the orally available Nutlin-3A analog, namely RG7112, in patients with liposarcoma (prior to de-bulking surgery), solid tumors, hematologic neoplasms and soft tissue sarcomas (NCT01143740, NCT01164033, NCT00559533, NCT00623870 and NCT01605526 studies) have been completed or are in progress. A second generation MDM2 inhibitor developed by Hoffman-Roche, RG7388, has even higher potency and selectivity [32][33][34]. Nevertheless, a new frontier seems to combine this treatment with other agents that would tip the balance toward a rapid response. Moreover, given that MDMX levels may

balance out MDM2 levels [35], efforts have been focused on the identification of dual MDM2/MDMX antagonists, i.e., 'two in one' inhibitors which can offer an effective therapy for a broader range of tumors [22].

In spite of substantial improvements during the last decade, further studies are still needed in order to elucidate molecular mechanisms and efficacy of this agent in long term cancer treatment.

d. p53: to kill or not to kill?

It is therefore of utmost importance to understand which p53 function is activated by these compounds in various cancers. How does p53 react to genotoxic versus non-genotoxic

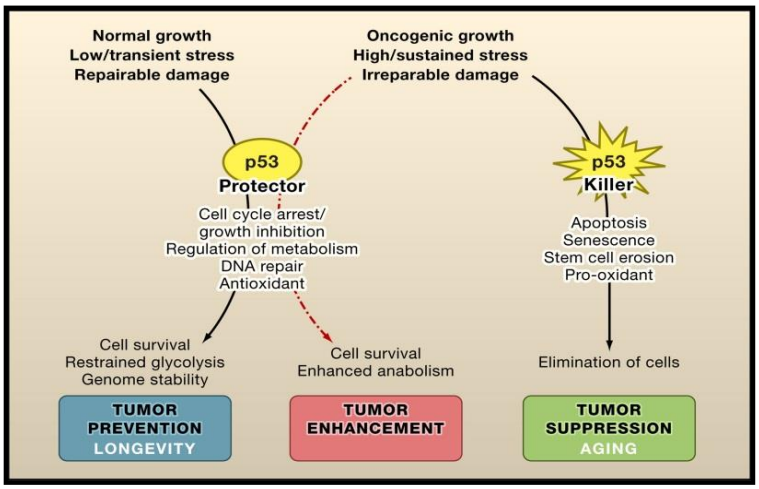

Figure 3: Dual mechanisms of p53 function in tumor suppression. P53 can promote repair and survival of damaged cells or it can promote elimination of cells [3].

activating agents? Indeed, within its role as TF, the responses p53 can elicit are complex (**Figure 3**). For instance, many of our models for p53 function suppose that induction of programmed cell death is the key mechanism by which p53 induces the elimination of cancer cells. In other words, p53 is a direct trans-activator of many genes acting in the intrinsic and extrinsic branches of the apoptotic pathway, including BAX, PUMA and NOXA [36]. Being p53 a cell fate controller, the second most obvious tumor suppressor activity it can exert is the inhibition of cell proliferation and growth. p53 can effectively block cell cycle progression by activating the transcription of the cyclin-dependent kinase inhibitor p21, although several other p53-target genes such as 14-3-3 σ (SFN) and miRNA-34a also contribute to this response [3][37]. Moreover, each cancer type reacts differently. Of course, cell cycle arrest is deemed the least preferred outcomes from a therapeutic perspective, as it is reversible and would lead only to a temporary stall in tumor growth for as long as the therapy is administered. This brings us to the interesting question of what determines the outcome of p53 activation.

2.2. Translational control mechanisms

In the first section, I presented an overview of how complex is the response that p53 can elicit. Although an high degree of control takes place at the transcriptional level, the final p53 response can be considered as the outcome of a circuit made of collections of factors co-regulating a given p53 target gene not only at transcriptional, but also at translational and post-translational level [38]. In this thesis, I will analyze the mechanisms implicated in translational control of p53 targets.

Originally studied in early stages of development in oocytes and embryos [39] [40], translational control is now widely accepted as an additional layer of gene expression regulation in somatic cells. Compared to transcriptional regulation, it allows rapid changes in protein synthesis rate for existing mRNAs [41]. Thus, translational control can be considered a fast and dynamic force shaping cell phenotypes. Moreover, these mechanisms can partially explain the lack of correlation between mRNAs levels, namely the transcriptome, and protein levels, namely the proteome.

a. The process of translation: an overview.

Translation proceeds by initiation, elongation, termination, and ribosome recycling, with most of the regulatory mechanisms thought to occur during the rate-limiting initiation step [42] [43].
In the canonical model, during the first steps of cap-dependent translation initiation, mRNAs are associated at their 5'UTR with the eukaryotic initiation factor eIF4F, comprising the cap-binding protein eIF4E, the scaffold protein eIF4G, and the 5'UTR unwinding RNA helicase eIF4A that operates in conjunction with eIF4B. At the 3'UTR end, associated poly-A binding proteins (PABP) bind eIF4G leading to the circularization and activation of mRNAs. The 43S pre-initiation complex [composed of the 40S ribosomal subunit, the eIF2 ternary complex (eIF2, GTP, and Met-tRNA), eIF3, eIF1, eIF1A, and eIF5] joins the activated RNA structure (via eIF4G and eIF3 interaction) and scans 5'UTR until AUG start codon recognition occurs, followed by the hydrolysis of eIF2-bound GTP and the release of eIF2-bound GDP, eIF5, eIF3, and eIF1. The subsequent association of the 60S ribosomal subunit with eIF5B-bound to GTP leads to eIF5B-mediated GTP hydrolysis and the release of eIF5B-GDP and eIF1, thus allowing the assembly of the 80S complex, which is then ready for translation elongation [43][44].

mRNAs encoding some stress response proteins must be able to evade this intricate regulatory process, especially in conditions of translation inhibition (*i.e.* hypoxia, nutrient deprivation), and several mechanisms have evolved to achieve this. One such mechanism is to bypass cap-dependent recruitment. An estimated 10% of mRNAs contain internal ribosome entry sites (IRESs) in their 5'UTRs and therefore have the potential to be translated by a process which allows

recruitment of the translation machinery downstream of the 5'm7G cap at a position within the 5'UTR. Originally identified in viruses, IRESs are typically structured RNA elements that facilitate the binding of the mRNA to 40S subunits, usually involving a subset of cofactors known as ITAFs (IRES trans-acting factors). Changes in the abundance or activity of these ITAFs allow precise control of IRES-mediated translation, and this mode of initiation is frequently used during stress conditions when cap-dependent translation is compromised [45].

The complex nature of the entire translation process offers a number of regulatory points to finely control the translation rate of each mRNA in particular in stress conditions. Most commonly used regulatory mechanisms modulate the phosphorylation states of eIFs by stress-related kinases and phosphatases (the GCN2, PERK, HRI, and PKR kinases) to control the ternary complex, the phosphorylation of the initiation factor eIF2 or of eIF4E-binding protein [45]. Moreover, sequences and structural elements, called cis-elements, bound by various kinds of regulators (RNA binding proteins or non-coding RNAs) may operate to influence the translation process before the ribosome scanning - by the inhibition or, vice versa, the induction of nuclear export and of mRNA stability- and during the translation steps influencing capping, alternative splicing, polyadenilation and also translation rates (**Figure 4**).

b. cis-elements

Found mainly in the untranslated regions of the mRNA (5'- or 3'-UTR), a cis-element is a recurrent sequence or secondary structure shared by a number of transcripts and defined by a specific combination of nucleotides, namely consensus sequence, to which specific trans-factors bind to exert their control over the mRNA. TOP-elements (5' terminal oligopyrimidine tract), IRES (internal ribosome entry segments) and G-quadruplexes structures are examples of cis-elements in the 5'-UTR [46][47]. Regulatory elements bound by RBPs or non-coding RNAs are mainly located in the 3'-UTR. Different crosslinking and immunoprecipitation techniques (CLIP, PAR-CLIP, iCLIP, CLASH) have allowed the identification of sequence elements, namely motifs, bound by specific trans-factors [48]. A well-known example of cis-element is the AAUAAA polyadenilation sequence. The CPSF RNA-binding protein binds the sequence and, together with the PABPN1 nuclear protein, stimulates the activity of the poly(A) polymerase, which is essentially inactive on its own [49].

c. RNA-binding proteins

RBPs often bind to the 5' UTR of a transcript to modulate translation initiation, and to its 3' UTR to influence its stability or *translatability*; nevertheless, they have also been well characterized

for modulating the initial step of transcripts life; when pre-mRNAs emerge from the transcription sites, they are associated with RBPs and RNAs, to form RNA-protein complexes also referred to as ribonucleoprotein (RNP) complexes [50]. The RNPs assembled on each mRNA by recruiting selected components, which are recombined during the different stages of the RNA maturation, from the splicing to the mRNA alternative nuclear polyadenylation, the export from the nucleus, the localization in the cytoplasm and cytoplasmic polyadenylation, and the final translation potential [51][49][50].

A diversity in their composition corresponds to this functional complexity: the human genome complement of RBPs is composed at least by 800 genes [52][53] which are characterized by the presence of different functional domains, among which the most represented are the zinc-finger C2H2 domain (787 genes), the RNA-recognition motif (RRM, 233 genes), the sterile alpha motif (SAM, 93 genes) and the K-homology domain (KH, 38 genes). Among the least abundant domains, we find the Pumilio RNA binding repeat (PUM, 4 genes) and Piwi proteins domain (PIWI, 8 genes).

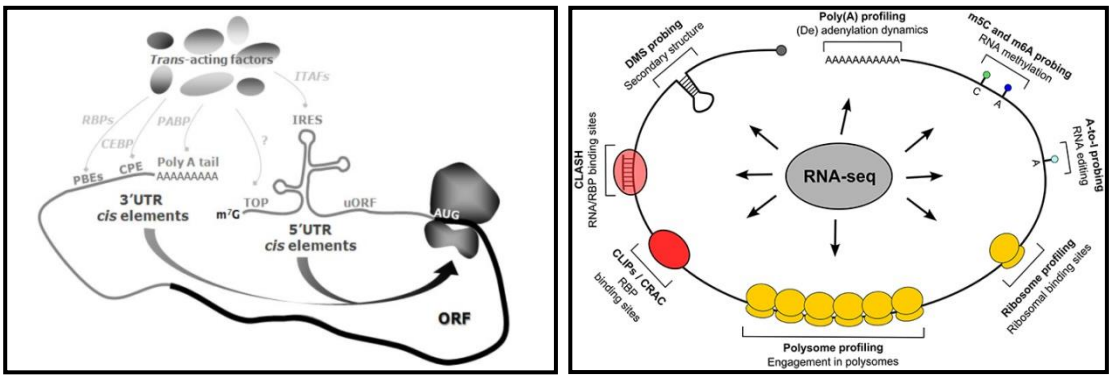

Figure 4: On the right, schematic representation of translation initiation regulation through *cis* elements and trans-acting factors operating in the mRNAs 5' UTR and 3' UTR [46]. On the left techniques allowing to study translatomes at various observational levels are presented [48].

To obtain a specific cellular outcome, some RBPs may cooperate to modulate a group of transcripts, while some may antagonize each other. Various RBPs may share the same binding element: the interaction with one RBP may be mutually exclusive, thus, affecting a second binding. For instance, ELAVL1 (HuR) and AUF1 (hnRNPD) compete with each other for binding to the same AU-rich elements on specific target mRNAs, thus, exerting opposing influences on target mRNA stability [54].

However, in general, the amount of data available on these RBPs, their coordinated modulation of groups of mRNAs (RNA regulons) or their combinatorial interactions on individual mRNAs is at present rather limited.

d. Non-coding RNAs

Non-coding RNAs have emerged as key post-transcriptional regulators of gene expression, involved in diverse physiological and pathological processes. Among them, long non-coding RNA (lncRNAs) were recently discovered and their molecular functions are only beginning to be revealed [55]. LncRNAs are more than 200 nucleotides in length. They are currently annotated as: 1*) Intronic lncRNAs* that are entirely transcribed from within a single intron of a protein-coding gene. (2) *Bidirectional lncRNAs* which share promoters with protein-coding genes but they are transcribed in the opposite direction and therefore have no overlapping sequence. 3) *Intervening lncRNAs* (lincRNAs) transcribed from regions that are at least 5 kb from protein-coding genes. 4) *Antisense lncRNAs* (natural antisense transcripts, NATs) which are transcribed from the opposite strand of protein-coding genes. It is estimated that 70% of mammalian protein-coding genes have an overlapping NAT [56]. The few lncRNAs studied in some depth have been characterized as transcriptional modulators or enhancers, while others have been associated to nuclear speckles structure [57]. Moreover, new insights suggest their implication in post-transcriptional control: they are implicated in the splicing; they may act as molecular decoy for microRNAs, or inhibit protein translation. For instance, linc-p21 has been described as inhibitor of translation, cooperating with HuR in the regulation of a subset of mRNAs [58]. Their implication in translation has been investigated at the level of the ribosomes as well: recent studies suggest the ability of lncRNAs to target the ribosome directly. Initially described as "contaminants", these lncRNAs are now studied as an emerging class of non-coding ribo-regulators of protein biosynthesis [59].

Beyond the biological implications, lncRNAs have been considered also as a therapeutic tool to specifically boost protein expression in mammalian systems, as suggested by an elegant work about an antisense lncRNA transcribed in the opposite strand of the mouse Ubiquitin carboxy-terminal hydrolase L1 (Uchl1) gene which can specifically induce the translation of Uchl1 under certain stress condition [60][61].

On the other hand, non-coding RNAs of ≈22nt length are defined as microRNAs (miRNAs). A lot of work has been already devoted to the characterization of this class of small RNAs; the primary transcripts of miRNA genes (pri-miRNAs) are cleaved into hairpin intermediates (pre-miRNAs) by the nuclear RNase III Drosha and further processed to mature miRNAs by cytosolic Dicer, another RNase-III-related enzyme [62]. In their final form, they most often bind to the 3'UTR of a transcript, inhibiting translation or destabilizing of target messenger RNAs including those coding for oncogenes and tumor suppressors. Dis-regulation in miRNAs expression has been reported in various cancers and can contribute to tumorigenesis [63].

2.3. Translation control in cancer

During cancer progression, cells are exposed to different types of stress. Rapid responses based on the expression of selected proteins may allow their further growth. Translation regulation is a rapid way of tuning gene expression by regulating protein synthesis from existing mRNAs, and thus also saves transcription-related energy [43]. Thus, translation regulation may act to the advantage of cancer cells. The major signaling pathways that promote carcinogenesis (AKT, RAS, MAPK signaling) are involved in this process controlling phosphorylation and regulation of translation factors or ribosomal proteins. For instance, AKT signaling inactivates the tuberous sclerosis tumor-suppressor TSC1/2 complex, which negatively regulates the mammalian target of rapamycin complex 1 (mTORC1), a major regulator of protein synthesis. In its active form, mTORC1 phosphorylates 4E-BP, leading to the release and activation of the cap-binding protein eIF4E. Inactivation of 4E-BPs by down-regulation or hyper-phosphorylation correlates with higher tumor grades and reduced patient survival in prostate and breast cancer, and leads to an increase in cap-dependent translation [43]. At the same time, overexpression of eIF4E, a key player in cap-dependent translation, leads to oncogenic transformation, and increased eIF4E protein levels are found in the majority of human cancers, where its expression correlates with a poor prognosis [42][64].

Lack of oxygen (hypoxia), starvation, and response to DNA-damage inducing therapy repress cap-dependent translation and lead to a reduction in overall protein synthesis, mostly by suppression of eIF4F and eIF2 ternary complex assembly by various mechanisms [45].

On the other hand, inhibition of protein synthesis allows the enhancement or activation of the translation of specific mRNA in a cap-independent manner using IRES. Of importance, these structures are present in mRNAs encoding proteins with oncogenic activity that promote the development, progression, and survival of cancer cells, such as c-MYC, lymphoid enhancer factor (LEF)-1, VEGF, hypoxia-inducible factor (HIF)-1a. In addition, IRES mutations or deregulated ITAFs can further increase the translation of oncogenic proteins. In multiple myeloma, mutations in c-myc-IRES were shown to enhance its translation initiation, and a more recent study in the same cancer type showed an increase in IRES-dependent c-myc translation via ITAFs such as Y-box binding protein 1 (YB-1) and polypyrimidine tract-binding protein 1 (PTB-1) [43].

Considering the low number of known mRNAs carrying an IRES in their 5'UTRs and also the lower level of knowledge about involved mechanisms, HIF1α and VEGF are the only targets that have become attractive in the development of anticancer drugs. Vice versa, the blocking of deregulated signaling pathways by kinase inhibitors has shown greater promise for cancer treatment. mTORC1 can be inhibited by rapalogs (rapamycin and its derivatives) that bind to

FKBP-12 and inhibit mTOR in complex 1. mTORC1/2 inhibitors (*e.g.,* PP242) were more efficient in the inhibition of global protein synthesis and in eIF4F complex formation than rapamycin, illustrating the more-effective approach of targeting cap-dependent translation in cancer. As an alternative to the inhibition of signaling pathways, therapeutic approaches that interfere with the deregulated translation typical of some cancers have been studied. Treatment with eIF4E-specific antisense oligonucleotides reduces eIF4E expression as well as eIF4E-regulated proteins, and suppresses tumor growth in nude mice bearing human breast and prostate tumor xenografts [43][65].

2.4. p53 in the translation control landscape

Translational control can be considered as an additional level of control also in shaping p53 outcomes. Indeed, signaling to mTOR appears to occur also through a p53-dependent pathway requiring transcriptional activation of Sestrin1 and Sestrin2, which in turn activate AMP-responsive protein kinase (AMPK), which then activates the repressor of mTOR TSC2 [43].

The synthesis of the p53 protein itself has been shown to be modulated by different trans-factors, miRNAs targeting its mRNA 3'-UTR and by the binding of ribosomal proteins such as RPL26 and nucleolin, that showed opposite effect on p53 translation rates [66]. Moreover, p53 targets can also be regulated at the post-transcriptional level in their protein synthesis rates, and the impact of this regulation has been recently reviewed [67]. Indeed, very well-known p53 targets undergo translational regulation through the action of miRNAs or RBPs that can modulate what has to be degraded or stored in the cytoplasm rather than being actively translated (**Figure 5**). For instance, the miR-17-92 cluster binds to the CDKN1A(p21) mRNA 3'-UTR promoting p21 degradation, although p53 enhances its transcription[68]; on the other hand, RBPs such as HuR promote p21 mRNA stability and translation[69]. However, HuR was shown to impact also on MDM2 [70], thus outlining a complex regulatory network also at the post-transcriptional level.

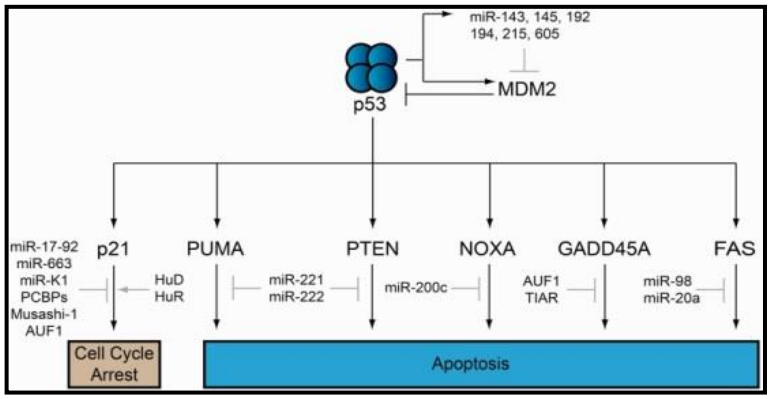

Figure 5: Post-transcriptional regulation of p53 target genes. miRNAs and RBPs work to enhance or repress the expression of p53 target protein-coding genes [67].

On the contrary, p53 has a direct role on post-transcriptional regulation through 1) the direct *activation* of miRNAs gene expression [71][72][73], 2) the direct interaction with Drosha, impacting on the processing of primary miRNAs to precursor miRNAs [74]. By regulating miRNAs, the net effect of p53 activation can be modulated in a context-dependent manner by negative regulation at the post-transcriptional level, moderating what would otherwise be a much greater impact on protein expression of p53 target genes. Therefore, this finely tuned regulatory response has a key role in managing the phenotypic outcomes in response to p53 activation: in particular, miRNA-34a is the most intensely investigated among p53-miRNAs [75]. In the same regulatory context, there are isolated evidences that a few RBPs - namely RNPC1, Quaking (QKI), PCBP4- are p53 or p53-family targets [76][77][78]. For instance, RNPC1 was shown to be a direct transcriptional target gene of both p53 and p63, and to be capable of stimulating p21 mRNA translation [79]; instead, PCBP4 resulted as a p53 target that can down-regulate p21 translation in a p53-independent manner [76].

3. Our approach

The mechanisms defining which cellular response is adopted upon p53 activation remain poorly characterized. As mentioned before, lots of efforts have been devoted to clarify the p53-dependent transcription mechanisms upon p53 induction, under a variety of stress conditions. Thus, along with the advance of new technologies, studies on p53-dependent gene expression have exponentially increased. New targets are continuously identified, increasing the complexity of known p53 cellular responses. However, these analyses are insufficient to explain the observed outcome, and more is needed: for instance, translational studies of p53 mRNA targets could better reveal why some of these are translated only in specific stress condition, thus producing proteins affecting the final phenotype.

In order to study translational control mechanisms as an additional level in shaping p53-dependent cellular response, we performed translatome analyses upon its activation (**Figure 6**). In our approach the translatome is analyzed by using the polysomal profiling technique: considered as a proxy for the proteome, the polysomal profiling approach allows us to separate actively translated mRNAs, bound by polysomes, from not actively translated ones. Thus, guided by the comparison between the translatome and the transcriptome, we characterized *coupled* genes -those mRNAs with homo-directional expression changes at both transcriptional and translational level upon p53 activation – and *uncoupled* genes – mRNAs whose transcription did not correlate with translation.

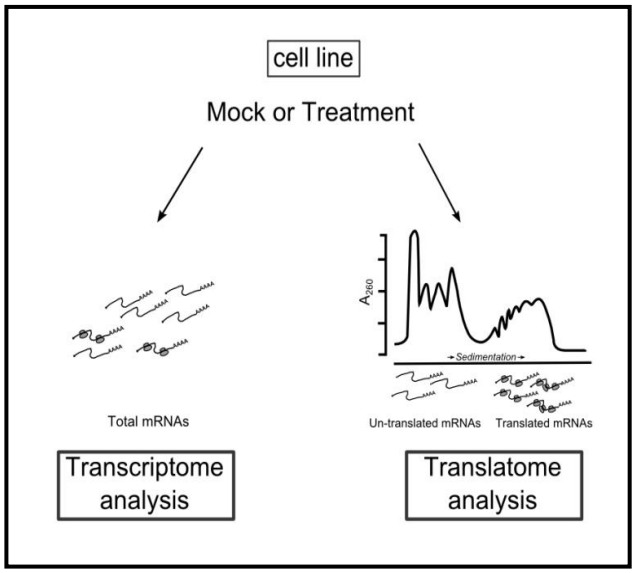

Figure 6: Schematic representation of our workflow. We compared the transcriptome (measure of the total mRNAs) with the translatome in order to characterize the mRNA fate in the cytoplasm before and after p53 activation.

We first performed treatment-specific *translatome* profiling in MCF7 cells upon Doxorubicin and Nutlin-3a treatments. Then, we analyzed the cell-type specific *translatome* of SJSA1, HCT116 and MCF7 cells, which exhibit different cellular responses to the MDM2 inhibitor Nutlin-3a (cell cycle arrest, apoptosis, or both, respectively) to study in detail whether different groups of uncoupled genes are associated with different outcomes.

4. RESULTS

This section will present the results obtained in the two main tasks on which I focused during my doctoral period. The first one highlights my specific contributions to the published manuscript that is included (Paper 1). The second task is still ongoing and I will present the results obtained so far in more details.

4.1. Translatome profiling upon different treatments in MCF7 cells

a. Project summary and my contributions

This study represented the first attempt to provide a global view of the comparison between changes at the transcriptional levels and changes in the translation efficiency of mRNAs in response to p53-activating stimuli. The well-characterized cell line MCF7, that expresses wild type p53, was chosen and the cells were treated with either Doxorubicin or Nutlin-3A, resulting in activation of the p53 pathways through different routes, the DNA damage response pathway in the first case, and non-genotoxic activation of p53 via inhibition if its interaction with MDM2, for the second treatment. Sub-toxic doses of Doxorubicin and Nutlin-3A and a relatively late time point (16 hours) were selected, also for the high levels of treatments similarity on cell viability levels, status of apoptosis markers and activation of p53 (*Figure S1 in the accompanying paper 1*). Three RNA samples were collected for each treatment: total RNA, cytoplasmic RNA not associated with polysomes, cytoplasmic RNA associated with two or more ribosomes -the latter two samples collected from sucrose-gradient fractionation-. These RNA samples were analyzed using expression microarrays, as described in the accompanying paper. Upon identification of differentially expressed genes (DEGs) for each treatment, the correlation between treatment-dependent changes at the transcriptional and translational level was first analyzed (*Figure 1 in the accompanying paper 1*).

We identified a high number of genes exhibiting homo-directional changes both in terms of transcriptome and translatome (defined as coupled). The majority of p53 targets, such as CDKN1A, MDM2 and BBC3, are included in this category. Even for these well-established p53 targets, quantitative differences among the transcriptome and polysomal (pol) mRNA levels were evident, suggesting a fine-tuning in their expression. Given the significantly higher fold

change in the pol fraction than in total RNA, we defined CDKN1A and MDM2 as 'translational thrust' genes. Vice versa, genes such as BBC3 with an opposite finding were proposed as 'translational drag' genes.

The focus of the study was then directed towards the differentially expressed genes identified in the translatome; analyses on these genes categories led us to identify the contribution of translational control mechanisms within p53 responses, considering that p53 does not modulate these genes in transcription. Interestingly, when we looked at uncoupled genes enhanced in the translatome that did not change in the transcriptome, gene ontology revealed enrichment for the term 'apoptosis' upon both treatments. Selected genes were validated by qPCR; PHPT1 protein increase was also checked by Western Blot analysis (*Figure 2 in the accompanying paper 1*). This suggests that enhanced translation of these uncoupled genes might reinforce the apoptotic phenotype, a process that could be important given the generally weaker transcriptional control of p53 targets involved in apoptosis.

Seeking mechanisms controlling the translation of these genes, we identified that a number of RBP genes were regulated by either Doxorubicin (67 RBPs) or Nutlin-3a (30 RBPs) or were common to both treatments (22 RBPs). Beside the well-known miRNAs role, these 22RBPs can be considered primary candidates modulators of the p53-directed translational control. In this part of the project, the p53-dependent expression of selected RBPs was validated; we confirmed YBX1, SRSF1, DDX17, TARDBP, HNRNPD and CPEB4 as targets (*Figure 6 in the accompanying paper 1*). More specifically, HNRNPD and CPEB4 were proposed as direct p53 targets, considering their modulation not only at the polysomal levels, but also at transcriptional level, as suggested by previously published ChIP-seq data (*Figure 5 in the attached paper 1*). Through their modulation, p53 may impact on its functions, either by acting on the p53 mRNA or on the mRNAs of its target genes. In particular, HNRNPD (also known as AUF1) is a member of the best characterized family of *cis*-acting mRNA stability determinants which bind adenylate/uridylate-rich elements (AU-rich elements or AREs) frequently contained within the 3-UTRs of mRNAs encoding cytokines or proto-oncogenes. In general, the presence of an ARE accelerates mRNA turnover [80]. Specifically, HNRNPD promotes transcripts decay though the downstream recruitment of the mRNA decay machinery [80]. Ample opportunity exists for combinatorial as well as competitive relationships among HNRNPD and other ARE-binding proteins on specific ARE target sites. For instance, HuR and HNRNPD can compete with each other for binding to the same AU-rich elements on specific target mRNAs, with an opposite influence [54]. For instance, HuR stabilizes while HNRNPD destabilizes BAX mRNA. In view of several reports, we propose that the p53-dependent HNRNPD down-regulation may promote

the mRNA stability of p53, BAX and other important cancer genes, acting in a reciprocal relation with HuR.

Vice versa, CPEB4 resulted up-regulated. It is one of the four members in the CPEB-family of proteins which bind cytoplasmic polyadenilation element (CPE) in the 3'UTR, thus regulating the length of the poly(A) tail and therefore the recruitment of 3' poly(A) tail-binding protein (PABP) and the pseudo-circularization of the mRNA [81]. These proteins may mediate both translation activation and repression according to selected factors, such as their abundance, the arrangement of CPEs sites in the 3'UTR. CPEB1 and CPEB4 have partially redundant functions as suggested by previous studies on the poly(A) tail length of mRNAs encoding mitotic factors [82]. CPEB1 has been studied more in detail; recent reports suggest that CPEB1 controls the polyadenylation-induced translation of p53 mRNA, and thus its mRNA stability [83]. We hypothesize that, as its functionally-related CPEB1 family member, the p53-dependent up-regulation of CPEB4 could influence p53 translation fitness at its own mRNA level.

At the same time, genes involved in mRNA processing and nucleotide binding resulted translationally down-regulated at the polysomal and sub-polysomal level. Thus, our analyses focused on the validation of RBPs annotated to this ontology category. DDX17, TARDBP, SRSF1 and YBX1 mRNAs were confirmed as modulated at the translational level by qPCR. Overall, in almost all the analyses, protein levels reflect the translatome changes, suggesting that these mRNA variations could have a significant impact on the final proteome (*Figure 3 and 4 of the attached paper 1*). Nevertheless, when the same validation experiments were performed at an earlier time point (8hours), temporal differences upon Doxorubicin and Nutlin-3a treatments were found. Indeed, p53 levels and activity may vary over time after the treatments, thus affecting the expression levels of its targets, as previously reported.

DDX17 (also known as p72) is a putative RNA helicase that by interacting with DDX5 (p68) can act as a modulator of p53-dependent transcription [84]. Moreover, p72 is also required for recognition of a subset of primary miRNAs in Drosha-mediated processing: p72 knockdown abolishes the increase of these selected miRNAs at the precursor and mature levels upon p53 activation, indicating that p72 is essential for the post-transcriptional up-regulation of several p53 targets miRNAs [74]. Thus, p53-dependent modulation of p72 may impact not only on its own transcriptional activity, but also on its ability to regulate miRNAs processing.

SRSF1, also known as alternative splicing factor 1 (ASF1), is the prototypical member of the SR protein family, a conserved class of splicing regulators. Besides its central roles in constitutive and alternative splicing, SRSF1 regulates other aspects of RNA metabolism, including mRNA stability, nuclear export, nonsense-mediated mRNA decay, translation, and miRNA processing.

The depletion of the protein triggers genomic instability, cell-cycle arrest, and apoptosis [85]. According to recent reports, SRSF1 binds RPL5-MDM2 [86]. Being thus involved in the p53 stabilization process, its p53-dependent modulation would represent an additional auto-regulatory mechanism to control p53 levels.

We explored in more detail two mechanisms linking p53 activation with YBX1 mRNA and protein down-regulation, namely the inhibition of the mTOR pathway and the up-regulation of miR-34a (*Figure 4 of the attached paper 1*). Being YBX1 a 5'-terminal oligo-pyrimidine tract-like mRNA, and thus, modulated by mTOR, we examined that the p53-dependent mTOR inhibition had an indirect effect on YBX1 translation. Moreover, on YBX1 3'UTR we found a binding site of one of the main and well-known miRNA target of p53, miR-34a; through its binding, miRNA-34a contributed to YBX1 mRNA down-regulation. Although we validated two independent mechanisms influencing YBX1 translational modulation, we don't exclude the presence of additional ones, participating to the eventual mRNA control.
YBX1 has been shown to be a multitasking protein with many functions including the regulation of both transcription and translation of several genes implicated in cell survival, DNA replication and repair, drug resistance and epithelial-mesenchymal transition [87]. Moreover, YBX1 is an IRES trans-acting factors implicated in the cap-independent translation initiation mechanism [46][65]. Thus, p53-dependent down-regulation of YBX1 may determine a reduction in the cap-independent translation of specific genes.

Preliminary results to clarify the specific impact of these RBPs on translational regulation after p53 activation were also obtained. We chose SRSF1 and YBX1 to explore these potential regulatory effects by a siRNA approach, as they both control cell proliferation, cell-cycle progression and apoptosis. More specifically, both RBPs have been independently associated to c-MYC translation. In our experiments, SRSF1 silencing led to a decrease also in YBX1 protein levels, suggesting a cross-talk between the two RBPs via unexplored mechanisms, and this resulted in a down-modulation of c-MYC. Hence, we suggested that p53-dependent negative regulation of both YBX1 and SRSF1, could lead to an even more robust repression of c-MYC. Besides their modulatory effect on c-MYC, both RBPs have been implicated in several aspects of cancer progression. In particular, from a clinic prospective, YBX1 has also been associated to patient prognosis: its protein levels are elevated in more aggressive tumors and strongly associated with poor disease-free survival and distant metastasis-free survival [88].

I contributed since the beginning to the project starting from the sample's collection to the microarray hybridization. I realized most of the data analysis process in order to identify each DEGs group. After performing pathways and ontologies analyses, I moved on to the validation experiments with the aim of investigating p53-dependent RBPs' modulation more in detail. Then, thanks to the AURA2 database and reagents available through an independent project in the lab, I focused my analysis on the translation control of YBX1 mRNA. Finally, I co-wrote the attached Paper 1.

4.2. Cell type-specific translatome profiling upon Nutlin-3A treatment

The previous study constituted the backbone for a larger project that is still ongoing, which I developed thanks to a collaboration with the Espinosa lab at UC Boulder, Colorado.

As mentioned before, p53 activation may offer a "smart" and effective therapeutic strategy. However, for clinical utility, the challenge is to be able to direct the outcome of p53-activation towards the induction of apoptosis, given that p53-activation can also result in robust cell cycle arrest, which in this context is much less desirable as it could provide for tumor resistance. This issue is exemplified by the observation that treating a panel of cancer cell lines with Nutlin-3a results in variable responses from overt cell cycle arrest, to massive apoptosis, to intermediate phenotypes. What is dictating these differences in responses and how will it be possible to shift the balance towards the apoptotic phenotype, thus reducing the probability of cell-cycle arrest choice [38]? Is the p53-dependent transcriptional network different among cell lines treated with Nutlin-3a that undergo cell cycle arrest versus apoptosis, namely are the p53 target genes that promote apoptosis less responsive in some cell lines? Is the outcome due to p53-independent factors, such as the levels or activity of survival proteins? Initial reports suggested that Nutlin-3A treatment determines mainly the cell-cycle arrest phenotype, an undesirable outcome in cancer therapy, and that MDM2 amplification was the main factor determining cells susceptibility to Nutlin-3-induced apoptosis [22]. On the contrary, nude mice bearing xenografts established from cells with normal MDM2 levels showed a reduction in the median tumor volume as in cells with MDM2 amplification, suggesting that, beyond MDM2, additional factors may be involved [4].

Given our finding that apoptotic genes appear to be controlled also at the level of translation efficiency, we decided to explore whether mRNA translational control mechanisms are indeed an additional checkpoint to the phenotype that can be variably active in different cell lines contributing to the licensing of the apoptotic response. Hence, we chose three cell lines (HCT116, SJSA1 and MCF7), confirmed their specific response to the treatment with Nutlin-3a (cell-cycle arrest, apoptosis and an intermediate phenotype between the two, respectively), and examined transcriptome as well as translatome changes using RNA-seq. With these datasets we were in the position to ask the extent by which the transcriptome of the three cell lines differ, to compare the subset of mRNAs that are Nutlin-3a induced or repressed both at transcriptional and translational levels, but also potentially identify mRNAs undergoing treatment-induced, cell-line selective changes in translation efficiency.

a. Coupled genes are necessary but not sufficient to shape the phenotype.

Because of its promising pre-clinical results [33][22], we selected the MDM2 inhibitor Nutlin-3a as p53 stimuli, while HCT116, SJSA1 and MCF7 were chosen as model cell lines. Indeed, these exhibit different cellular responses (cell cycle arrest, apoptosis, or both, respectively) to Nutlin-3A upon 24 and 48 hours treatment [4]. Being an earlier time point a better window to observe the mechanisms causing these phenotypes, we performed our analyses upon 12 hours treatment, with the goal to capture factors implicated in phenotypic choices implicated in the cell cycle choices. Moreover, at this time point, p53 stabilization and activity on its targets was previously described in all the three cell lines [89]. A graphical workflow of the experiment is presented in **Figure 8A**. Briefly, we collected total and cytoplasmic RNA, the latter was separated on a sucrose gradient and then fractionated in order to recover the fraction of

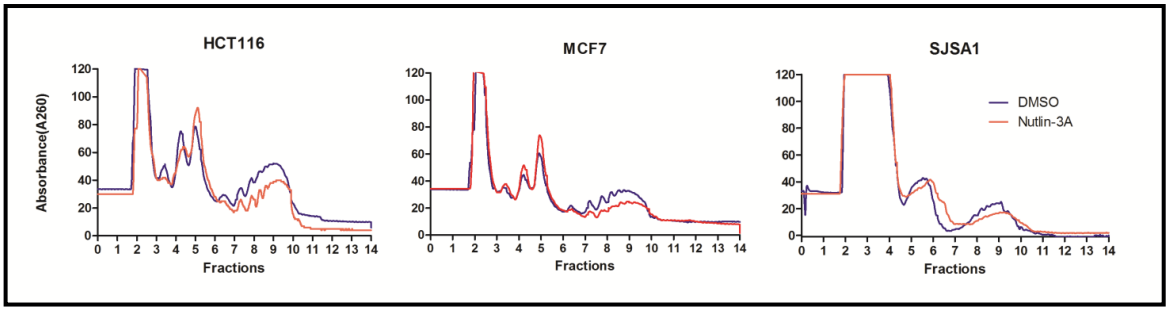

Figure 7: Polysomal profiles upon DMSO or Nutlin-3A treatment in the three cell lines.

mRNAs associated with polysomes (considered as actively translated mRNAs) from those that are not (un-translated mRNAs) [90]. Polysomal profiles showed a low variation between control and Nutlin-3A samples, indicating small changes in global translational rates (**Figure 7**). While a small increase in the proportion of 80S to polysomes was apparent, the treatment had a similar impact at this level of analysis in the three cell lines. The slight reduction in absorbance of the polysomal fractions values may be due to a p53-dependent inhibition of the mTOR pathway [91].

Following high-throughput sequencing of poly-A^+ selected RNA libraries, we firstly analyzed coupled genes. Being transcribed and then translated upon p53 activation, these may embody "direct-functional targets" better than genes identified only by a classical transcriptomic analysis. Notably, while HCT116 and MCF7 cells displayed a similar number of coupled genes, there were fewer in SJSA1 cells: compared to the other two cell lines, a nearly ≈50% reduction in the proportion of coupled DEGs was observed (**Figure 8B**). Thus, more pervasive translational control mechanisms could be envisioned in SJSA1 cells that could control the output of "direct-

functional genes" and the related apoptotic phenotype. Among coupled genes, only 33 up-regulated and 79 down-regulated genes were in common among the three cell lines (**Figure 8C**). These genes numbers were smaller compared to those revealed by analyses of the transcriptomes alone –around 40% of common genes-, suggesting that several targets which are commonly modulated at their total mRNA levels are then differently controlled at the translational level: the translatome acts as a filter defining which genes, previously selected by transcription, need to be translated. Taking into account the translatome status for transcriptionally modulated mRNAs, we further analyze common coupled genes. In principle, if p53 transcriptional selectivity defines the outcome, well-known p53 targets with regulatory functions only in one phenotype should be differentially expressed across the cell lines. For instance, in HCT116 cells, cell-cycle arrest inducers such as p21, GADD45 and 14-3-3σ should be expressed and induced at higher level than in SJSA1 cells; vice versa, apoptotic triggers such as BBC3, BAX and KILLER might be more abundant to start with and should be more differentially expressed in SJSA1 than in HCT116 cells. Results are presented in **Figure 8D**, where both the level of treatment-dependent induction and the normalized level of expression in the polysomes (RPKM) are reported: all well-known p53 targets listed above were included in the 33 coupled genes; in other words, these were common across all cell lines independently from the

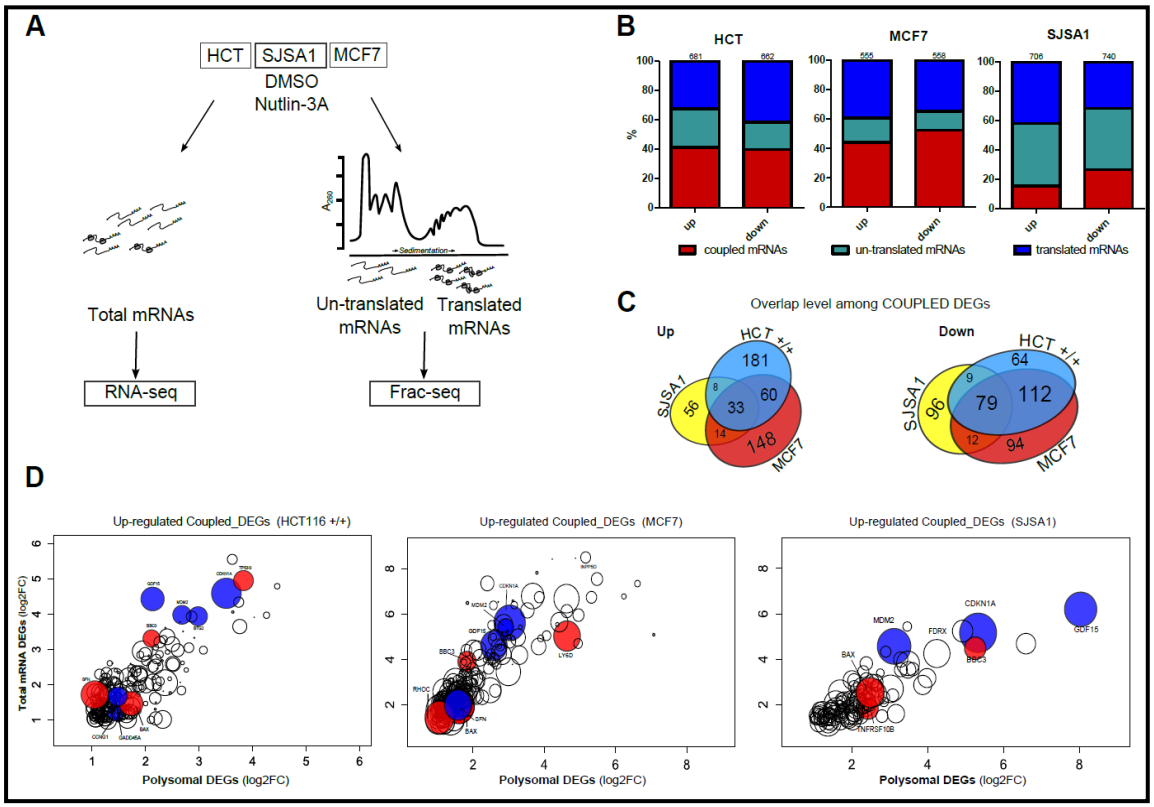

Figure 8: **Coupled differentially expressed genes**. A. Schematic workflow. B. Percentage of coupled and uncoupled DEGs in the three cell lines. C. Overlap among coupled DEGs across the three cell lines. D. Scatter plots comparing log2FC values of the total and polysomal fractions for coupled DEGs. Dots dimension is proportional to RPKM values in the polysomal fraction after Nutlin-3A treatment. Red circles = apoptotic genes; Blue circles = arrest genes.

phenotype they are known to display (**Figure 8D**). Additionally, even their expression levels in the polysomal fraction were comparable, suggesting thus their constitutive induction upon p53 activation, independently from the cellular outcome. Taken together, these data strongly support the hypothesis that coupled genes cannot justify the difference in the observed phenotypes by themselves. In other words, transcriptional selectivity by itself, although present, does not seem to explain the different cellular responses to Nutlin-3a treatment.

b. Uncoupled polysomal genes are different across cell lines

Besides coupled genes, we proceeded to identify uncoupled genes showing a significant increase or decrease in their polysomal level, namely genes with enhanced or reduced translation, respectively. First of all, we checked whether the treatment affected their fold change distribution. Excluding some outliers genes in MCF7 cells, uncoupled polysomal genes have comparable up- and down-regulation levels across all the three cell lines (**Figure 9A**).

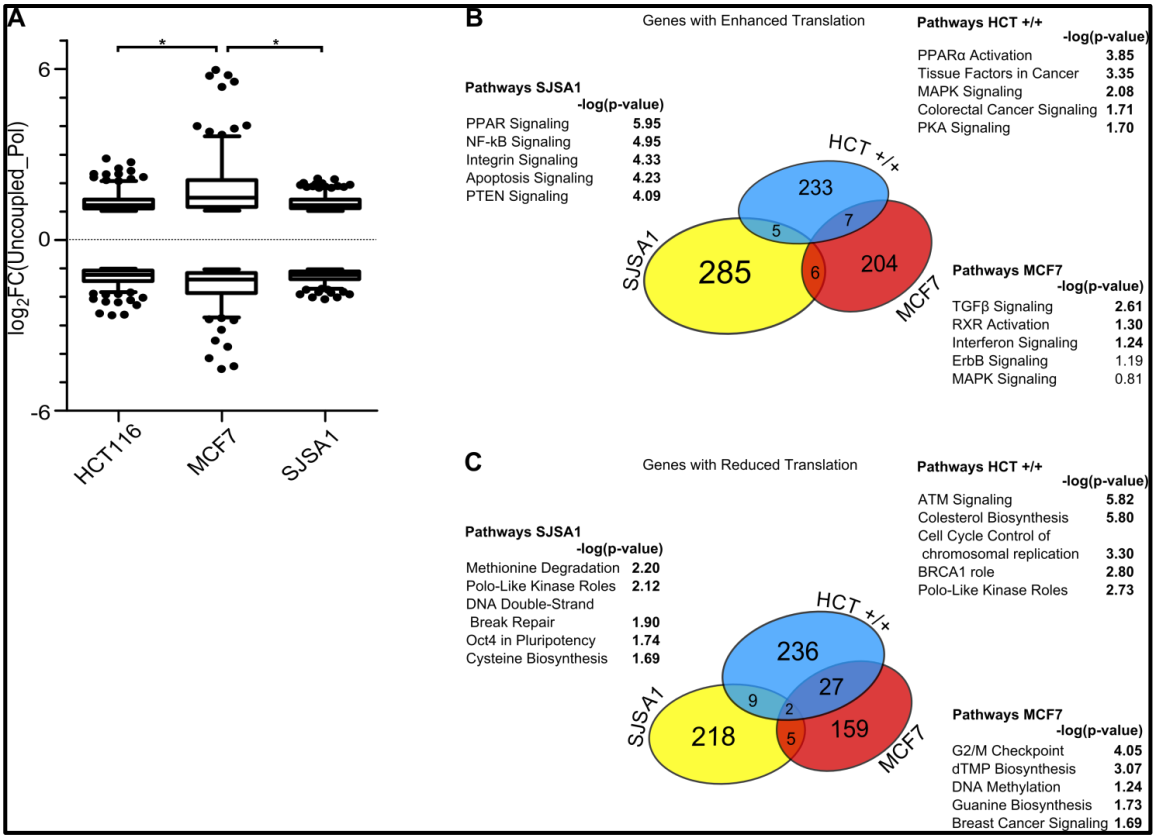

Figure 9: Uncoupled polysomal genes upon p53 induction. A. Log2FC distribution of the genes in all the three cell lines. * = p-value <0.5; B. Overlap among uncoupled DEGs with enhanced translation. For each category enriched pathways are reported; C. Overlap among uncoupled DEGs with reduced translation level and corresponding enriched pathway.

Despite this similarity, none of the genes enhanced in translation was in common among the three cell lines and only two genes were commonly reduced in their translation rates (**Figure 9B-9C**). Along with the lack of overlap, the pathway analysis [92] revealed different genetic signatures across the cell lines. Notably, in SJSA1 cells uncoupled genes exhibiting enhanced translation efficiency were more enriched for the apoptotic signature pathway. Given that, and bearing in mind the apoptotic phenotype of these cells, we can suggest that this outcome may be regulated also at the translational level. This brought us to the interesting question of what determines the translation selectivity of these genes, in spite of the apparent absence of transcriptional selectivity.

c. SJSA1 uncoupled translated mRNAs are enriched for a C-rich motif in their 3'UTRs.

Given the lack of overlap among uncoupled genes enhanced in translation, the three cell lines may have different translational tools, namely trans-factors acting on cis-elements, actively influencing the translation of different genes. To test this hypothesis, we further investigated the existence of enriched sequence motifs in the 5' and 3'UTRs of all gene categories by means of Weeder [93]. Employing the longest 5' or 3'UTR of each gene, we looked for motifs with a length ranging from 6 to 12nt and found in at least 25% of all sequences. When comparing results for each category, a motif with a "TGTAC" consensus was found as enriched among uncoupled, translated genes in HCT116 cells. Nevertheless, this motif was also present both in genes with reduced translation rates of the same cell line and of SJSA1 cells, and, thus, couldn't be considered as a selective feature (**Figure 10**). On the contrary, a C-rich motif (consensus TGGCCCCCATGGCCT) was found as enriched in the 3'UTRs selectively of SJSA1 uncoupled translated genes (**Figure 10A**). Merging all genes list that strongly support the presence of at least one C-rich motif in their 3'UTRs (numbered as n°2, n°5, n°8, n°7), we obtained a final list of 194 out of the 296 translated genes which have at least one instance of this motif in their 3'UTRs, denoting a widespread distribution. None of the other 5' or 3'UTRs categories of coupled or uncoupled genes carried this motif, not even in the other cell lines; only a minority of translated genes in MCF7 cells - 24 out of 218 of which only one, namely FOSL2, is also an uncoupled translated gene in SJSA1 cells - carried this motif. Moreover, we found an enrichment for the "regulation of apoptosis" gene ontology term (p-value of 4.2E-2) on the 194 genes carrying the motif that are significantly up-regulated in the translatome only in SJSA1 cells, suggesting a correlation between these regulated genes and the final phenotype (**Table1**).

Collectively, we hypothesized a role of this C-rich motif in enhancing the translation of uncoupled translated genes only in SJSA1 cells, thus contributing to define the observed phenotype.

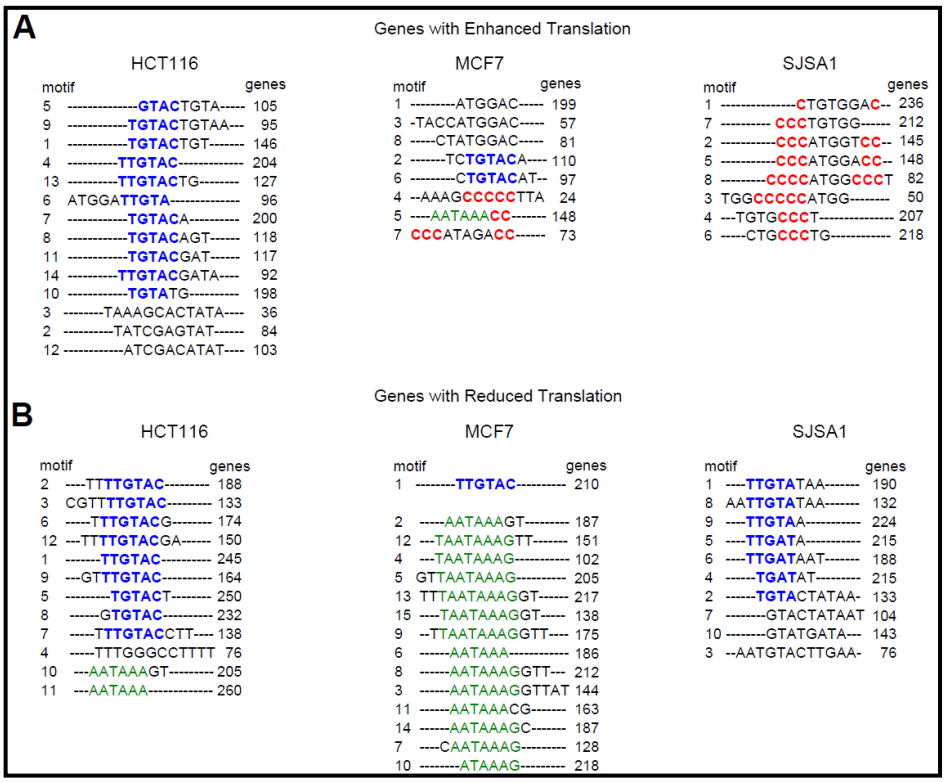

Figure 10: Motif discovery analysis suggested by Weeder. A. Alignment of motifs enriched in the 3'UTRs of uncoupled DEGs enhanced in translation. B. Alignment of motifs enriched in the 3'UTRs of uncoupled DEGs with reduced translation. Motifs are numbered in the "motif" column according to the order in which they were presented by Weeder. The "genes" column lists the number of genes harboring the reported motif at least once. Common nucleotides patterns across the motifs are highlighted by different colors.

Gene Ontology Term	Genes	p-value
Nucleotide binding	36	2.7E-2
Protein transport	15	5.0E-2
Regulation of apoptosis	15	4.2E-2
G1/S checkpoint	4	6.5E-3

Table 1: Gene Ontology Analysis. GO terms enriched in the 194 genes carrying at least one copy of the C-rich motif in their 3'UTRs.

d. The C-rich motif is functional only in SJSA1 cells treated with Nutlin-3A.

We are currently performing experiments to identify the role of the C-rich motif: preliminary data will be presented in this paragraph.

Firstly, selected translated genes of SJSA1 cells, harboring at least one instance of the C-rich motif in their 3'UTR, were validated by qPCR (**Figure 11A**). Indeed, those genes were up-regulated only in the polysomal mRNA fraction compared to total mRNA upon Nutlin-3A treatment, and in SJSA1 cells only, thus confirming the cell line selective, treatment-dependent translational uncoupling. Genes were selected for validation because of their higher level of induction in the polysomal mRNA fraction upon Nutlin-3A according to their log2 fold changes and corrected p-values level. Considered as a proxy of the proteome [90], mRNAs levels in the polysomal fraction may reflect proteins' expression: thus, EIF5A and BAK1 –two known apoptotic targets- up-regulation at the polysomal level was confirmed, by means of Western Blot, to be mirrored in protein levels upon Nutlin-3A treatment, once again in SJSA1 cells only (**Figure 11B**).

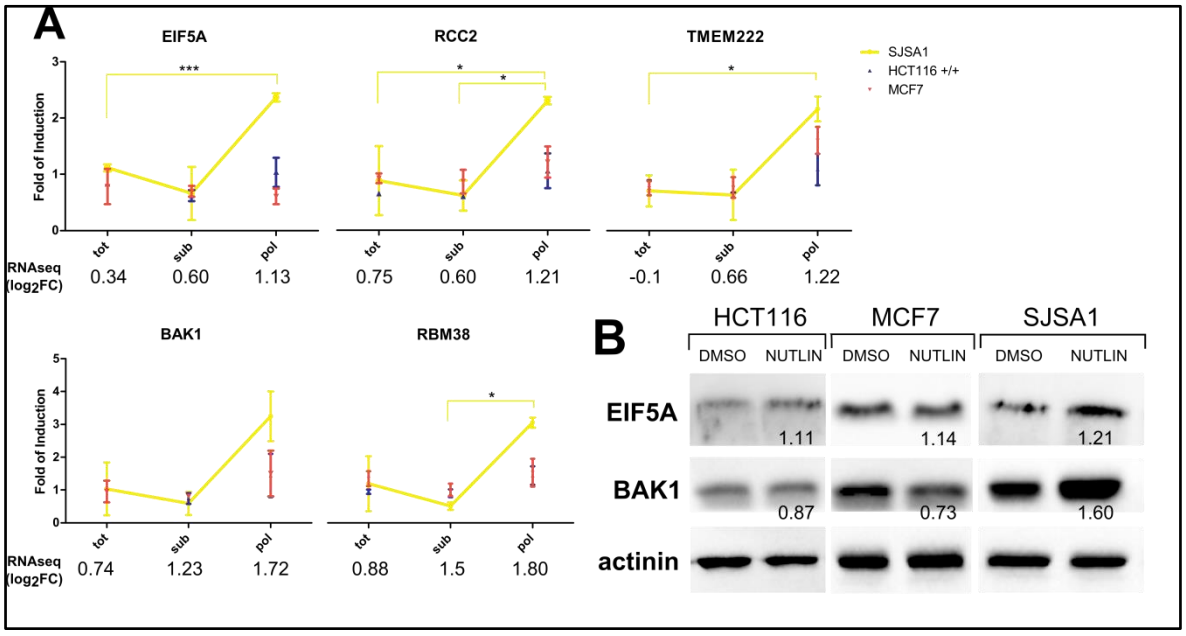

Figure 11: Validation experiments for selected genes harboring a C-rich motif in their 3-UTRs. A. mRNA expression levels in total (tot), sub-polysomal (sub) and polysomal (pol) fractions. qPCR results are presented as fold of induction (ΔΔCq) upon 12hours of Nutlin-3A treatments in the three cell lines. Log2 Fold Change values (log2FC) obtained by RNAseq in SJSA1 cells are reported. B. EIF5A and BAK1 were validated also at protein level by Western Blot analysis. α-actinin was used as reference gene. Numbers report the band quantification values after normalization with actinin levels and DMSO level in each cell line.

Is the C-rich motif in their 3'UTR responsible for the enhanced mRNA translation efficiency and the increase in protein levels? To answer this question, we are currently analyzing whether the C-rich motif can ectopically influence mRNA translation and if mutations in the motif sequence can inhibit or abolish this enhancement of translation in response to Nutlin-3A treatment. For these experiments, we tested the "TGGCCCCCATGGCCT" motif consensus in a luciferase system; in details, we cloned the motif in the 3'UTR of the β-actin reference gene lacking any C-rich motif. Given the absence of any positional preference for the C-rich motif along the 3'UTRs of the SJSA1 uncoupled mRNAs (**Figure 12A**), the motif was inserted both at the beginning and at the end of the β-actin 3'UTR. When these C-rich β-actin 3'UTRs were tested in SJSA1 cells, the relative luciferase activity was increased upon Nutlin-3A treatment, compared to the levels obtained with the reporter vector containing the wild-type β-actin 3'UTR (**Figure 12B**). The activity was even higher when two motifs, one at the 5'- the other at the 3' of the UTR, were present, especially upon 24 hours of Nutlin-3A treatment. Interestingly, when the same experiments were performed in the other two cell lines, we didn't obtain the same increase. This latter finding suggests that the C-rich motif is necessary but not sufficient for the observed effects: a trans-factor, such as an RBP, likely differentially expressed in SJSA1 cells with respect to the other cell lines, may be needed to mediate its regulatory role. Additional analyses are currently ongoing (*see Discussion*).

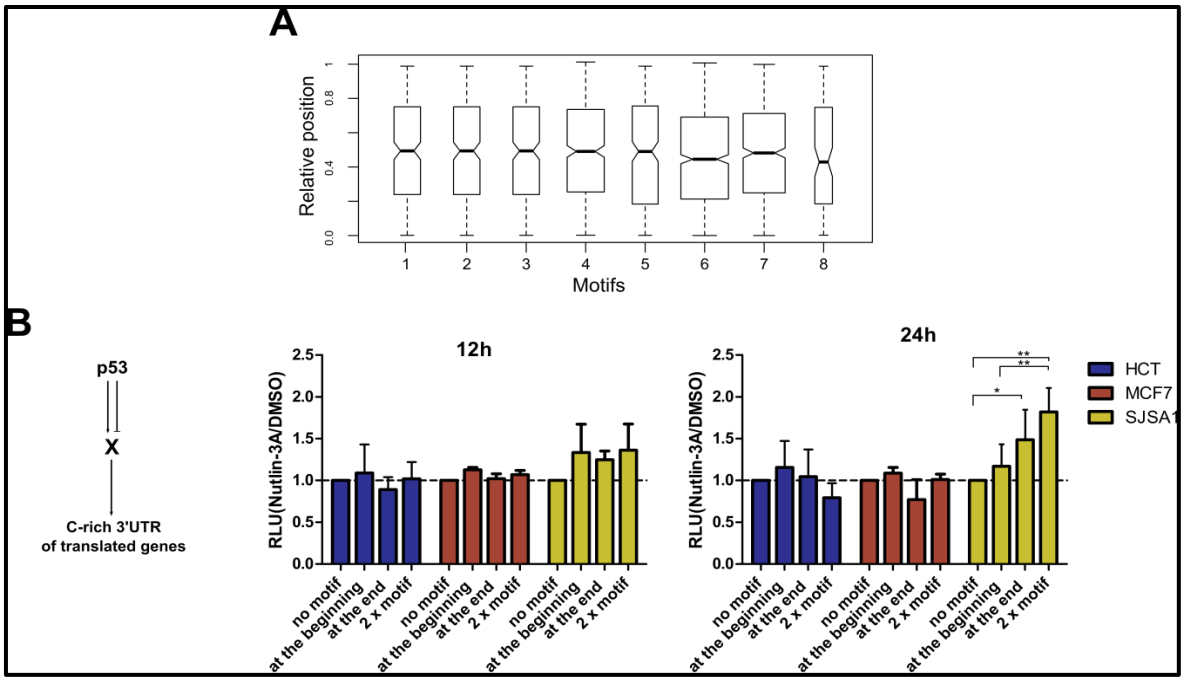

Figure 12: C-rich motif in the 3'UTR. A. Relative position of the C-rich motifs along the 3'UTR. Motifs numbers resulted from Weeder (see Figure 9). B. Relative luciferase values upon transfection of the β-actin 3'UTR and Nutlin-3A treatment in its wild-type form (no motif), with the motif in at least one position (at the beginning/at the end), with two motifs (2xmotif). Results are presented for the three cell lines upon 12h or 24h of Nutlin-3A treatment (Nutlin-3A/DMSO values). ** = p-value< 0.01; * = p-value<0.05.

e. My contributions

The project started as a collaboration with the Espinosa Lab at the University of Colorado Boulder where I spent my period abroad from January 2014 to September 2014. While Matthew Galbraith (University of Colorado Boulder) started the analysis of the total RNA-seq data, I performed samples collection for the translatome analysis. Then, after completing all libraries preparation, I set up the machine to sequence polysomal samples and then I analyzed all the results; the motif analysis was performed with the collaboration of Erik Dassi (CIBIO). Since my return in the Inga Lab, I'm working on all the validation experiments.

f. Materials and methods

Cell lines and culture condition: HCT116 and SJSA1 were maintained in RPMI (Gibco) and MCF7 in DMEM, both supplemented with 10% FBS, antibiotics (100 units/mL penicillin plus 100 mg/mL streptomycin) and 2mM L-glutamine. After seeding in 10cm tissue culture dishes and allowed to reach 70-80% of confluence, cells were treated with 10µM Nutlin-3A (Alexis Biochemicals). After 12 hours, polysomal separation was performed as previously described [94]. Three biological samples were analyzed. Concentration, purity and integrity were measured with the Agilent 2100 Bioanalyzer (Agilent Technologies) discarding RNA preparations with RIN (RNA integrity number) value <8.

Library preparation and data analysis: PolyA+ mRNA isolation was performed using the Dynabeads mRNA DIRECT Micro kit (Life Technologies) following the "mRNA isolation from purified total RNA" protocol and using 15µg of RNA as input. Then, we proceeded to the library preparation according to the Ion Total RNA-Seq Kit instructions. As indicated, we assigned the quality and efficiency of each preparation step using the Agilent RNA 6000 Pico kit with Agilent 2100 Bioanalyzer instrument. After that, each library template was clonally amplified on Ion Sphere Particles for sequencing on the Ion Proton System, producing ≈60-80 M raw reads per sample. After quality filtering and trimming (minimum read length: 30nt; maximum read length: 150nt) by FASTX-Toolkit, mapping to the hg19 build of the human genome (February 2009 GRCh37, NCBI Build 37.1) was performed using GSNAP [95]. Mapping parameters allowed for 0.03% mismatches. To compute the per-gene reads counts, we used HTSeq [96]. We chose the intersection non-empty mode with reads overlapping more than one exonic feature. DESeq R

package [97] was used to call Differentially Expressed Genes (DEGs) starting from two replicates for each condition. For all analyses on DEGs, two thresholds were set: (1) log_2FC >1 and <1 for up-regulated and down-regulated genes, respectively; (2) FDR-corrected p-value <0.1.

Gene ontology and pathway analysis of DEGs: Pathways enrichment analysis for all our selected categories of coupled or uncoupled DEGs was performed with ingenuity pathway analysis (www.ingenuity.com). Only direct interactions were considered in setting parameters.

Motif discovery analysis: To search for common sequence motifs in each category of coupled or uncoupled DEGs, we used the Weeder tool, setting the following parameters: (1) longest 5' or 3'UTR of each gene as input, (2) motifs had to be found in at least 25% of all input sequences, (3) the motif could have a length ranging from 6 to 12nt. When the analyses were completed, the "adviser" program was started to select the best motifs, especially according to their redundancy [93] .

Cloning strategy and luciferase assay: Full-length β-actin 3'-UTR, β-actin 3'-UTR with the addition of a C-rich motif at the 3'UTR beginning or at the 3'UTR end or both, were cloned at the luciferase end of a pGL4.13 vector using XbaI as restriction enzyme. Dual-luciferase reporter assay was done according to the manufacturer's instructions (Promega). Briefly, cells were plated on a 24-well plate, and then transfected with control pGL4.13 reporter vector or the same vector containing the different 3'UTRs, and a Renilla luciferase vector. After 24h, cells were treated with DMSO or Nutlin-3A. Luciferase activity was measured on triplicate wells using Infinite 200 PRO microplate reader (TECAN) 12 or 24 h post-treatment.

5. DISCUSSION

We described translational control as an additional dimension shaping the p53-directed gene response. While lots of efforts have been devoted to study p53-dependent transcriptional modulation, we aimed at investigating the less known translational control, using polysomal profiling and thus focusing on relative changes in mRNA loading on polysomes as a proxy to investigate changes at protein levels, closer to the phenotype. At the same time, we did not aim to quantify the proteins amounts upon p53 induction, but rather to determine the translational state of p53 target mRNAs and the mechanisms by which those mRNAs are/aren't driven to translation. Indeed, proteomic approaches allow to characterize proteins in a particular context although many technological challenges still remain (reproducibility or sensitivity levels, still lower than those from a classical transcriptomic analysis), especially if one needs to quantify changes across conditions rather than just determine whether a protein is produced or not [98][99]. For instance, when iTRAQ analysis was performed to investigate Nutlin-3A changes at proteomic levels and at different time points, full coverage of the proteome was not possible, and MDM2 binding proteins such as p53 and E2F1 were not quantified [100]. Besides all technical issues, relative protein quantification is not instrumental in defining the mechanisms behind the choice to translate a particular mRNA. To this purpose, we opted for a polysomal profiling approach, a method allowing to characterize the translatome and thus we can distinguish actively translated mRNAs from non-actively translated ones [90]; in other words, we can determine the mRNAs fate in the cytoplasm to elucidate mechanisms behind the choice to translate obtaining an indirect estimate of proteome changes at the same time. Additionally, considering the possibility to analyze those mRNAs by means of high-throughput technologies, sensitivity and reproducibility levels remain similar to a classic transcriptomic analysis.

Firstly, a translatome study upon p53 activation by two stimuli, Doxorubicin and Nutlin-3A, was performed; we selected drugs and time conditions by which our cell model (MCF7 cells) would show a mild phenotype, similar between treatments. Indeed, after 16 hours of sub-toxic doses of Nutlin-3A and Doxorubicin, MCF7 cells exhibit a similar viability level associated to low apoptotic rates. In summary, by our analysis we demonstrated that translation control mechanisms define transcripts' fate upon p53 induction by both stimuli. Indeed, besides a good overall correlation between transcription and translation rate changes, a considerable level of uncoupled mRNAs was found. Interestingly, apoptotic genes were enriched among the group of uncoupled mRNAs exhibiting enhanced translation in response to the treatments. Given the absence of a significant transcriptional modulation, those mRNAs might be considered *indirect p53 targets,* controlled at the translational level in order to synthesize the right amount of pro-

phenotype proteins. In general, apoptotic genes have been already characterized to be heavily regulated, not only by selective p53 cofactors and specific post-translational modifications of its protein, but also at their promoter level where a selection pressure exists at the binding site level to limit the intrinsic potential of p53 to bind [101]. In this scenario, the translational control of apoptotic genes is an additional level to modulate, once again, the irreversible decision to the programmed cell-death fate.

Influenced by temporal differences in p53 stabilization upon treatment, also these mechanisms of control showed changes with time, as suggested by our data at an earlier time point (8 hours): several validated targets were confirmed at both time points, while others were not.

The even more significant involvement of translated mRNAs in the apoptotic phenotype for cells treated with Nutlin-3A led us to the interesting question of what determines their translation rates. Indeed, understanding this mechanism may improve our knowledge on how a cell decides whether or not to die in response to p53 activation. To further investigate on this aspect, we decided to perform a second translatome study, employing a panel of cell lines exhibiting different cellular responses to Nutlin-3A [4]. What determines the apoptotic choice instead of the cell cycle arrest one upon Nutlin-3A treatment in different cell lines? Are the mechanisms controlling mRNAs translation different? A previous study already pointed out the existence of several and mostly un-known pro-cell cycle arrest factors, including but not limited to 14-3-3, miRNA-34a and p21; in particular, dying cells required a progressive suppression of p21 at translational level -p21 gene resulted transcriptionally activated to similar extent in apoptotic or not-apoptotic cells [89]-. Since we decided to investigate an early time point, canonical p53 targets such as p21 didn't show differences in their transcriptional/translational expression rates in cells undergoing apoptosis with respect to HCT116 cells (Nutlin-3A-induced cell-cycle arrest phenotype). In other words, this result suggests that canonical and well-known *p53 direct targets* cannot completely explain the difference in the phenotype. Instead, we can determine all those additional and still un-known factors involved in defining the phenotype from an earlier time of the signal transduction. Indeed, our preliminary results suggest that cells undergoing cell death choice have *indirect p53 targets* involved in the apoptotic pathway, not significantly translated in cells exhibiting a cell-cycle arrest phenotype. The enrichment of this pathway is even higher than what we found in MCF7 cells, confirmed to have a milder phenotype that is a combination between cell-cycle arrest and apoptosis, according to our first experimental data.

A large majority of these *indirect p53 targets* appear to share a redundant C-rich motif in their 3'UTR. At this site, the binding of several RBPs may be envisioned, thus contributing to define

the translation rates of bound transcripts. Although their translational role is considered even more complex and broader than the miRNAs one [49], RBPs involvement in p53 response and the identification of the complete mechanisms by which p53 controls their expression remains to be investigated. In our study, we confirmed HNRNPD and CPEB4 as targets of a p53-dependent modulation at the total mRNA. These RBPs can be added to the small list of already known RBPs targets of p53 - RNPC1, Quaking (QKI), PCBP4 [67]. Moreover, we validated YBX1, SRSF1, DDX17, and TARDBP as indirect p53-targets. For these second RBPs category, their translational modulation is not a direct consequence of p53 induction; several upstream factors which may or may not be p53 targets cause their changes in translation upon treatment. For instance, we investigated more in detail upstream factors involved in YBX1 translational down-regulation: the inhibition of the mTOR pathway and the up-regulation of miR-34a. These results suggest the presence of a p53-dependent regulon made at least by YBX1 mRNA, mTOR factors and the miR-34a, contributing to the specific stage of YBX1 mRNA translation. Although we validated two independent mechanisms influencing YBX1 translational modulation, we don't exclude the presence of additional ones, participating to the final mRNA control. At the same time, we cannot exclude a p53-dependent/independent recombination of all these factors during the lifetime of the YBX1 transcript from its transcription to the final translation.

Mechanisms by which the other identified RBPs are modulated remain to be studied, as well as further investigations are needed to clarify their specific impact on the phenotype: which are their specific targets? Are those RBPs cooperating with each other in combinatorial fashion to determine their and their mutual targets' translation rates?

Considering what is already known about the RBPs that we identified as direct/indirect p53 targets, none of those show binding the C-rich motif that is enriched in mRNAs exhibiting enhanced translation in SJSA1 cells undergoing Nutlin-3a dependent apoptosis. Nevertheless, PCBP family members (poly-C binding proteins) are our primary candidates: first of all, they are known to bind poly-C elements [102]; moreover, in our RNA-seq data, they show different expression levels among the analyzed cell lines; hnRNPK, PCBP1, PCBP2, PCBP3 and PCBP4 are all members of this family. Besides the shared structure and origins [102], they have been studied in different context: hnRNPK mainly as a transcription co-factor [103][104], while PCBP1, PCBP2 and PCBP4 also as translational modulators, especially influencing poly(A) processing sites [102][105]. In particular, PCBP4 has been reported to regulate p21 in a p53-independent manner, although transcription from the PCBP4 locus can be induced by DNA damage in a p53-dependent manner [76]. Ongoing studies will further elucidate whether these factors contribute to the translation of apoptotic genes and which of them is more prominent.

In any case, we hypothesize that the direct/indirect modulation of one or more of these RBPs upon Nutlin-3A may change the translational fate of more than one target at once, potentially more than 140 translated genes in cells undergoing apoptosis containing the C-rich motif. If this is true, this small RBPs family may be considered as factors contributing to determine the apoptotic response to Nutlin-3A and, at the same time, to avoid the less desired cell-cycle arrest phenotype. Thus, their modulation may be envisioned as a new therapeutic approach in combination with Nutlin-3A.

Besides the hypothesized impact on translational control, we cannot exclude the involvement of a divergent transcriptional program in defining cell fate choices. Indeed, data obtained by analyzing total mRNA differences upon treatment suggests that only 40% of genes are commonly differentially induced upon treatment in all cell lines. This dissimilarity may be due to the different tissue derivation of our cell lines and to the presence of a different transcriptional landscape. In other words, the potential for combined activation of transcription factors, generating transcriptional cooperation – e.g. p53 and ER, p53 and NFκB – may lead to different starting combinations of expressed genes associated to the final response. In our hypothesis, translational control is a filter for transcriptional modulation and a rapid way of tuning gene expression through protein synthesis regulation.

Further aspects may make the scenario even more complicated: studies on the p53 protein gave rise to the idea that its isoforms and/or post-translational modifications may influence the apoptotic phenotype as well; indeed, according to the “Barcode Hypothesis”, different p53 protein products arising by alternative promoter usage and alternative splicing may be involved considering their divergent transcriptional selectivity [106][37]. Concerning post-translation modifications, phosphorylation of Ser6, -15, -20, -37, -46 and -392 are suggested as dispensable for p53-dependent apoptosis, comparing cells treated with Nutlin-3A versus other DNA damaging agents [30][37]. Implications of these aspects for the apoptotic response are not considered by our analyses.

In summary, selectivity at the level of mRNAs translation, in addition to transcriptional selectivity, may be considered a critical determinant in shaping the p53-directed apoptotic response. In this scenario, RBPs that are direct/indirect p53 targets represent relevant contributing factors, strictly implicated in these mRNAs translation.

6. APPENDIX a

During my PhD, I collaborated to a project focused on the cooperative interaction between two transcription factors, p53 and NFκB.

Indeed, cellular responses to changes in the microenvironment require coordinated activation of different sequence-specific transcription factors, among which NFκB and p53 have a prominent role and often opposing functions. While, the canonical functions of p53 and NFκB are consistent with the co-occurrence of p53 inactivation and NFκB hyper-activation that is frequent in cancer, recent studies provided examples of positive cooperation between p53 and NFκB that would occur in specific cell types, such as antigen presenting cells or macrophages, and contribute to physiological responses, such as for example in the process of innate immunity and inflammation. Thus, the functional interaction between p53 and NFκB remains an open question. To investigate more globally the transcriptional crosstalk between these two factors we performed a proof of concept study using breast cancer-derived MCF7 cells treated with Doxorubicin, Tumor Necrosis Factor alpha (TNFα) and a combination of the two compounds (Doxo+TNFα). Our results demonstrated a synergistic interaction between p53 and NFκB transcription factors, which can lead to the reprogramming of cell fate and enhanced migratory potential. Seven genes (PLK3, LAMP3, ETV7, UNC5B, NTN1, DUSP5, SNAI1) were established as synergistically up-regulated after Doxo+TNFα and dependent both on p53 and NFκB. A 29 genes signature of highly synergistic genes up-regulated by Doxo+TNFα appeared to have prognostic value in a cohort of luminal breast cancer patients.

All project results were published (*see the attached paper 2 by Bisio et al.*).

I contributed to this work analyzing the microarray data, identifying the list of differentially expressed genes (DEGs) after single or combined treatment. For those genes, I performed functional analysis by means of DAVID, seeking for most significant gene ontology terms of down- or up-regulated DEGs, thus, confirming apoptosis induction as the most significantly enriched GO terms among up-regulated DEGs, while TNFα treatment resulted in gene annotation terms consistent with NFκB activation. By IPA analysis, I investigated the presence of predicted upstream regulators of the DEGs for the indicated treatments (Doxorubicin, TNFα, Doxorubicin and TNFα), confirming TP53 as an upstream regulator. Interestingly, this TP53 enrichment was less significant in the double treatment compared to the Doxorubicin single treatment. In a similar manner, I analyzed the DEGs that were synergistically regulated by the double treatment. I also contribute to identify the 29 genes signature used to define a prognostic signature in breast cancer patients. Moreover, I performed validation experiments

for our candidate genes in MCF7 cells by qPCR and Western Blot analyses. For the paper layout, I took care of the preparation of Figure 1.

7. APPENDIX b

During my PhD, I collaborated to develop of a pattern search algorithm that maps p53 response elements and predicts their transactivation potential.

The canonical p53 response element (RE) found in many identified binding sites of mostly up-regulated p53 target genes consists of two copies of the palindromic half-site RRRCWWGYYY separated by a spacer of 0–13 bp, in which R = purine, W = adenine or thymidine and Y = pyrimidine. Because of mismatches, recent reports, including ChIP-seq and ChIP-exo data, highlight the extensive presence of non-canonical REs, such as half-sites and 3/4 sites (3Q), which have different p53 transactivation potential.

Functional assays in the yeast *S. cerevisiae* have been extensively used to characterize the transactivation potential of p53 RE and thus to identify functional half-site and 3/4 site (3Q). Considering the high correlation reported between results in yeast and transactivation or occupancy data in cancer cell lines, we have combined all the data obtained so far with the yeast-based p53 transactivation assay and developed an algorithm, *p53retriever*, to scan human DNA sequences, identify p53 REs and classify them based on predicted transactivation potential into five broad categories, from 5 (= highly functional REs activity) to 1 (= unlikely functional REs). The resulting algorithm has several distinctive features compared to previous tools, particularly for scoring interactions among groups of mismatches, non-canonical 3Q sites and half sites p53 REs, weighting the impact of consensus mismatches considering their position within the full site RE sequence, *i.e.* giving higher penalty to mismatches in the two internal quarter sites, and weighs consensus sequence variations within dinucleotide motifs in the core and flanking regions. A prevalence of grade 2 category REs was identified.

The initial scan of REs in the proximity of all annotated transcriptional start sites of coding genes, was then extended at distal enhancers, defined by ENCODE chromatin codes, where the frequency of REs of the highly functional group is significantly higher than the frequency found in human promoters. To infer the predictive power of the pattern search on p53-dependent transcriptional changes, 13 genes were selected and their expression were tested followed by qPCR in cell lines differing for p53 status (two derivative MCF7clones, the so called MCF7 vector and MCF7shp53, HCT $p53^{+/+}$ and HCT $p53^{-/-}$) and at different time points (8, 16, 24 hours) after

p53 activation by two different treatments, i.e. Doxorubicin -a genotoxic chemotherapeutic drug- and Nutlin-3A. Although the induction was not directly proportional to the REs category grade, we confirmed p53-dependent induction by qPCR for all of the 13 chosen gene in time/cell line dependent manner and propose DNAJA1, MAP2K3 and potentially YAP1 as new direct p53 target genes.

I contributed to define the pattern search rules for p53retriever. When we obtained the complete list of REs, I selected 13 genes for qPCR analysis: these experiments had to reflect the algorithm output variety, taking into account candidates with/without REs already reported by ChIPseq data, as well as the grade attributed to the RE by p53*retriever*. Moreover, besides their p53 binding sites, I selected these candidates because of their reported involvement in cell-cycle control and tumor progression (PDE2A, E2F7, GAS6, TRIM32, HRAS, KITLG and TGFA), in transcription (KCTD1), and DNA editing (APOBEC3H). Although our algorithm considers the p53 transactivation potential, it cannot account for the system complexity of transcriptional regulation in living cells and the response variability upon each different p53 stimuli. Thus, I validated the selected targets in five cell lines systems and using two p53 activators. Additionally, I co-wrote Paper 3 with Toma Tebaldi and Alberto Inga. Paper 3 was submitted to BMC Genomics; it was recently accepted, and is now in press.

8. DECLARATION OF AUTHORSHIP

I (Sara Zaccara) confirm that this is my own work and the use of all material from other sources has been properly and fully acknowledged.

9. REFERENCES

[1] a J. Levine, W. Hu, and Z. Feng, “The P53 pathway: what questions remain to be explored?,” *Cell Death Differ.*, vol. 13, no. 6, pp. 1027–1036, Mar. 2006.

[2] M. Farnebo, V. J. N. Bykov, and K. G. Wiman, “The p53 tumor suppressor: a master regulator of diverse cellular processes and therapeutic target in cancer.,” *Biochem. Biophys. Res. Commun.*, vol. 396, no. 1, pp. 85–9, May 2010.

[3] K. H. Vousden and C. Prives, “Blinded by the Light: The Growing Complexity of p53.,” *Cell*, vol. 137, no. 3, pp. 413–31, May 2009.

[4] C. Tovar, J. Rosinski, Z. Filipovic, B. Higgins, K. Kolinsky, H. Hilton, X. Zhao, B. T. Vu, W. Qing, K. Packman, O. Myklebost, D. C. Heimbrook, and L. T. Vassilev, “Small-molecule MDM2 antagonists reveal aberrant p53 signaling in cancer: implications for therapy.,” *Proc. Natl. Acad. Sci. U. S. A.*, vol. 103, no. 6, pp. 1888–93, Feb. 2006.

[5] D. Menendez, A. Inga, and M. a Resnick, “The expanding universe of p53 targets.,” *Nat. Rev. Cancer*, vol. 9, no. 10, pp. 724–37, Oct. 2009.

[6] F. Nikulenkov, C. Spinnler, H. Li, C. Tonelli, Y. Shi, M. Turunen, T. Kivioja, I. Ignatiev, A. Kel, J. Taipale, and G. Selivanova, “Insights into p53 transcriptional function via genome-wide chromatin occupancy and gene expression analysis.,” *Cell Death Differ.*, vol. 19, no. 12, pp. 1992–2002, Dec. 2012.

[7] P. A. J. Muller and K. H. Vousden, “Mutant p53 in cancer: new functions and therapeutic opportunities.,” *Cancer Cell*, vol. 25, no. 3, pp. 304–17, Mar. 2014.

[8] T. Soussi and K. G. Wiman, “Shaping genetic alterations in human cancer: the p53 mutation paradigm.,” *Cancer Cell*, vol. 12, no. 4, pp. 303–12, Oct. 2007.

[9] Y. Wang and C. Prives, “Increased and altered DNA binding of human p53 by S and G2/M but not G1 cyclin-dependent kinases.,” *Nature*, vol. 376, no. 6535, pp. 88–91, Jul. 1995.

[10] M. S. Rodriguez, J. M. Desterro, S. Lain, C. A. Midgley, D. P. Lane, and R. T. Hay, “SUMO-1 modification activates the transcriptional response of p53.,” *EMBO J.*, vol. 18, no. 22, pp. 6455–61, Nov. 1999.

[11] S. Das, L. Raj, B. Zhao, Y. Kimura, A. Bernstein, S. A. Aaronson, and S. W. Lee, “Hzf Determines cell survival upon genotoxic stress by modulating p53 transactivation.,” *Cell*, vol. 130, no. 4, pp. 624–37, Aug. 2007.

[12] M. Lion, A. Bisio, T. Tebaldi, V. De Sanctis, D. Menendez, M. A. Resnick, Y. Ciribilli, and A. Inga, “Interaction between p53 and estradiol pathways in transcriptional responses to chemotherapeutics.,” *Cell Cycle*, vol. 12, no. 8, pp. 1211–24, Apr. 2013.

[13] A. Bisio, J. Zámborszky, S. Zaccara, M. Lion, T. Tebaldi, V. Sharma, I. Raimondi, F. Alessandrini, Y. Ciribilli, and A. Inga, “Cooperative interactions between p53 and NFκB enhance cell plasticity.,” *Oncotarget*, vol. 5, no. 23, pp. 12111–25, Dec. 2014.

[14] J. M. Espinosa, “Mechanisms of regulatory diversity within the p53 transcriptional network.,” *Oncogene*, vol. 27, no. 29, pp. 4013–23, Jul. 2008.

[15] Y. Samuels-Lev, D. J. O’Connor, D. Bergamaschi, G. Trigiante, J. K. Hsieh, S. Zhong, I. Campargue, L. Naumovski, T. Crook, and X. Lu, “ASPP proteins specifically stimulate the apoptotic function of p53.,” *Mol. Cell*, vol. 8, no. 4, pp. 781–94, Oct. 2001.

[16] J. J. Jordan, D. Menendez, A. Inga, M. Noureddine, M. Nourredine, D. A. Bell, D. Bell, and M. A. Resnick, “Noncanonical DNA motifs as transactivation targets by wild type and mutant p53.,” *PLoS Genet.*, vol. 4, no. 6, p. e1000104, Jun. 2008.

[17] A. G. Jegga, A. Inga, D. Menendez, B. J. Aronow, and M. A. Resnick, “Functional evolution of the p53 regulatory network through its target response elements.,” *Proc. Natl. Acad. Sci. U. S. A.*, vol. 105, no. 3, pp. 944–9, Jan. 2008.

[18] M. M. Horvath, X. Wang, M. A. Resnick, and D. A. Bell, “Divergent evolution of human p53 binding sites: cell cycle versus apoptosis.,” *PLoS Genet.*, vol. 3, no. 7, p. e127, Jul. 2007.

[19] G. S. Chang, X. A. Chen, B. Park, H. S. Rhee, P. Li, K. H. Han, T. Mishra, K. Y. Chan-Salis, Y. Li, R. C. Hardison, Y. Wang, and B. F. Pugh, “A comprehensive and high-resolution genome-wide response of p53 to stress.,” *Cell Rep.*, vol. 8, no. 2, pp. 514–27, Jul. 2014.

[20] J. Zeron-Medina, X. Wang, E. Repapi, M. R. Campbell, D. Su, F. Castro-Giner, B. Davies, E. F. P. Peterse, N. Sacilotto, G. J. Walker, T. Terzian, I. P. Tomlinson, N. F. Box, N. Meinshausen, S. De Val, D. A. Bell, and G. L. Bond, “A polymorphic p53 response element in KIT ligand influences cancer risk and has undergone natural selection.,” *Cell*, vol. 155, no. 2, pp. 410–22, Oct. 2013.

[21] X. Xiong, Y. Zhao, H. He, and Y. Sun, “Ribosomal protein S27-like and S27 interplay with p53-MDM2 axis as a target, a substrate and a regulator.,” *Oncogene*, vol. 30, no. 15, pp. 1798–811, Apr. 2011.

[22] G. Selivanova, “Wild type p53 reactivation: from lab bench to clinic.,” *FEBS Lett.*, vol. 588, no. 16, pp. 2628–38, Aug. 2014.

[23] L. T. Vassilev, “MDM2 inhibitors for cancer therapy.,” *Trends Mol. Med.*, vol. 13, no. 1, pp. 23–31, Jan. 2007.

[24] J.-C. Marine and A. G. Jochemsen, “Mdmx as an essential regulator of p53 activity.,” *Biochem. Biophys. Res. Commun.*, vol. 331, no. 3, pp. 750–60, Jun. 2005.

[25] X. Wang and X. Jiang, “Mdm2 and MdmX partner to regulate p53.,” *FEBS Lett.*, vol. 586, no. 10, pp. 1390–6, May 2012.

[26] Q. Li and G. Lozano, “Molecular pathways: targeting Mdm2 and Mdm4 in cancer therapy.,” *Clin. Cancer Res.*, vol. 19, no. 1, pp. 34–41, Jan. 2013.

[27] Y. Pommier, E. Leo, H. Zhang, and C. Marchand, “DNA topoisomerases and their poisoning by anticancer and antibacterial drugs.,” *Chem. Biol.*, vol. 17, no. 5, pp. 421–33, May 2010.

[28] R. L. Momparler, M. Karon, S. E. Siegel, and F. Avila, “Effect of adriamycin on DNA, RNA, and protein synthesis in cell-free systems and intact cells.,” *Cancer Res.*, vol. 36, no. 8, pp. 2891–5, Aug. 1976.

[29] J. Zawacka-Pankau and G. Selivanova, “Pharmacological reactivation of p53 as a strategy to treat cancer.,” *J. Intern. Med.*, Dec. 2014.

[30] L. T. Vassilev, B. T. Vu, B. Graves, D. Carvajal, F. Podlaski, Z. Filipovic, N. Kong, U. Kammlott, C. Lukacs, C. Klein, N. Fotouhi, and E. A. Liu, “In vivo activation of the p53 pathway by small-molecule antagonists of MDM2.,” *Science*, vol. 303, no. 5659, pp. 844–8, Feb. 2004.

[31] M. A. Allen, Z. Andrysik, V. L. Dengler, H. S. Mellert, A. Guarnieri, J. A. Freeman, K. D. Sullivan, M. D. Galbraith, X. Luo, W. L. Kraus, R. D. Dowell, and J. M. Espinosa, “Global analysis of p53-regulated transcription identifies its direct targets and unexpected regulatory mechanisms,” *Elife*, vol. 3, pp. e02200–e02200, May 2014.

[32] K. H. Khoo, K. K. Hoe, C. S. Verma, and D. P. Lane, “Drugging the p53 pathway: understanding the route to clinical efficacy.,” *Nat. Rev. Drug Discov.*, vol. 13, no. 3, pp. 217–36, Mar. 2014.

[33] C. Tovar, B. Graves, K. Packman, Z. Filipovic, B. Higgins, M. Xia, C. Tardell, R. Garrido, E. Lee, K. Kolinsky, K.-H. To, M. Linn, F. Podlaski, P. Wovkulich, B. Vu, and L. T. Vassilev, “MDM2 small-molecule antagonist RG7112 activates p53 signaling and regresses human tumors in preclinical cancer models.,” *Cancer Res.*, vol. 73, no. 8, pp. 2587–97, Apr. 2013.

[34] S. Biswas, E. Killick, A. G. Jochemsen, and J. Lunec, “The clinical development of p53-reactivating drugs in sarcomas - charting future therapeutic approaches and understanding the clinical molecular toxicology of Nutlins.,” *Expert Opin. Investig. Drugs*, vol. 23, no. 5, pp. 629–45, May 2014.

[35] M. Hirose, K. Yamato, S. Endo, R. Saito, T. Ueno, S. Hirai, H. Suzuki, M. Abei, Y. Natori, and I. Hyodo, “MDM4 expression as an indicator of TP53 reactivation by combined targeting of MDM2 and MDM4 in cancer cells without TP53 mutation.,” *Oncoscience*, vol. 1, no. 12, pp. 830–43, Jan. 2014.

[36] T. Riley, E. Sontag, P. Chen, and A. Levine, “Transcriptional control of human p53-regulated genes.,” *Nat. Rev. Mol. Cell Biol.*, vol. 9, no. 5, pp. 402–12, May 2008.

[37] H. Mellert and J. M. Espinosa, “Tumor Suppression by p53: Is Apoptosis Important or Not?,” *Cell Rep.*, vol. 3, no. 5, pp. 1335–1336, 2013.

[38] K. D. Sullivan, C. L. Gallant-Behm, R. E. Henry, J.-L. Fraikin, and J. M. Espinosa, “The p53 circuit board.,” *Biochim. Biophys. Acta*, vol. 1825, no. 2, pp. 229–44, Apr. 2012.

[39] S. a Terman, “Relative effect of transcription-level and translation-level control of protein synthesis during early development of the sea urchin.,” *Proc. Natl. Acad. Sci. U. S. A.*, vol. 65, no. 4, pp. 985–92, Apr. 1970.

[40] M. G. Gurdon JB, Lane CD, Woodland HR, “Use of frog eggs and oocytes for the study of messenger RNA and its translation in living cells.,” *Nature*, vol. 233, no. 5316, pp. 177–82, 1971.

[41] E. Szostak and F. Gebauer, “Translational control by 3’-UTR-binding proteins.,” *Brief. Funct. Genomics*, vol. 12, no. 1, pp. 58–65, Jan. 2013.

[42] D. Silvera, S. C. Formenti, and R. J. Schneider, “Translational control in cancer.,” *Nat. Rev. Cancer*, vol. 10, no. 4, pp. 254–66, Apr. 2010.

[43] M. Grzmil and B. a Hemmings, “Translation regulation as a therapeutic target in cancer.,” *Cancer Res.*, vol. 72, no. 16, pp. 3891–900, Aug. 2012.

[44] N. Sonenberg and A. G. Hinnebusch, “Regulation of translation initiation in eukaryotes: mechanisms and biological targets.,” *Cell*, vol. 136, no. 4, pp. 731–45, Feb. 2009.

[45] K. A. Spriggs, M. Bushell, and A. E. Willis, “Translational regulation of gene expression during conditions of cell stress.,” *Mol. Cell*, vol. 40, no. 2, pp. 228–37, Oct. 2010.

[46] X. Pichon, L. a Wilson, M. Stoneley, A. Bastide, H. a King, J. Somers, and A. E. E. Willis, “RNA binding protein/RNA element interactions and the control of translation.,” *Curr. Protein Pept. Sci.*, vol. 13, no. 4, pp. 294–304, Jun. 2012.

[47] A. Bugaut and S. Balasubramanian, “5’-UTR RNA G-quadruplexes: translation regulation and targeting.,” *Nucleic Acids Res.*, vol. 40, no. 11, pp. 4727–41, Jun. 2012.

[48] E. Dassi and A. Quattrone, “Fingerprints of a message: integrating positional information on the transcriptome.,” *Front. cell Dev. Biol.*, vol. 2, p. 39, Jan. 2014.

[49] T. Glisovic, J. L. Bachorik, J. Yong, and G. Dreyfuss, “RNA-binding proteins and post-transcriptional gene regulation.,” *FEBS Lett.*, vol. 582, no. 14, pp. 1977–86, Jun. 2008.

[50] J. D. Keene, “RNA regulons: coordination of post-transcriptional events.,” *Nat. Rev. Genet.*, vol. 8, no. 7, pp. 533–43, Jul. 2007.

[51] M. G. Romanelli, E. Diani, and P. M.-J. Lievens, “New insights into functional roles of the polypyrimidine tract-binding protein.,” *Int. J. Mol. Sci.*, vol. 14, no. 11, pp. 22906–32, Jan. 2013.

[52] A. Castello, B. Fischer, K. Eichelbaum, R. Horos, B. M. Beckmann, C. Strein, N. E. Davey, D. T. Humphreys, T. Preiss, L. M. Steinmetz, J. Krijgsveld, and M. W. Hentze, “Insights into RNA Biology from an Atlas of Mammalian mRNA-Binding Proteins,” *Cell*, vol. 149, no. 6, pp. 1393–1406, 2012.

[53] A. G. Baltz, M. Munschauer, B. Schwanhäusser, A. Vasile, Y. Murakawa, M. Schueler, N. Youngs, D. Penfold-Brown, K. Drew, M. Milek, E. Wyler, R. Bonneau, M. Selbach, C. Dieterich, and M. Landthaler, “The mRNA-Bound Proteome and Its Global Occupancy Profile on Protein-Coding Transcripts,” *Mol. Cell*, vol. 46, no. 5, pp. 674–690, 2012.

[54] K. Mazan-Mamczarz, P. R. Hagner, B. Dai, W. H. Wood, Y. Zhang, K. G. Becker, Z. Liu, and R. B. Gartenhaus, “Identification of transformation-related pathways in a breast epithelial cell model using a ribonomics approach.,” *Cancer Res.*, vol. 68, no. 19, pp. 7730–5, Oct. 2008.

[55] M. Haemmerle and T. Gutschner, “Long Non-Coding RNAs in Cancer and Development: Where Do We Go from Here?,” *Int. J. Mol. Sci.*, vol. 16, no. 1, pp. 1395–1405, Jan. 2015.

[56] G. G. C. Editor and J. M. Walker, *Regulatory Non- Coding RNAs IN Series Editor*. 2015.

[57] M. Huarte, "LncRNAs have a say in protein translation.," *Cell Res.*, vol. 23, no. 4, pp. 449–51, Apr. 2013.

[58] J.-H. Yoon, K. Abdelmohsen, S. Srikantan, X. Yang, J. L. Martindale, S. De, M. Huarte, M. Zhan, K. G. Becker, and M. Gorospe, "LincRNA-p21 suppresses target mRNA translation.," *Mol. Cell*, vol. 47, no. 4, pp. 648–55, Aug. 2012.

[59] A. Pircher, J. Gebetsberger, and N. Polacek, "Ribosome-associated ncRNAs: An emerging class of translation regulators.," *RNA Biol.*, vol. 11, no. 11, pp. 1335–1339, Nov. 2014.

[60] M. Huarte, "LncRNAs have a say in protein translation.," *Cell Res.*, vol. 23, no. 4, pp. 449–51, Apr. 2013.

[61] C. Carrieri, L. Cimatti, M. Biagioli, A. Beugnet, S. Zucchelli, S. Fedele, E. Pesce, I. Ferrer, L. Collavin, C. Santoro, A. R. R. Forrest, P. Carninci, S. Biffo, E. Stupka, and S. Gustincich, "Long non-coding antisense RNA controls Uchl1 translation through an embedded SINEB2 repeat.," *Nature*, vol. 491, no. 7424, pp. 454–7, Nov. 2012.

[62] J. Han, Y. Lee, K.-H. Yeom, Y.-K. Kim, H. Jin, and V. N. Kim, "The Drosha-DGCR8 complex in primary microRNA processing.," *Genes Dev.*, vol. 18, no. 24, pp. 3016–27, Dec. 2004.

[63] L. He and G. J. Hannon, "MicroRNAs: small RNAs with a big role in gene regulation.," *Nat. Rev. Genet.*, vol. 5, no. 7, pp. 522–31, Jul. 2004.

[64] Anne-Claude Gingras, and Brian Raught, and N. Sonenberg, "eIF4 INITIATION FACTORS: Effectors of mRNA Recruitment to Ribosomes and Regulators of Translation," Nov. 2003.

[65] C. C. Thoreen, S. A. Kang, J. W. Chang, Q. Liu, J. Zhang, Y. Gao, L. J. Reichling, T. Sim, D. M. Sabatini, and N. S. Gray, "An ATP-competitive mammalian target of rapamycin inhibitor reveals rapamycin-resistant functions of mTORC1.," *J. Biol. Chem.*, vol. 284, no. 12, pp. 8023–32, Mar. 2009.

[66] J. Chen and M. B. Kastan, "5'-3'-UTR interactions regulate p53 mRNA translation and provide a target for modulating p53 induction after DNA damage.," *Genes Dev.*, vol. 24, no. 19, pp. 2146–56, Oct. 2010.

[67] J. a Freeman and J. M. Espinosa, "The impact of post-transcriptional regulation in the p53 network.," *Brief. Funct. Genomics*, vol. 12, no. 1, pp. 46–57, Jan. 2013.

[68] K. Conkrite, M. Sundby, S. Mukai, J. M. Thomson, D. Mu, S. M. Hammond, and D. Macpherson, "miR-17 ~ 92 cooperates with RB pathway mutations to promote retinoblastoma," pp. 1734–1745, 2011.

[69] W. Wang, H. Furneaux, H. Cheng, M. C. Caldwell, D. Hutter, Y. Liu, N. Holbrook, and M. Gorospe, "HuR regulates p21 mRNA stabilization by UV light.," *Mol. Cell. Biol.*, vol. 20, no. 3, pp. 760–9, Feb. 2000.

[70] M. Ghosh, H. L. Aguila, J. Michaud, Y. Ai, M. Wu, A. Hemmes, A. Ristimaki, C. Guo, H. Furneaux, and T. Hla, "Essential role of the RNA-binding protein HuR in progenitor cell survival in mice," vol. 119, no. 12, 2009.

[71] A. Bisio, V. De Sanctis, V. Del Vescovo, M. A. Denti, A. G. Jegga, A. Inga, and Y. Ciribilli, "Identification of new p53 target microRNAs by bioinformatics and functional analysis.," *BMC Cancer*, vol. 13, p. 552, Jan. 2013.

[72] M. T. N. Le, N. Shyh-Chang, S. L. Khaw, L. Chin, C. Teh, J. Tay, E. O'Day, V. Korzh, H. Yang, A. Lal, J. Lieberman, H. F. Lodish, and B. Lim, "Conserved regulation of p53 network dosage by microRNA-125b occurs through evolving miRNA-target gene pairs.," *PLoS Genet.*, vol. 7, no. 9, p. e1002242, Sep. 2011.

[73] M. T. N. Le, C. Teh, N. Shyh-chang, H. Xie, B. Zhou, V. Korzh, H. F. Lodish, and B. Lim, "MicroRNA-125b is a novel negative regulator of p53," pp. 862–876, 2009.

[74] H. I. Suzuki, K. Yamagata, K. Sugimoto, T. Iwamoto, S. Kato, and K. Miyazono, "Modulation of microRNA processing by p53.," *Nature*, vol. 460, no. 7254, pp. 529–33, Jul. 2009.

[75] M. Rokavec, H. Li, L. Jiang, and H. Hermeking, "The p53/miR-34 axis in development and disease.," *J. Mol. Cell Biol.*, vol. 6, no. 3, pp. 214–30, Jun. 2014.

[76] A. Scoumanne, S. J. Cho, J. Zhang, and X. Chen, "The cyclin-dependent kinase inhibitor p21 is regulated by RNA-binding protein PCBP4 via mRNA stability.," *Nucleic Acids Res.*, vol. 39, no. 1, pp. 213–24, Jan. 2011.

[77] J. Zhang and X. Chen, "Posttranscriptional regulation of p53 and its targets by RNA-binding proteins.," *Curr. Mol. Med.*, vol. 8, no. 8, pp. 845–9, Dec. 2008.

[78] R. Rahman-roblick, U. J. Roblick, U. Hellman, P. Conrotto, T. Liu, S. Becker, G. Auer, K. G. Wiman, D. Hirschberg, and H. Jo, "p53 targets identified by protein expression profiling," vol. 104, no. 13, pp. 5401–5406, 2007.

[79] J. Zhang, S. J. Cho, and X. Chen, "RNPC1 , an RNA-binding protein and a target of the p53 family , regulates p63 expression through mRNA stability," pp. 1–6, 2010.

[80] G. Stoecklin, O. Mühlemann, E. J. F. White, G. Brewer, and G. M. Wilson, "Post-transcriptional control of gene expression by AUF1: Mechanisms, physiological targets, and regulation," *Biochim. Biophys. Acta - Gene Regul. Mech.*, vol. 1829, no. 6, pp. 680–688, 2013.

[81] G. Fernández-Miranda and R. Méndez, "The CPEB-family of proteins, translational control in senescence and cancer.," *Ageing Res. Rev.*, vol. 11, no. 4, pp. 460–72, Sep. 2012.

[82] I. Novoa, J. Gallego, P. G. Ferreira, and R. Mendez, "Mitotic cell-cycle progression is regulated by CPEB1 and CPEB4-dependent translational control.," *Nat. Cell Biol.*, vol. 12, no. 5, pp. 447–56, May 2010.

[83] D. M. Burns, A. D'Ambrogio, S. Nottrott, and J. D. Richter, "CPEB and two poly(A) polymerases control miR-122 stability and p53 mRNA translation.," *Nature*, vol. 473, no. 7345, pp. 105–8, May 2011.

[84] F. V Fuller-Pace, "The DEAD box proteins DDX5 (p68) and DDX17 (p72): multi-tasking transcriptional regulators.," *Biochim. Biophys. Acta*, vol. 1829, no. 8, pp. 756–63, Aug. 2013.

[85] S. Das, O. Anczuków, M. Akerman, and A. R. Krainer, “Oncogenic splicing factor SRSF1 is a critical transcriptional target of MYC.,” *Cell Rep.*, vol. 1, no. 2, pp. 110–7, Feb. 2012.

[86] O. I. Fregoso, S. Das, M. Akerman, and A. R. Krainer, “Splicing-factor oncoprotein SRSF1 stabilizes p53 via RPL5 and induces cellular senescence.,” *Mol. Cell*, vol. 50, no. 1, pp. 56–66, Apr. 2013.

[87] D. N. Lyabin, I. A. Eliseeva, and L. P. Ovchinnikov, “YB-1 protein: functions and regulation.,” *Wiley Interdiscip. Rev. RNA*, vol. 5, no. 1, pp. 95–110.

[88] A. Lasham, W. Samuel, H. Cao, R. Patel, R. Mehta, J. L. Stern, G. Reid, A. G. Woolley, L. D. Miller, M. A. Black, A. N. Shelling, C. G. Print, and A. W. Braithwaite, “YB-1, the E2F pathway, and regulation of tumor cell growth.,” *J. Natl. Cancer Inst.*, vol. 104, no. 2, pp. 133–46, Jan. 2012.

[89] R. París, R. E. Henry, S. J. Stephens, M. McBryde, and J. M. Espinosa, “Multiple p53-independent gene silencing mechanisms define the cellular response to p53 activation,” *Cell Cycle*, vol. 7, no. 15, pp. 2427–2433.

[90] Y. Arava, “Isolation of polysomal RNA for microarray analysis,” *Methods Mol Biol.*, vol. 224, pp. 79–87, 2003.

[91] Z. Feng, “p53 regulation of the IGF-1/AKT/mTOR pathways and the endosomal compartment.,” *Cold Spring Harb. Perspect. Biol.*, vol. 2, no. 2, p. a001057, Feb. 2010.

[92] “Ingenuity Pathways Analysis.” [Online]. Available: www.ingenuity.com/variants.

[93] G. Pavesi, P. Mereghetti, G. Mauri, and G. Pesole, “Weeder Web: discovery of transcription factor binding sites in a set of sequences from co-regulated genes.,” *Nucleic Acids Res.*, vol. 32, no. Web Server issue, pp. W199–203, Jul. 2004.

[94] A. Bisio, S. Nasti, J. J. Jordan, S. Gargiulo, L. Pastorino, A. Provenzani, A. Quattrone, P. Queirolo, G. Bianchi-Scarrà, P. Ghiorzo, and A. Inga, “Functional analysis of CDKN2A/p16INK4a 5’-UTR variants predisposing to melanoma.,” *Hum. Mol. Genet.*, vol. 19, no. 8, pp. 1479–91, Apr. 2010.

[95] T. D. Wu and S. Nacu, “Fast and SNP-tolerant detection of complex variants and splicing in short reads.,” *Bioinformatics*, vol. 26, no. 7, pp. 873–81, Apr. 2010.

[96] S. Anders, P. T. Pyl, and W. Huber, “HTSeq - A Python framework to work with high-throughput sequencing data.,” *Bioinformatics*, vol. 31, no. 2, pp. 166–9, Sep. 2014.

[97] S. Anders and W. Huber, “Differential expression analysis for sequence count data.,” *Genome Biol.*, vol. 11, no. 10, p. R106, Jan. 2010.

[98] G. Dittmar and M. Selbach, “SILAC for biomarker discovery.,” *Proteomics. Clin. Appl.*, Dec. 2014.

[99] T. C. Walther and M. Mann, “Mass spectrometry-based proteomics in cell biology.,” *J. Cell Biol.*, vol. 190, no. 4, pp. 491–500, Aug. 2010.

[100] J. Nicholson, K. Neelagandan, A.-S. Huart, K. Ball, M. P. Molloy, and T. Hupp, “An iTRAQ Proteomics Screen Reveals the Effects of the MDM2 Binding Ligand Nutlin-3 on Cellular Proteostasis,” *J. Proteome Res.*, vol. 11, no. 11, pp. 5464–78, Nov. 2012.

[101] T. Riley, E. Sontag, P. Chen, and A. Levine, “Transcriptional control of human p53-regulated genes.,” *Nat. Rev. Mol. Cell Biol.*, vol. 9, no. 5, pp. 402–12, May 2008.

[102] A. V Makeyev and S. A. Liebhaber, “The poly(C)-binding proteins: a multiplicity of functions and a search for mechanisms.,” *RNA*, vol. 8, no. 3, pp. 265–78, Mar. 2002.

[103] A. Moumen, P. Masterson, M. J. O’Connor, and S. P. Jackson, “hnRNP K: an HDM2 target and transcriptional coactivator of p53 in response to DNA damage.,” *Cell*, vol. 123, no. 6, pp. 1065–78, Dec. 2005.

[104] E. F. Michelotti, G. A. Michelotti, A. I. Aronsohn, and D. Levens, “Heterogeneous nuclear ribonucleoprotein K is a transcription factor.,” *Mol. Cell. Biol.*, vol. 16, no. 5, pp. 2350–60, May 1996.

[105] A. Charlesworth, H. A. Meijer, and C. H. de Moor, “Specificity factors in cytoplasmic polyadenylation.,” *Wiley Interdiscip. Rev. RNA*, vol. 4, no. 4, pp. 437–61.

[106] J.-C. Bourdon, K. Fernandes, F. Murray-Zmijewski, G. Liu, A. Diot, D. P. Xirodimas, M. K. Saville, and D. P. Lane, “p53 isoforms can regulate p53 transcriptional activity.,” *Genes Dev.*, vol. 19, no. 18, pp. 2122–37, Sep. 2005.

10. PAPERS

PAPER 1:

"p53-directed translational control can shape and expand the universe of p53 target genes"

Zaccara S., et al. *Cell Death Differ. 2014 Oct;21(10):1522-34.*

Supplementary Files accompanying this paper are in the "Supplementary Files.zip" file. 49

PAPER 2:

"Cooperative interactions between p53 and NFκB enhance cell plasticity"

Bisio A., et al. *Oncotarget. 2014 Dec 15;5(23):12111-25.*

Supplementary Files accompanying this paper are available on-line. 62

PAPER 3:

"Whole-genome cartography of p53 response elements ranked on transactivation potential"

Tebaldi T., Zaccara S., et al. *(BMC Genomics, in press)*

Supplementary Files accompanying this paper are in the "Supplementary Files.zip" file. 77

Cell Death and Differentiation (2014), 1–13

www.nature.com/cdd

p53-directed translational control can shape and expand the universe of *p53* target genes

S Zaccara[1], T Tebaldi[2], C Pederiva[1], Y Ciribilli[1], A Bisio[1] and A Inga*[,1]

The increasing number of genome-wide transcriptome analyses focusing on p53-induced cellular responses in many cellular contexts keeps adding to the already numerous p53-regulated transcriptional networks. To investigate post-transcriptional controls as an additional dimension of p53-directed gene expression responses, we performed a translatome analysis through polysomal profiling on MCF7 cells upon 16 hours of doxorubicin or nutlin-3a treatment. The comparison between the transcriptome and the translatome revealed a considerable level of uncoupling, characterized by genes whose transcription variations did not correlate with translation variations. Interestingly, uncoupled genes were associated with apoptosis, DNA and RNA metabolism and cell cycle functions, suggesting that post-transcriptional control can modulate classical p53-regulated responses. Furthermore, even for well-established p53 targets that were differentially expressed both at the transcriptional and translational levels, quantitative differences between the transcriptome, subpolysomal and polysomal RNAs were evident. As we searched mechanisms underlying gene expression uncoupling, we identified the p53-dependent modulation of six RNA-binding proteins, where hnRNPD (AUF1) and CPEB4 are direct p53 transcriptional targets, whereas SRSF1, DDX17, YBX1 and TARDBP are indirect targets (genes modulated preferentially in the subpolysomal or polysomal mRNA level) modulated at the translational level in a p53-dependent manner. In particular, YBX1 translation appeared to be reduced by p53 via two different mechanisms, one related to mTOR inhibition and the other to miR-34a expression. Overall, we established p53 as a master regulator of translational control and identified new p53-regulated genes affecting translation that can contribute to p53-dependent cellular responses.
Cell Death and Differentiation (2014) advance online publication, 13 June 2014; doi:10.1038/cdd.2014.79

Discovered nearly 35 years ago, tumor suppressor p53, which is often described as the 'guardian of the genome,' acts prominently as a transcription factor in many biological processes including DNA metabolism, apoptosis and cell cycle regulation.[1] Although the role of p53 is generally considered to be at the level of transactivation via binding to target sequences, there are several other ways by which it can determine its cellular responses including, for example, interaction with other transcription factors.[2]

Post-transcriptional and translational controls provide fine tuning of transcriptional outcomes in eukaryotic somatic cells.[3] More than 90% of all coding transcripts appear to be subject to this regulation, especially at translation initiation,[4] considered as the rate-limiting step of the whole process.[3,5] By binding mainly to the 5′ and 3′ untranslated regions (5′UTR; 3′UTR) of mRNAs, miRNAs—other non-coding RNAs and RNA-binding proteins (RBPs)—were shown to participate in the regulation of translation.[6] An unexpected complexity in the modulation of the fate of mRNAs along with a widespread alteration of that process in cancer cells was found in recent studies.[7–9] The synthesis of the p53 protein itself has been shown to be modulated by miR-125b[10] or by RPL26 and nucleolin, that produce opposite effects on the rate of p53 mRNA translation.[11] Moreover, p53 target genes, including CDKN1A (p21), BBC3 (PUMA) and BAX, can be regulated post-transcriptionally by miRNAs or RBPs, some of which can be direct p53 target genes. The impact that this additional level of regulation can have on the p53 response networks has been recently reviewed.[12–17]

All these mechanisms to control the fate of mRNAs may account for the lack of correlation—referred to as uncoupling—between relative changes in the total cellular mRNA levels (corresponding to the transcriptome (transcripts examined from total RNA extractions)) and protein abundances (the proteome) after p53 activation.[18] To investigate p53-dependent uncoupling at the genome level, we compared the transcriptome after doxorubicin (Doxo) or nutlin-3a (Nutlin) treatment with the translatome (transcript examined from polysomal mRNA extractions, considered as actively translated), analyzed by polysomal profiling, a technique that allows quantification of mRNAs associated with the polysomes as a proxy for the proteome.[19]

Overall, we identified an evident translation selectivity that we considered to be an additional dimension by which p53 can tailor its gene response network.

Results

Coupled differentially expressed genes after doxorubicin and nutlin-3a treatments are enriched for p53 targets. To characterize the impact of post-transcriptional

[1]Laboratory of Transcriptional Networks, Centre for Integrative Biology, CIBIO, University of Trento, Trento, Italy and [2]Laboratory of Translational Genomics, Centre for Integrative Biology, CIBIO, University of Trento, Trento, Italy
*Corresponding author: A Inga, Laboratory of Transcriptional Networks, Centre for Integrative Biology, CIBIO, University of Trento, via delle Regole 101, Mattarello, Trento 38123, Italy. Tel: +39 0461 283099/283714; Fax: +39 0461 283091; E-mail: inga@science.unitn.it
Abbreviations: *Tot*, total RNA; sub, subpolysomal RNA; pol, polysomal RNA; up, upregulated; down, downregulated; RBPs, RNA-binding proteins; Doxo, doxorubicin; Nutlin, nutlin-3a; DEGs, differentially expressed genes
Received 17.10.13; revised 23.4.14; accepted 30.4.14; Edited by M Oren

regulation in shaping the p53-dependent gene response, we combined polysomal profiling with microarray analysis on MCF7vector cells[20] (containing wild-type p53) upon doxorubicin (Doxo, 1.5 μM) or nutlin-3a (Nutlin, 10 μM) treatment for 16 h. Both treatments resulted in high p53 induction and similar low levels of toxicity (Supplementary Figure S1). Experiments were conducted also on MCFshp53 cells, which express an shRNA targeting p53.[20] Residual p53 expression was detected in MCF7shp53 cells, but p21 was not induced by either Doxo or Nutlin (Supplementary Figure S1C).

No significant effects of the treatments on overall polysomal distributions were evident (Figure 1a). For the microarray analysis, we collected subpolysomal ('sub') and polysomal ('pol') mRNA fractions so as to analyze mRNAs that are not actively translated separately from those that are in active translation.[21] Total mRNA ('tot') was also collected to quantify transcriptome changes (see Materials and Methods).

When we measured the global overlap between expression changes of 'tot' (transcriptome) and 'pol' (translatome), we obtained Spearman correlations of 0.65 and 0.67 after Doxo and Nutlin treatment, respectively (Figure 1b). Hence, many genes exhibited homodirectional changes both in terms of transcriptome and translatome (defined as coupled differentially expressed genes (DEGs)). In the three RNA preparations (tot, pol and sub), we found 239 and 155 commonly upregulated coupled DEGs (DEGs with homodirectional expression changes in transcriptome and translatome) after Doxo and Nutlin treatment and 216 and 301 commonly repressed coupled DEGs (Figure 1c, green, overlapping areas). Among them, we counted 107 upregulated coupled and 118 downregulated-coupled DEGs in both Doxo and Nutlin treatment. (Supplementary Table S1A). A p53 pathway signature was revealed by ingenuity pathway analysis for Doxo and Nutlin upregulated and downregulated coupled DEGs (Figure 1d). Sixty-four out of 225 genes had expression changes consistent with p53 activation (*P*-value: 7.5^{-39}) (Supplementary Table S2A). Moreover, ingenuity pathway analysis identified p53 as the main upstream regulator especially among coupled DEGs (Supplementary Table S3). Interestingly, gene ontology enrichment did not reveal differences between Doxo and Nutlin DEGs (Supplementary Table S2B), consistent with the similarity in cell phenotypes observed at the doses and time point used (Supplementary Figure S1).

Three well-established p53 target genes (MDM2, p21 and PUMA) were validated as coupled DEGs by quantitative PCR (qPCR), whose sensitivity is higher than the microarray's (Figure 1e). Given the significantly higher fold change in the pol fraction compared with the subpolysomal fraction, particularly after Nutlin treatment, p21 and MDM2 translation appeared to be enhanced. We defined this finding a 'translational thrust'. An 8 h treatment time point was added for comparison (Figure 1e); (Supplementary Figure S2). At the earlier time point the induction of the three p53 target genes, and particularly MDM2, was more robust in response to Nutlin than to Doxo. The PUMA transcript can also be classified as a thrust gene after 8 h of Nutlin treatment. However, at the 16 h time point PUMA-relative expression changes were higher in total RNA compared with sub and pol, suggesting that, unlike MDM2 and p21, the PUMA transcript could be subject to an opposite regulation we define here as 'translational drag.' This latter phenomenon could be dependent on several factors, including delayed transactivation, slow pre-mRNA maturation, regulation at the nuclear export level or slow assembly of ribosomes on mRNAs. No evidence of transcriptional or translational changes was seen in treated MCF7shp53 cells (Figure 1e).

The majority of direct p53 target genes are coupled. Nevertheless, we found that expression is uncoupled for about 70% of DEGs.

The uncoupled, translationally upregulated gene group is enriched for apoptotic functions. Uncoupled DEGs are genes with a major change in relative expression levels compared with mock treatment in only one of the three mRNA preparations: (a) transcriptome (tot); (b) translatome (pol); (c) non-translated subpolysomal mRNAs (sub) (red, blue and yellow circular sectors, respectively, in Figure 1c). We identified 1432 uncoupled DEGs after Doxo and 987 after Nutlin treatment.

First, we focused on uncoupled DEGs that were induced in the translatome but did not change in the transcriptome (Figure 2a); (Supplementary Table S1B). We found 55 translatome-uncoupled DEGs common to the two treatments (Figure 2a). Among them, PHPT1 (14-kDa phosphohistidine

Figure 1 Differentially expressed genes in the transcriptome and translatome of doxorubicin- and nutlin-3a-treated MCF7 cells. Overall results and coupled differentially expressed genes (DEGs). (**a**) Profiles after sucrose gradient fractionation of cytoplasmic extracts prepared from MCF7vector (upper plot) and MCF7shp53 (lower plot) cell lines. The conditions tested were mock, doxorubicin (Doxo, 1.5 μM) and nutlin-3a (Nutlin, 10 μM) after 16 h of treatment. The subpolysomal fractions (sub: free RNA, small-40S and large-60S and monosomes-80S) and the polysomal fractions (pol) were separated. Sub and pol fractions (see numbers on *x*-axis) were combined in two separated tubes for RNA extraction. (**b**) Scatter-plots representing transcriptional and translational $\log_2$ fold changes. Spearman correlation was calculated. DEGs in each category (transcriptome only, translatome only and homodirectional changes) are classified according to $\log_2$ fold change >1 and <-1 for induced and repressed genes, respectively, and Benjamini–Hochberg corrected *P*-value <0.05. Genes without significant changes are shown in gray. (**c**) Venn diagrams showing the level of coupling/uncoupling for upregulated (up) and downregulated (down) DEGs after Doxo and Nutlin treatment. The green overlapping areas represent coupled DEGs that are enriched in all conditions: total RNA (tot), subpolysomal fraction (sub) and polysomal fraction (pol). (**d**) Coupled DEGs are mainly involved in the p53 pathway. Ingenuity pathways analysis (IPA) was performed on coupled DEGs after Doxo and Nutlin treatment and each of these genes is considered by IPA according to their $\log_2$ fold change and BH corrected *P*-value, integrating up- and downregulated DEGs (up and down). Results on the coupled DEGs that are common to both Doxo and Nutlin treatments are also presented (common coupled DEGs). The *y*-axis displays the significance of the association between DEGs and the canonical pathways measured by Fisher's exact test. A *P*-value cutoff of 0.05 was used to identify significantly enriched pathways. The plot shows four among the most enriched pathways. (**e**) Relative expression levels of three established p53 target genes. MCF7vector cells were treated with Doxo and Nutlin for 8 h (upper plots) or 16 h (lower plot). MDM2, p21 and PUMA transcript levels were validated by qPCR in total RNA (tot), subpolysomal (sub) and polysomal (pol) fractions as positive controls. To establish p53 dependence, all experiments were conducted also in MCF7shp53 cells. Data are plotted relative to each mock condition and three reference genes. $n=3$. Means $\pm$ S.D. are shown. $^*P<0.05$. The basal expression levels in each RNA fraction are presented in Supplementary Table S7

phosphatase)[22] and TP53RK (p53-related protein kinase)[23] were chosen for validation by qPCR owing to their biological relevance in post-translational control, and because they had not been previously reported as p53-regulated genes. PHPT1 and TP53RK proved to be translational upregulated genes, particularly after 16 h of treatment (Figure 2b).

We also compared changes in protein levels by western blot analysis (Figure 2c). Considered as a

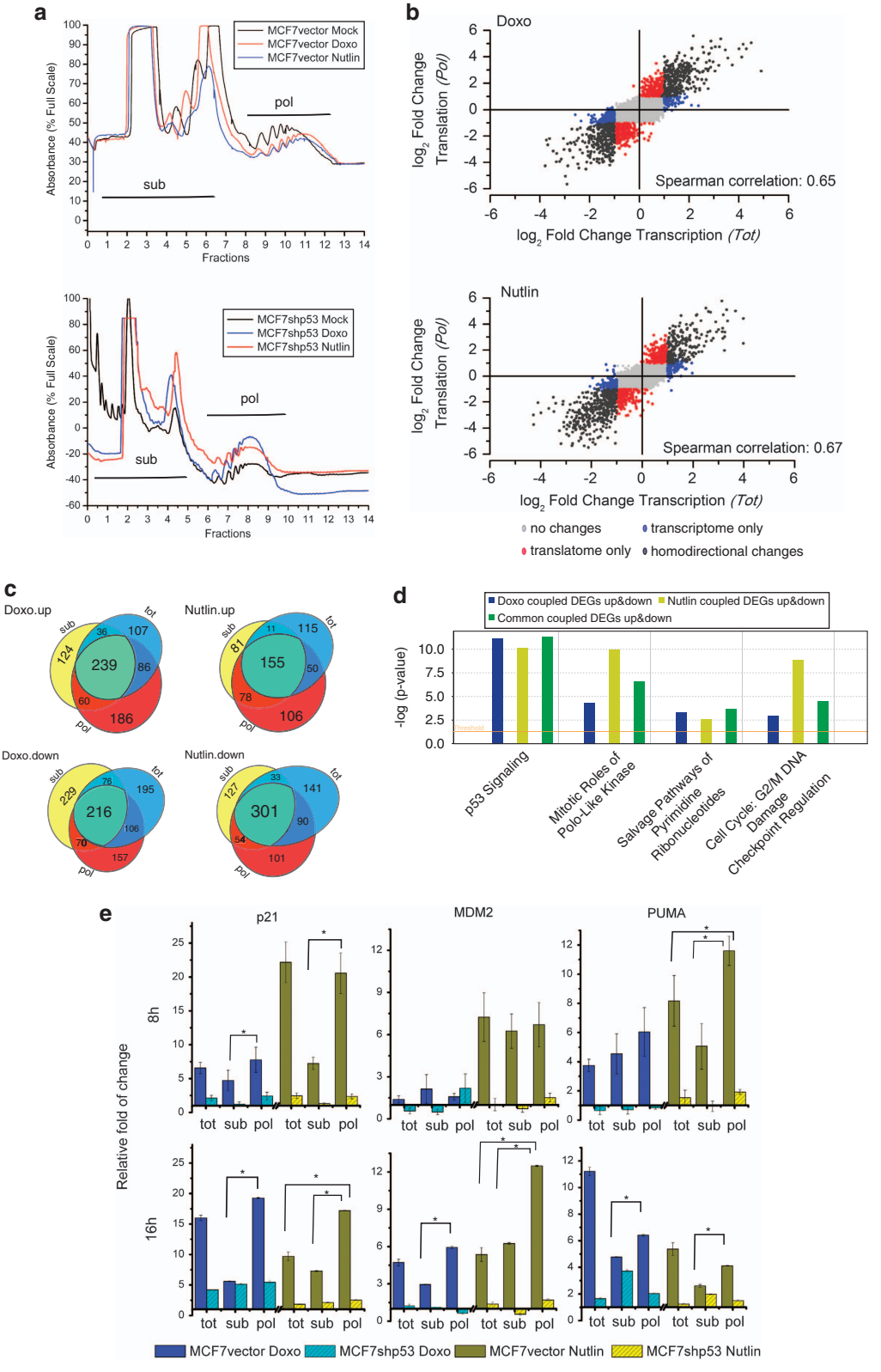

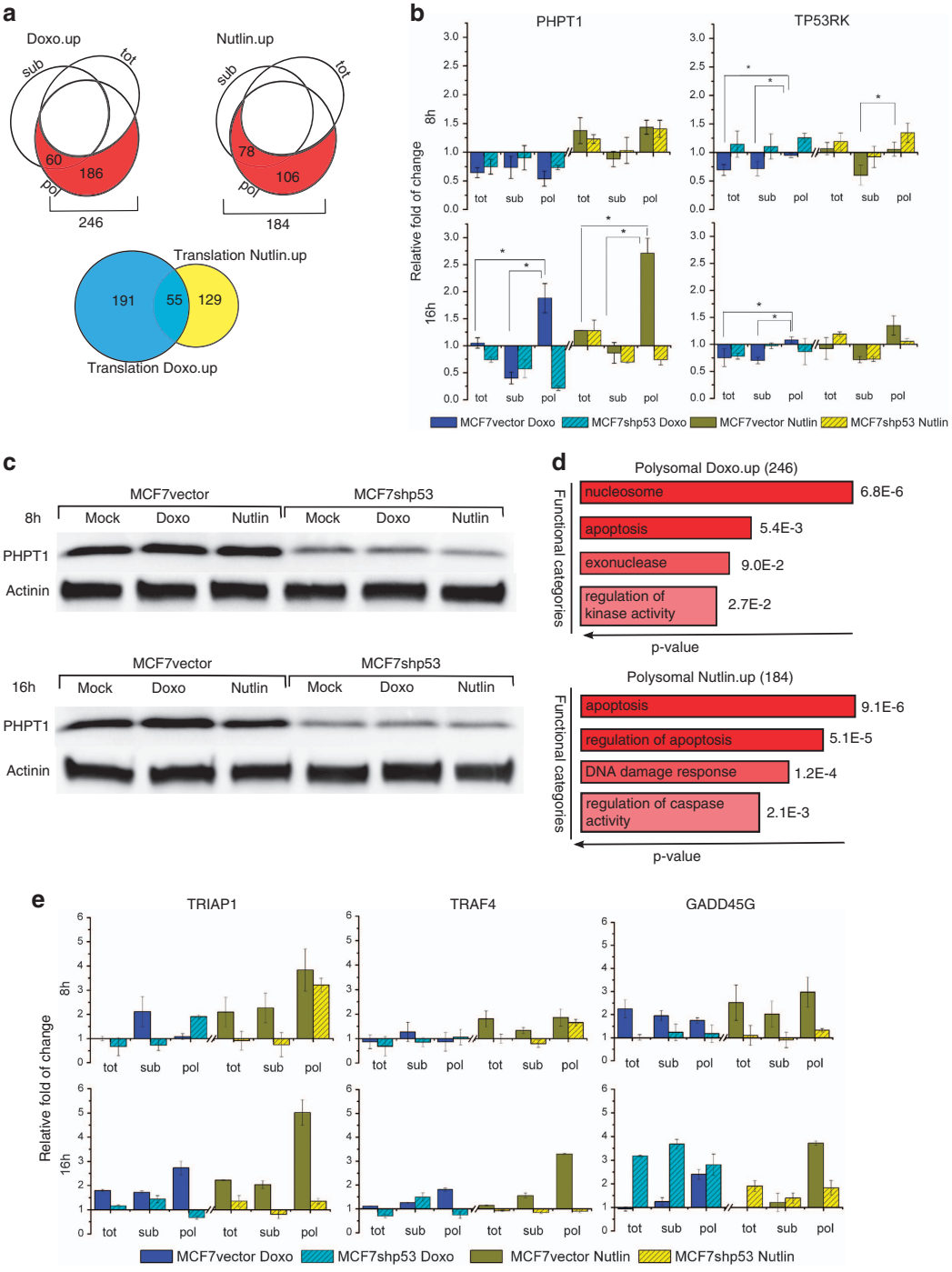

Figure 2 Uncoupled DEGs upregulated only in translation are enriched in apoptosis function. (**a**) Top: Venn diagrams from Figure 1b, highlighting the uncoupled DEGs that are upregulated in translation after doxorubicin and nutlin-3a treatments. Bottom: Venn diagram showing the level of overlap between DEGs with high translation levels after Doxo and Nutlin treatment. (**b**) p53 promotes the translation of PHPT1, a modulator of DNA accessibility, and of TP53RK, a putative activator of p53 itself. MCF7vector and MCF7shp53 cell lines were treated with Doxo and Nutlin for 8 h (upper plots) or 16 h (lower plots). PHPT1 and TP53RK mRNA levels were validated by qPCR starting from total RNA (tot), subpolysomal (sub) and polysomal (pol) fractions. Data are plotted relative to each mock condition and three reference genes. $n=3$. Means ± S.D. are shown. $^*P<0.05$. (**c**) Western Blot analysis of PHPT1 protein level in MCF7vector and MCF7shp53 cells after 8 h (top) and 16 h (bottom) of treatment with Doxo or Nutlin. Actinin was used as reference protein for loading control. (**d**) Gene ontology (GO) analysis on upregulated DEGs in the polysomal fraction that did not change in the total RNA. Plots represent the most enriched GO terms obtained by DAVID analysis. *P*-values of the enriched categories are reported. The analysis was performed on upregulated DEGs after both Doxo and Nutlin treatments. (**e**) p53 promotes the translation of TRIAP1, TRAF4 and GADD45G, three p53 target genes involved in the apoptotic process. MCF7vector and MCF7shp53 cells were treated with Doxo and Nutlin for 8 h (upper plots) or 16 h (lower plots). mRNA levels were measured by qPCR starting from total RNA (tot), subpolysomal (sub) and polysomal (pol) fractions. Data are plotted relative to each mock condition and three reference genes. $n=3$. Means ± S.D. are shown. $^*P<0.05$

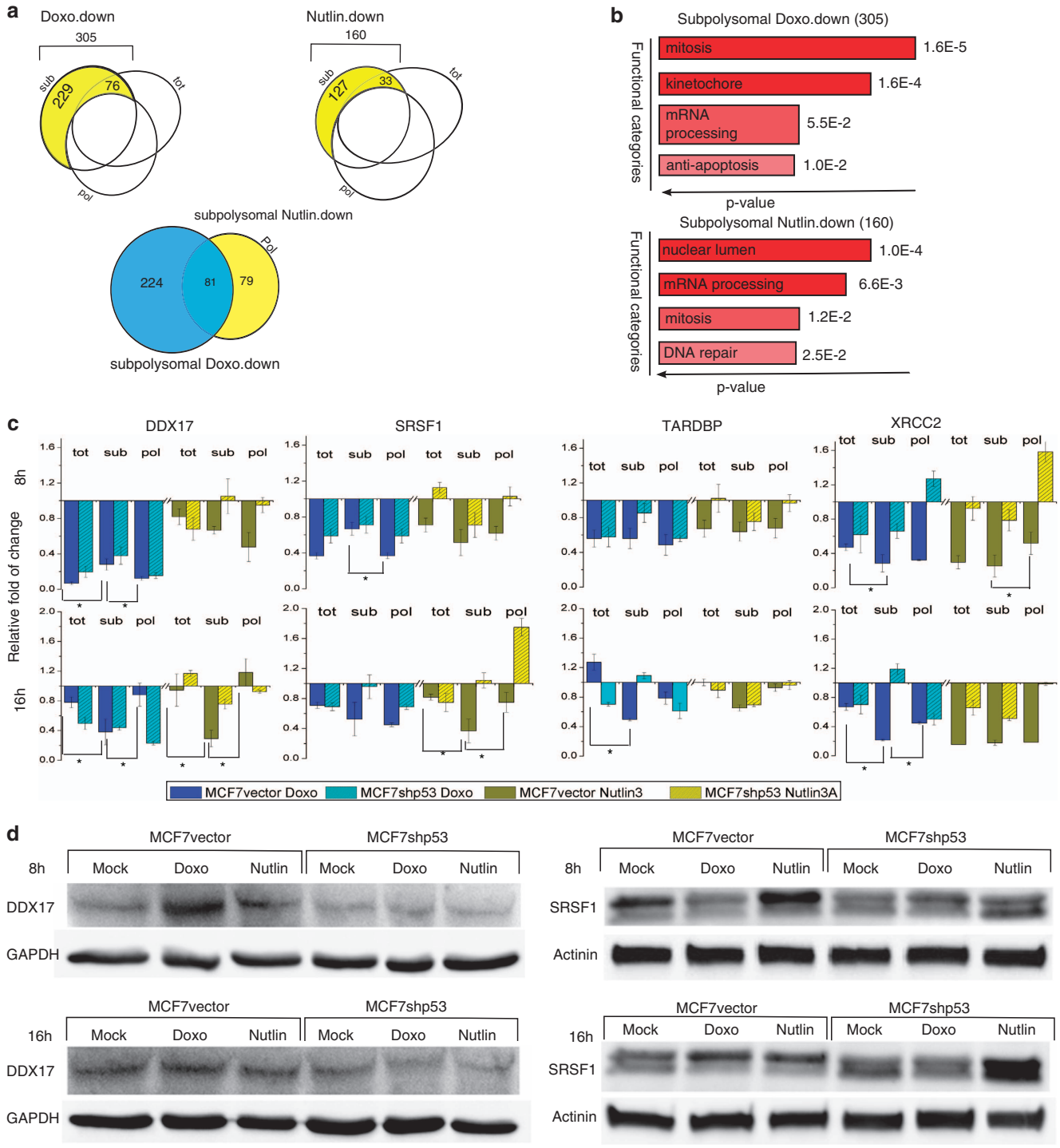

Figure 3 Subpolysomal downregulated DEGs are involved in mitosis and RNA splicing regulation. (**a**) Top: Venn diagrams from Figure 1b, highlighting the uncoupled DEGs that were downregulated in the subpolysomal fraction without significant changes at polysomal levels. Bottom: Venn diagram showing the level of overlap between DEGs downregulated in the subpolysomal fraction after doxorubicin and nutlin-3a treatments. (**b**) Gene ontology (GO) analysis on DEGs downregulated in the subpolysomal fraction that did not change in polysomal RNA. Graphs represent the most enriched GO terms obtained by DAVID analysis. *P*-values of the enriched categories are indicated. The analysis was performed on downregulated DEGs after both Doxo and Nutlin treatments. (**c**) DDX17, SRSF1, TARDBP and XRCC2 are indirect p53 targets. MCF7vector and MCF7shp53 cell lines were treated with Doxo and nutlin-3a for 8 h (upper plots) and 16 h (lower plots). mRNA levels were measured by qPCR in total RNA (tot), subpolysomal (sub) and polysomal (pol) fraction. Data are plotted relative to each mock condition and three reference genes. $n = 3$. Means ± S.D. are shown. $^*P < 0.05$. (**d**) Western Blot analysis of DDX17 (left side) and SRSF1 (right side) protein levels in MCF7vector and shp53 cells after 8 h (top) and 16 h (bottom) of treatment with Doxo or Nutlin. GAPDH and actinin were used as reference proteins for loading control. The actinin-loading control for SRSF1 is the same used as the loading control for PHPT1 in Figure 2c

proxy of the proteome, the pol level should reflect the protein level of each transcript. PHPT1 protein levels were slightly induced by both Doxo and Nutlin in MCF7vector cells, whereas no changes occurred in MCF7shp53 (the basal levels were significantly lower) (Figures 2b and c).

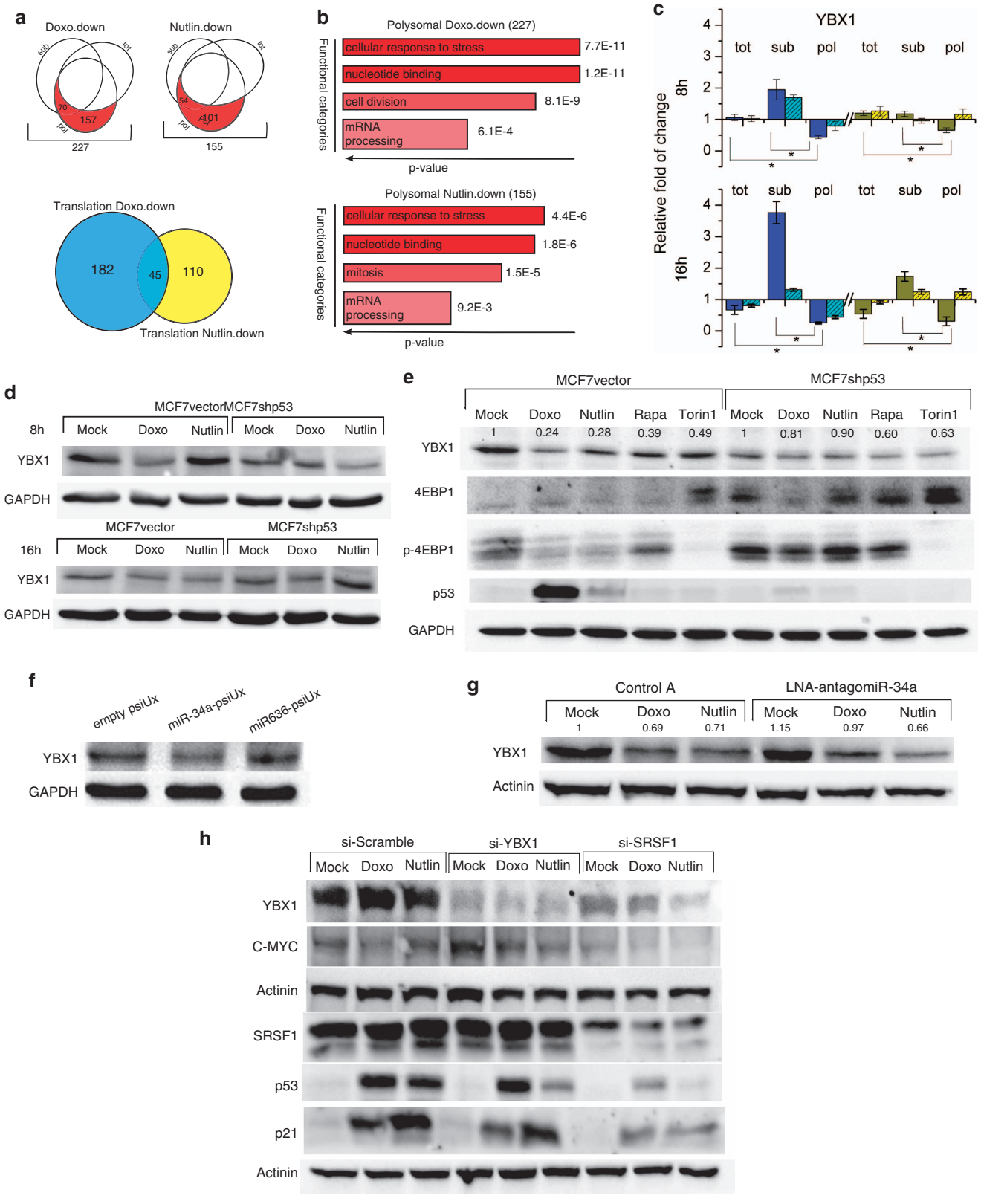

Among induced translatome-uncoupled DEGs, gene ontology analysis revealed enrichment for apoptosis terms after both Doxo and Nutlin treatments (Figure 2d). This observation suggests that modulation of translation efficiency might reinforce the activation of p53-dependent apoptosis, a process that could be important given the generally weaker transcriptional control of p53 target genes in the apoptosis group.[24] We validated by qPCR TRIAP1,[25] TRAF4[26] and GADD45G[27] (the full list of genes is presented in Supplementary Figure S3A). According to ChIP-seq data on MCF7 cells, these genes are direct p53 targets.[28] For all of them, the increase at the polysomal level, especially after Nutlin treatment, was confirmed at both time points. For GADD45G, high level of induction was observed also in the MCF7shp53 cells (Figure 2e).

Overall, we conclude that even if there was a weak modulation at the total mRNA level, p53 or p53-inducing treatments enhanced the translation of these apoptotic genes.

p53 activation reduced the subpolysomal mRNA levels of DDX17, SRSF1, TARDBP and XRCC2. Relative translation efficiency can decrease by inhibiting translation without impacting mRNA stability, or by destabilizing mRNAs. Given that p53 controls the expression of many miRNAs and RBPs,[12] it could indirectly impact both mechanisms. DEGs that were selectively downregulated in the sub fraction but did not change in translation might be considered as candidate targets for a regulation process that targets more selectively mRNA molecules not engaged in translation (Figure 3a). Following Doxo and Nutlin treatments, we observed, respectively, 305 and 160 subpolysomal downregulated DEGs (Supplementary Table S1C) and 81 were common to the two groups. (Figure 3a). 'Mitosis' was the mostly enriched functional category, among which XRCC2[29] was also validated by qPCR (Figure 3c). mRNA-processing categories, such as RNA splicing, were also enriched (Figure 3b); (Supplementary Figure S3B). As we were interested in how p53 might modulate post-transcriptional mechanisms, we also selected three RBPs—SRSF1, DDX17 and TARDBP—for further qPCR validation. DDX17 and SRSF1 mRNAs were confirmed to be downregulated in sub but did not change in tot nor pol after Nutlin treatment in MCF7vector cells. On the contrary, Doxo treatment led to a less-evident down-modulation in the pol fraction that generally was p53-independent (downregulation in the MCF7shp53 cells).

Changes in DDX17 and SRSF1 protein levels were investigated (Figure 3d). In general, protein levels were more in agreement with their matched pol changes at the 16 h time point. Moreover, SRSF1 was consistently upregulated in MCF7shp53 at 16 h post Nutlin treatment, confirming mRNA data and literature reports.[30]

p53 activation leads to translational inhibition of genes involved in mRNA processing and nucleotide binding, including YBX1. Although a reduction in subpolysomal RNA can be interpreted as evidence of reduced mRNA stability, lower polysomal RNA can be a hallmark for decreased translation efficiency of specific mRNAs.

Hence, we examined DEGs that were repressed in polysomal fraction, but did not change in total mRNA (Figure 4a); (Supplementary Table S1D). Although not as first enriched term, gene ontology analysis showed an enrichment for 'mRNA processing' after both treatments (Figure 4b); (Supplementary Figure S3C). DEGs (45) were common to the two treatments (Figure 4a) including five RBPs (YBX1, SNRPA, HNRNPA3, KIAA0020 and DGCR8) among a restricted list (see Materials and Methods).

YBX1 was chosen for validation also because of its reported interaction with p53.[31] Its mRNA was significantly downregulated in polysomal RNA, more than in the total RNA, with a p53-dependent shift from the polysomal to the subpolysomal fraction (Figure 4c). The same trend was observed after 8 h, but only in the Doxo treatment. Moreover, the reduction in pol mRNA corresponds to a reduction in YBX1 protein level (Figure 4d).

The YBX1 transcript was found to have a 5′-terminal oligopyrimidine tract-like mRNA that is suppressed in the polysomal fraction after mTOR inhibition.[32] Furthermore, p53 can negatively modulate the mTOR pathway via the

Figure 4 DEGs inhibited in translation are involved in mRNA processing and help shaping the p53-dependent response. (**a**) Top: Venn diagrams from Figure 1b, highlighting the uncoupled DEGs that were downregulated in the polysomal fraction without significant changes in total mRNA. Bottom: Venn diagram showing the overlap between DEGs downregulated in the polysomal fraction after Doxo and Nutlin treatments. (**b**) Gene ontology (GO) analysis on DEGs downregulated in the polysomal fraction that did not change in total RNA. Graphs represent the most enriched GO terms obtained by DAVID analysis. *P*-values of the enriched categories are reported. The analysis was performed on downregulated DEGs after both doxorubicin and nutlin-3a treatments. (**c**) YBX1 is an indirect p53 target. MCF7vector and MCF7shp53 cell lines were treated with Doxo and Nutlin for 8 h (upper plot) or 16 h (lower plot). YBX1 levels were measured by qPCR in total RNA (tot), subpolysomal (sub) and polysomal (pol) fractions. Data are plotted relative to each mock condition and three reference genes. $n = 3$. Means ± S.D. are shown. $^*P < 0.05$. (**d**) Western Blot analysis of YBX1 protein level in MCF7vector and shp53 cells after 8 h (upper panels) and 16 h (lower panels) of treatment with Doxo or Nutlin. GAPDH was used as reference protein for loading control, and is the same used as loading control for DDX17 in Figure 3d. (**e**) Western Blot analysis of MCF7vector and MCF7shp53 cell extracts after treatment with Doxo, Nutlin, rapamycin (Rapa) and Torin1. Protein levels of YBX1, total 4EBP1 and phosho(p-) 4EBP1 were measured as mTOR inhibition would lead to a reduction of 4EBP1 phosphorylation (p-4EBP1) and the consequent inhibition of cap-dependent translation. As control, p53 protein levels were measured. p53 is stabilized after 16 h of treatment with Doxo and Nutlin, whereas the treatment with mTOR inhibitors does not have an impact on p53 protein levels. GAPDH was used as a reference protein for loading control. For YBX1, numbers above the immunoreactive bands represent the relative amount of proteins normalized against both the reference protein and the mock condition (set to 1 separately for each cell line). (**f**) Ectopic overexpression of miR-34a in MCF7vector cell line. The empty miR-expression plasmid psiUx condition was used as negative control. miR-636 was overexpressed as an additional control of miR-34a specificity. GAPDH was used as a reference protein for loading control. (**g**) YBX1 protein levels in MCF7vector cells transfected with the negative Control A or an LNA-antagomiR-34a and treated after 48 h with Doxo or Nutlin. Actinin was used as a reference protein for loading control. Numbers above the immunoreactive bands represent the relative amount of proteins normalized using both the reference protein and the mock condition in the control experiment (set to 1). (**h**) Western Blot analysis on MCF7vector cell extracts after silencing YBX1, SRSF1 or scramble control, either in the mock condition or after Doxo or Nutlin treatment. Protein levels of YBX1 and SRSF1 confirm the silencing. c-MYC protein levels were measured because it is a recognized downstream target of both YBX1 and SRSF1. As additional controls, p53 as well as p21 levels were measured. Actinin was used as a reference protein for loading control

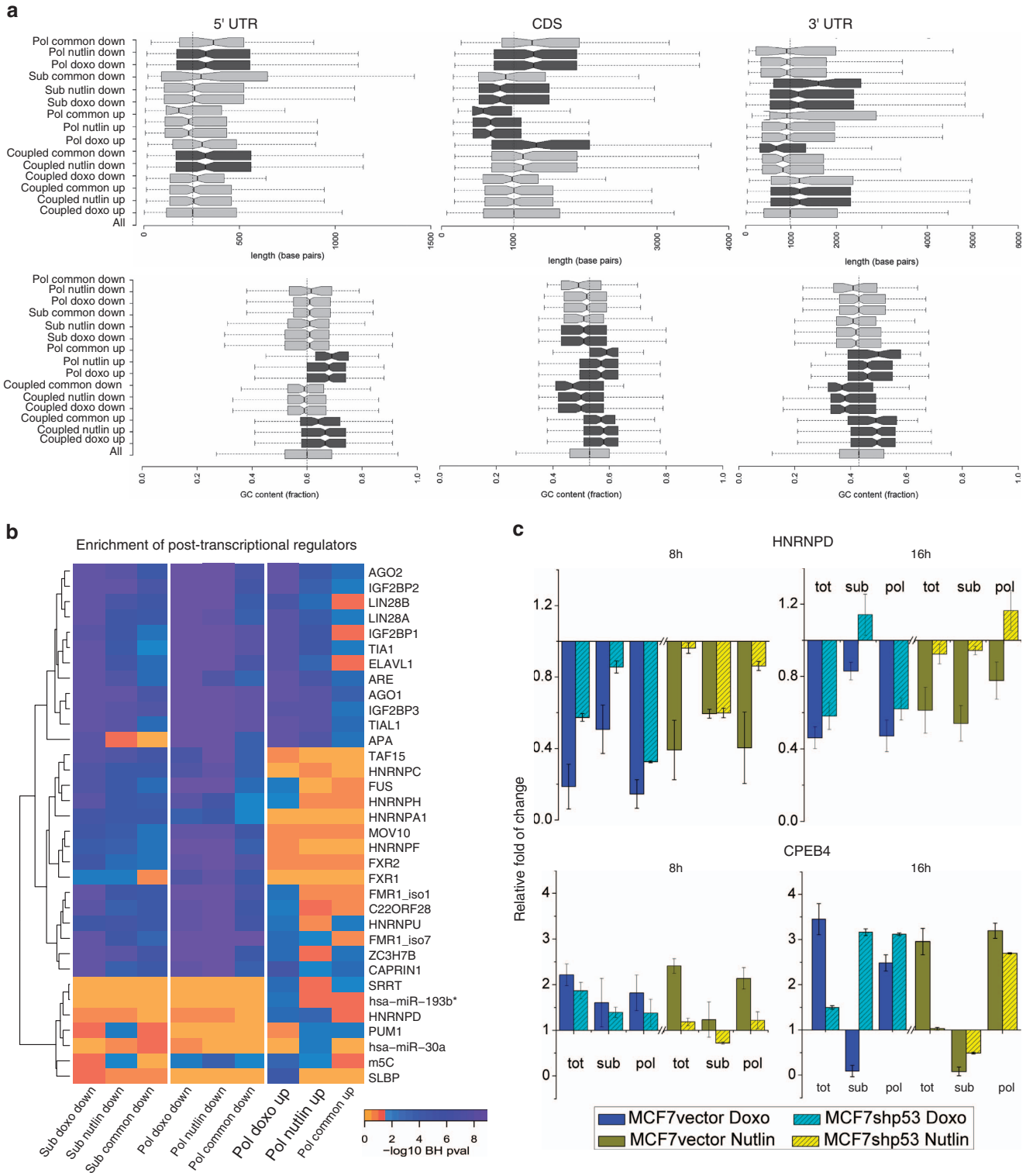

Figure 5 Enrichment of sequence features or of regulatory elements in the UTRs or coding sequence of uncoupled DEGs. (**a**) The upper plots show the length distribution for the 5′-untranslated region (UTR), coding region (CDS) and 3′-UTR of the indicated list of our DEGs. Common refers to the overlap between Doxo and Nutlin DEGs. The lower plots present the GC content for each of these categories. All distributions are compared with the background distribution of the whole set of human genes (all). The significant shifts in distribution are shown in dark gray (Mann–Whitney test, *P*-value < 0.01). (**b**) Heatmap based on the enrichment *P*-values adjusted for multiple testing with the Benjamini–Hochberg method. DEGs upregulated in the subpolysomal fraction, upregulated in the polysomal fraction or downregulated in the polysomal fraction are presented for each treatment (Doxo and Nutlin). The enrichment of regulatory elements for DEGs common to both treatments are also presented, referred to as 'common'. (**c**) hnRNPD and CPEB4 are direct p53 targets. MCF7vector and MCF7shp53 cell lines were treated with Doxo and Nutlin for 8 or 16 h. hnRNPD and CPEB4 levels were measured by qPCR in total RNA (tot), subpolysomal (sub) and polysomal (pol) fractions. Data are plotted relative to each mock condition and three reference genes. $n = 3$. Means ± S.D. are shown

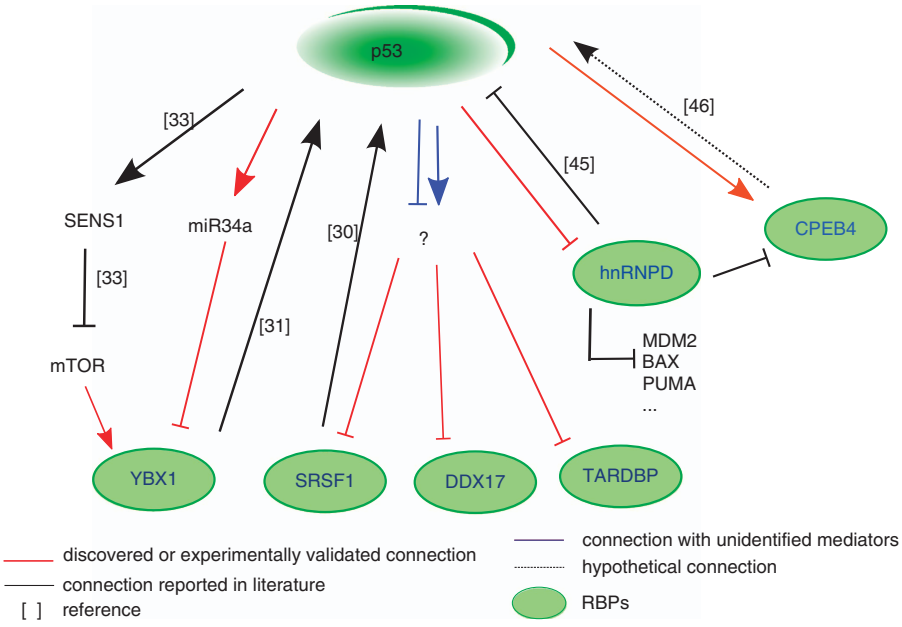

Figure 6 Five RBPs are regulated by p53 and can contribute to post-transcriptional control of p53 responses. Cartoon highlighting functional links between wild-type p53 and six RBPs that are established or confirmed in our work. Solid red lines and arrows represent functional interactions discovered or experimentally validated in this work. Black lines represent functional interactions reported in the literature (citation numbers are near those arrows). Blue lines are used when the mediators of the functional interactions are unknown. The impact of CPEB4 on p53 is hypothetical, based on results with the related CPEB1 protein

upregulation of Sestrins (SESN1–2).[33] SESN1 was among the coupled upregulated DEGs that we identified (Supplementary Table S1A). As apparently p53 could impact on YBX1 mRNA through the mTOR pathway, we examined the impact of Doxo and Nutlin treatments on mTOR activity in comparison with two mechanistically different mTOR inhibitors rapamycin (an allosteric mTORC1 inhibitor) and Torin1 (a selective ATP-competitive mTOR inhibitor) as controls. The amount of p-4EBP1 was reduced by Torin1 and, to a limited extent, by rapamycin, but also by Doxo or Nutlin treatment in MCF7vector cells (Figure 4e). Although YBX1 protein levels were markedly lower after Torin1 and rapamycin treatment independently from p53 status, the reduction was even more evident after both Doxo and Nutlin treatment in MCF7vector cells. This was despite the apparent lower inhibition of mTOR in MCF7shp53 cells, based on p-4EBP1 levels. Collectively, these results suggest an additional mTOR pathway-independent, p53-dependent mechanism of YBX1 translational regulation.

We searched for published evidence of RBPs or miRNAs that could modulate YBX1 mRNA translation/stability. YBX1 was reported as a target of miR-137 in multidrug-resistant MCF7/ADAM cells,[34] but we were unable to detect miR-137 in our cell lines, both in treated and untreated conditions. On the basis on a recent CLASH analysis,[35] miR-34a, a p53-target miRNA,[12] was found to bind YBX1 3′UTR. We confirmed that Doxo and Nutlin increased miR-34a expression only in MCF7vector cells (Supplementary Figure S4A). Moreover, miR-34a ectopic overexpression led to a reduction in YBX1 protein (Figure 4f; Supplementary Figure S4B). Vice versa, upon inhibition of miR-34a, YBX1 levels were slightly increased in the mock condition and were reduced less by Doxo, but not by Nutlin, treatment (Figure 4g; Supplementary Figure S4C). Therefore, an additional effect between p53-dependent miR-34a overexpression and p53-related reduction in the mTOR activity on YBX1 can be hypothesized.

Transcriptional and translational cross-talk between p53, YBX1, SRSF1 and c-MYC. We established that p53 indirectly modulates the expression of at least four RBPs (DDX17, SRSF1, TARDBP and YBX1). By binding to their target mRNAs, RBPs could in turn contribute to the tuning of the p53-induced responses both at the transcriptional and translational levels. We chose SRSF1 and YBX1 to explore these potential regulatory modules by an siRNA approach, as they both control cell proliferation, cell-cycle progression and apoptosis[36,37] (Figure 4h). We confirmed data indicating that SRSF1 reduction leads to a lower stabilization of p53 protein and to lower induction of p21.[30,38] We then examined c-MYC protein levels, given that c-MYC translation is reported to be upregulated by YBX1,[39] and SFSRF1 depletion was associated with reduced c-MYC oncogenicity.[36] Interestingly, silencing SRSF1 led to a concomitant decrease in YBX1 protein and even more so in the c-MYC protein. On the contrary, YBX1 silencing did not impact on SRSF1 or c-MYC protein levels in the mock condition.

CPEB4 and hnRNPD, mediators of translational control, are new p53 transcriptional targets. General RNA sequence features of the 5′ and 3′UTR as well as coding sequence (CDS) influence post-transcriptional regulation of each mRNA.[40,41] In order to identify potential post-transcriptional regulatory sequences embedded in the transcripts of our DEGs, we performed a distribution analysis of the length and the GC content of their 5′UTR, CDS and 3′UTR regions (Figure 5a). When compared with the

background distribution of the whole set of human genes, translatome upregulated DEGs showed significantly shorter CDS regions and higher GC content, both in the CDS and the UTRs. On the contrary, coupled downregulated genes showed a decreased GC content, more significantly in the 3′UTR region. UTR sequences of our DEGs were analyzed for the enrichment of specific regulatory elements using experimental annotation contained in the Atlas of regulatory UTR activity 2 (AURA 2)[42] (Figure 5b); (Supplementary Figure S5). Target mRNAs of hnRNP-A1, -C and -F were enriched among downregulated DEGs. Conversely, hnRNPD (AUF1)-binding sites were enriched among upregulated uncoupled DEGs for both Doxo and Nutlin treatments (BH *P*-value: 0.00027). Furthermore, our array data identified hnRNPD to be a downregulated coupled DEG upon Doxo treatment, a result confirmed by qPCR (Figure 5c). Hence, hnRNPD should be included in the growing list of p53 target genes coding for RBPs, also considering ChIP-seq data.[43]

ZNF469, ZNF488 and CPEB4 were instead upregulated-coupled RBP DEGs common to both treatments and CPEB4 was validated by qPCR. As already reported by ChIP-seq data,[28,43] we confirm that CEBP4 is a direct p53 target gene.

Other groups of transcriptionally/translationally uncoupled genes are described in Supplementary Figure S6.

Discussion

Genome-scale transcriptome analyses have been instrumental in describing the p53 gene response networks under a variety of stress responses.[28] Nevertheless, the mechanism defining which cellular response is adopted remains poorly characterized.[25]

Here, we describe post-transcriptional gene expression control as an additional dimension to potentially shape the p53-directed gene response. Moreover, the global implications of several RBPs on that mechanism are also taken into account, given their involvement in mRNA translation. Quantitative proteomics would theoretically be an ideal tool to assess the p53-dependent translational output. Nevertheless, the coverage of proteomic studies is still a limiting factor.[44] In our approach the translatome can be considered as a proxy for the proteome, although the experimental methods maintain the sensitivity typical of RNA expression studies.

To shape the downstream response networks p53 modulates RBPs that act as molecular sieves. Guided by the comparison of transcriptome and translatome data, but also considering DEGs within the free cytoplasmic pool (sub), we identified a number of RBPs that could be regulated by either Doxo (67 RBPs) or nutlin-3a (30 RBPs) or would be common to both treatments (22) (Supplementary Table S4). These 22RBPs are primary candidates for p53-directed control. Indeed, in the validation experiments we confirmed YBX1, SRSF1, DDX17, TARDBP, HNRNPD and CEBP4 as targets of p53-dependent modulation at the total mRNA or polysomal mRNA levels or both (Figure 6). In particular, we focused on targets that could directly or indirectly modulate p53 functions, either by acting on the p53 mRNA or on the mRNAs of p53 target genes.

Interestingly, hnRNPD had already been reported to target and destabilize the mRNAs of p53,[45] BAX and other important cancer genes, often in a reciprocal, alternating association with HuR, an mRNA-stabilizing factor.[45] We propose that through the transcriptional downregulation of hnRNPD, p53 can engage a positive feedback and potentially also a feed-forward regulatory loop. Consistently, we found enrichment for hnRNPD target mRNAs among the group of translationally upregulated DEGs (Figure 5a).

CPEB4 was an upregulated-coupled DEG whose enhanced expression was abated by p53 silencing. Notably, CPEB4 is a member of the CPEB family, and CPEB1, functionally related with CPEB4, was shown to sustain p53 translation, thereby participating in the activation of the senescence response.[46,47] We suggest that p53 could impact its own translation fitness and functions via its direct target gene CPEB4.

DDX17, TARDBP, SRSF1 and YBX1 are confirmed as modulated at the post-transcriptional level. Overall, in almost all the analyses, protein levels reflect the subpolysomal or polysomal mRNA changes, suggesting that these mRNA variations could have a significant impact on the final proteome. Although TARDBP functions are still under investigation, DDX17/p72 is a putative RNA helicase[48] that by interacting with DDX5 (p68) can act as a modulator of p53-dependent transcription and DNA damage response.

SRSF1 was repressed by both doxorubicin and nutlin-3a treatments particularly in the subpolysomal RNA fraction, and the p53-dependent negative modulation was apparent comparing MCF7vector with MCF7shp53 cells. As it was recently reported that SRSF1 overexpression provides resistance to oncogenic transformation via stabilization of p53,[30,49] we propose that we have uncovered a negative feedback loop by which p53 inhibits a positive regulator.

We explored in more detail two mechanisms linking p53 activation with YBX1 mRNA and protein downregulation, namely the inhibition of the mTOR pathway[32] and the upregulation of miR-34a.[12] Although p53 can negatively impact on mTOR, via the transcriptional activation of SESN1 and SESN2,[33] the high dependency of mTOR function on the cell metabolic state can also influence our results. The dynamics by which p53 modulates all these RBPs is an additional, critical point. Here, we measured the expression of these genes also after 8 h of treatments to begin exploring this issue. Temporal differences in p53 stabilization upon doxorubicin and nutlin-3a treatments have been already reported[50] and are confirmed by our analysis. Overall, the qPCR results revealed correlations (e.g., p21, PUMA, TRIAP1, TRAF4, XRCC2, hnRNPD and CPEBP4) as well as differences (MDM2, PHPT1, TP53RK, GADD45G, DDX17, SRSF1, TARDBP and YBX1), between the two time points and also between mRNA and protein levels.

Further investigations are needed to clarify the specific impact of RBPs on post-transcriptional regulation after p53 activation. In our experiments SRSF1 silencing led to a decrease also in YBX1 protein levels, suggesting a cross-talk between the two RBPs via unexplored mechanisms, and this resulted in down-modulation of c-MYC. Hence, p53-dependent negative regulation of both YBX1 and SRSF1, could lead to repression of c-MYC, and contribute to cell cycle

arrest. Importantly, for c-MYC and potentially many other targets, p53 could also impact indirectly on mRNA translation efficiency via transcriptional inhibition of the Fibrillarin gene.[51]

Apoptosis can be regulated also at the level of translation efficiency of p53 target genes. Gene ontology of DEGs that were uncoupled and upregulated only in the polysomal fraction revealed an enrichment for the term 'apoptosis', which was even more significant in cells treated with nutlin-3a. This finding uncovers a new layer of complexity in the modulation of the classical p53-dependent apoptosis (Supplementary Figure S7). Several studies have shown that transcriptional activation of apoptosis gene targets can be influenced by selective cofactors or specific post-translational modifications of the p53 protein.[24] We suggest that translational controls may promote the synthesis of those pro-apoptotic proteins contributing to the actual induction of programmed cell death. Recently, Ribo-seq was used to profile MCF7 cells treated with nutlin-3a.[52] Ribo-seq maps ribosome-protected fragments, but, unlike polysomal profiling, it does not separate actively translating polysomes from monosomes (80S), nor does it address subpolysomal RNA. Consistently with our results, downregulation of cell-cycle genes was observed but the modulation of apoptosis or mRNA-processing pathways was not apparent in Ribo-seq data.

In summary, our analysis of uncoupled mRNAs, namely mRNAs undergoing translational control, reveals a large number of new indirect p53-regulated targets that would not have been identified through a traditional transcriptome study. On the basis of the functions of these genes, it becomes apparent that selectivity at the level of mRNA translation, in addition to transcriptional selectivity, is a critical contributing factor in the shaping of p53-directed responses and at least six RBPs directly or indirectly modulated by p53 may be implicated. Our study opens up a scenario where further investigations will clarify the impact of p53-dependent post-transcriptional regulation as well as the involvement of RBPs on cellular outcomes.

Materials and Methods

Cell lines and culture conditions. MCF7 cells stably expressing an shRNA targeting p53 (MCF7shp53) or control cells (MCF7vector) were kindly provided by Dr Agami.[20] Cells were normally maintained in RPMI (Gibco, Life Technologies, Milan, Italy) supplemented with 10% FBS, antibiotics (100 units/ml penicillin plus 100 mg/ml streptomycin) and 2 mM L-glutamine. Puromycin (Sigma-Aldrich, Milan, Italy) was used to maintain the selection, at 0.5 μg/ml as final concentration.

Polysomal RNA fractionation and extraction. MCF7vector cells (3.5×10^6) were seeded into 10 cm tissue culture dishes and allowed to reach 70–80% confluence before treatment with 1.5 μM doxorubicin (Doxo) or 10 μM nutlin-3a (Nutlin). Doxo was purchased from Sigma-Aldrich, whereas nutlin-3a was obtained from Alexis Biochemicals (Enzo Life Science, Exeter, UK). After 8 or 16 h, polysomal separation was performed as previously described.[53] Briefly, samples were loaded in 15–50% linear sucrose gradients, ultra-centrifuged and fractionated with an automated fraction collector. All the fractions containing subpolysomal or polysomal RNA were identified and pooled in two separate tubes. RNA was purified by extraction with 1 volume of phenol–chloroform and adding a washing step in 70% v/v ethanol in order to remove phenol contaminations. DNAse treatment (RNase-Free DNase Set, Qiagen, Hilden, Germany) was performed to remove DNA contamination after the RNA extraction. Three biological replicates were performed. For validation studies, all these steps were repeated also for the MCF7shp53 cell line, seeding 2×10^6 cells/dish.

Total RNA extraction. MCF7vector and MCF7shp53 cell lines were seeded into six-well plates and allowed to reach 70–80% of confluency before treating with 1.5 μM Doxo or 10 μM Nutlin. After 8 or 16 h of treatment, cells were harvested and total RNA was extracted using the Agilent Total RNA Isolation Mini Kit (Agilent Technologies, Milan, Italy) according to the manufacturer's instructions. In-column DNAse treatment (RNase-Free DNase Set, Qiagen) was performed to remove DNA contamination during the extraction. Three biological samples were analyzed.

Microarray hybridization and data analysis. Purity of all extracted RNAs (A260/A280 value of 1.8–2.1) and concentrations were measured using the Nanodrop spectrophotometer. An additional quality control was performed with the Agilent 2100 Bioanalyzer (Agilent Technologies) discarding RNA preparations with RIN (RNA integrity number) value <8. mRNAs extracted after 16 h of treatment with Doxo or Nutlin were hybridized to an Agilent-014850 Whole Human Genome Microarray 4x44K G4112F-Probe following the manufacturer's protocol. Raw data and procedures were deposited in Gene Expression Omnibus (GSE50650). That output was analyzed with the tRanslatome package[54] using the Limma method (http://www.bepress.com/sagmb/vol3/iss1/art3) comparing each treatment of every tested RNAs with the mock condition. Moreover, Supplementary Table S5 shows the detailed list of all our DEGs. For all further analysis on DEGs, two thresholds were set for each comparison: (1) $\log_2$ (fold change) >1 and <-1 for upregulated and downregulated genes, respectively; (2) Benjamini–Hochberg (BH) corrected *P*-value <0.05.

Gene ontology and pathway analysis of DEGs. Gene-annotation enrichment analysis for all our selected categories of coupled or uncoupled DEGs was performed with the DAVID resource.[55] The significance of overrepresentation was determined at a false discovery rate of 5% with BH multiple testing correction and an enrichment score >1.5. All pathways analyses were performed using ingenuity pathway analysis (www.ingenuity.com). Only direct interactions were considered in setting parameters.

Analysis of UTR sequence features. UTR and CDS sequences were downloaded from the UCSC Genome Browser (http://genome.ucsc.edu/), assembly GRC37/hg19. For each HGNC gene the longest transcript variant was selected as representative of the gene. Distribution analysis was performed on the length and GC content of 5′UTR, CDS and 3′UTR regions of the lists of DEGs. All the distributions were compared with the background distribution corresponding to the whole set of human genes, and significant shifts were identified with the Mann–Whitney test, selecting a 0.01 significance threshold on the resulting *P*-value.

Analysis of 5′-3′UTRs and of RBP genes. The AURA 2 database (http://aura.science.unitn.it/) was used to perform the analysis of the enrichment of regulatory elements at the 5′–3′UTR of coupled or uncoupled DEGs. Given that AURA 2 is a database containing only experimentally validated post-transcriptional interactions at the UTR level, we used AURA to select enriched RBPs for further validations. The presented enrichment *P*-values were adjusted for multiple testing with the BH-method. We matched our DEG classes with a restricted RBPs' list to obtain the number of RBP genes that were modulated after Doxo and nutlin-3a treatments. The restricted list was compiled including all canonical RBPs (i.e., proteins containing at least one recognized RBP motif), translation factors and non-canonical RBPs reported in previous studies.[56,57]

RT-qPCR reaction. cDNA was generated from 1 μg of RNA using the RevertAid First Strand cDNA Synthesis Kit (Fermentas, Milan, Italy) in 20 μl final volume following manufacturer's instructions. All qPCR assays were performed on a CFX Touch Real-Time PCR Detection System (Bio-Rad, Milan, Italy) in a 384-well plate format. Assays contained 2X KAPA Probe FAST qPCR Master Mix (Kapa Biosystems, Resnova, Rome, Italy), 20$\times$ PrimeTime ZEN Double-Quenched Probes Assay (IDT, Tema Ricerca, Bologna, Italy) and 25 ng of cDNA. Primers are all commercially available according to their catalog number. In addition, we validated some targets using the 2$\times$ KAPA SYBR FAST qPCR Kit (Kapa Biosystems, Resnova) and specific primers purchased from Eurofins (MWG, Operon, Ebersberg, Germany). The list of primers is presented in Supplementary Table S6. All these primers were validated according to the MIQE

guidelines.[58] We present the mRNA quantification relative to the mock condition for each fraction (tot, sub and pol) in order to highlight changes upon treatment. To clarify variation in the mock variation, the ΔCq data of the mock condition are reported in Supplementary Table S7. The relative quantification was obtained using the comparative Cq method (ΔΔCq), where glyceraldehyde 3-phosphate dehydrogenase (GAPDH), β-2microglobulin and tyrosine 3-Monooxygenase/TRYPTOPHAN 5-Monooxygenase Activation Protein, Zeta Polypeptide (YWHAZ) served as reference genes. The relative folds of change were analyzed using a *t*-test approach considering three biological replicates ($P<0.05$).

Antibodies and western blot analysis. Antibodies used for western blot analysis were p53 (DO-1), p21(C-19), YBX1(59-Q), 4EBP1(R-113), GAPDH(6C5), alpha-Actinin (B-19), SRSF1 (3G268), MYC (9E10) and PHPT1 (N-23) from Santa Cruz Biotechnology (Heidelberg, Germany), p-4EBP1(Thr37/46) from Cell Signaling Technology (Milan, Italy) and DDX17 (ab70184) from Abcam (Cambridge, UK). MCF7vector and MCF7shp53 cells were seeded into six-well plates and allowed to reach 70–80% of confluency before treating with Doxo (1.5 μM), Nutlin (10 μM) for 16 or 8 h and rapamycin (250 nM) and Torin1 (250 nM) for 2 h. The concentration and time point used for rapamycin and Torin1 are based on a previous paper.[59] Rapamycin (Sigma-Aldrich)–Torin1 (Tocris Bioscience, Bristol, UK). Proteins were extracted using RIPA buffer as previously described,[2] supplemented with protease inhibitors and phosphatase inhibitor cocktail2 (Sigma-Aldrich) and quantified using the BCA assay (Thermo Scientific, Pierce, Milan, Italy). The relative molecular mass of the immunoreactive bands was determined using PageRuler Plus Prestained Protein Ladder (Fermentas). The semi-quantitative analysis was performed using GAPDH or Actinin as reference proteins for loading control.

Silencing of YBX1 and SRSF1 proteins. To perform YBX1 or SRSF1 silencing, we used DsiRNA Duplex purchased from IDT (si-YBX1: HSC.RNAI.N004559.12.3, si-SRSF1: HSC.RNAI.N006924.12.1). MCF7vector cells were seeded into six-well plates and allowed to reach 30–40% of confluence. After 24 h, 25 nM of the different DsiRNAs were transfected using INTERFERin (Polyplus, Euroclone, Milan, Italy). As a negative control, we transfected cells with the si-scramble si.NC1 at the same final concentration. Fifty-six hours after the transfection, cells were treated with doxorubicin and nutlin. Antisense effects were assessed 16 h after the treatments, thats is, 72 h after transfection.

Apoptosis assays. MCF7vector cells were seeded in 96-well plates (Corning, Lowell, MA, USA) at the density of 15 000 cells/well. After 24 h, cells were treated with 0.75, 1.5 and 3 μM of Doxo and 5 μM, 10 μM and 15 μM of Nutlin. After 16 h, cells were exposed to 10 μl/well of Cell Proliferation Reagent WST-1 (Roche, Milan, Italy) for 30 min before measuring the absorbance at 460 and 600 nm using an Infinite 200 PRO microplate reader (TECAN, Milan, Italy). A reduction in the absorbance signal is proportional to a reduction in the activity of mitochondrial dehydrogenases that is considered as a marker of cell viabilty. Doxo (1.5 μM) and 10 μM Nutlin were chosen for all subsequent experiments. We chose a 16 h time point after doxorubicin and nutlin treatment of MCF7 cells at relatively low doses because we were interested in identifying p53-directed or stress-response-directed mechanisms of post-transcriptional control. For Fluorescence-activated cell sorting analysis, MCF7vector cells were seeded into 10-cm dishes and treated the following day. In order to have more information about cells viability, we recovered and analyzed also cells that were in suspension after the treatments. The FITC AnnexinV Apoptosis Detection kit I (BD Pharmingen, Milan, Italy) was used for the staining following the manufacturer's protocol. TO-PRO-3 Iodide (1 μM) (642/661) was used as a nucleic acid dye (Life Technologies).

miRNA extraction and quantification. MCF7vector and MCF7shp53 cells were seeded into six-well plates and allowed to reach 70–80% confluence before treating with Doxo or Nutlin. After 16 h, cells were harvested and total RNA was extracted using 300 μl of TRIZOL reagent (Invitrogen, Life Technologies). After 5 min of incubation at room temperature, 60 μl of chloroform were added, followed by another incubation step of 3 min at room temperature. Three different phases were obtained following centrifugation at 4 °C for 15 min at 12 000 × *g*. We recovered only the aqueous phase containing the RNA to continue with isopropanol precipitation and subsequent ethanol 75% wash. mRNA quality was controlled as described above. Mature miR expression levels were quantified using pre-made Exiqon assays, using the small nuclear snRNA U6 as reference and following the manufacturer's instructions for cDNA reaction (Universal cDNA Synthesis kit, Exiqon, Woburn, MA, USA) and qPCR with the ExiLENT SYBRGreen Master Mix (Exiqon).

miRNA overexpression. To overexpress pre-miR-34a, we used an siRNA-expressing vector (psiUx) based on the strong and ubiquitous RNA PolII-dependent promoter of the human U1 small nuclear RNA (snRNA) gene.[60] Transfection of the empty psiUx was used as a control.[61] miR-636 was overexpressed as an additional control to confirm a specific effect of miR-34a. MCF7vector cells were seeded into six-well plates. After 24 h, cells were transfected with the different plasmids using FuGENE HD Transfection Reagent (Promega, Milan, Italy). Forty-eight hours after the transfection, cells were harvested and miRNAs or proteins were extracted for quantification assays, as described in the previous sections.

miRNA inhibition. To inhibit miR-34a, MCF7vector cell lines were seeded into six-well plates. When cells reached 30–40% of confluence, miRCURY LNA miR-34a Inhibitor (Exiqon) was transfected using INTERFERin transfection reagent (Polyplus). After optimization experiments, we used 50 nM of miR-34a inhibitor final concentration for the transfection. As a negative control, we transfected cells with miRCURY LNA microRNA Inhibitor Negative Control A at the same final concentration. Thirty-two hours after the transfection, cells were treated with Doxo and Nutlin. Effects were assessed 16 h after the treatments, that is, 48 h after transfection.

Conflict of Interest

The authors declare no conflict of interest.

Acknowledgements. We thank Dr. Valentina Adami (HTS facility at CIBIO) for technical assistance with the microarray experiments and Dr. Isabella Pesce with the FACS experiments (Cell Analysis and Separation facility at CIBIO). We thank Drs Matthew Galbraith, Mattia Lion, Daniel Menendez, Michael A Resnick and Maria del Huerto Flammia for critical evaluation of the paper content and style. We are grateful to Drs Erik Dassi and Alessandro Quattrone for access to AURA 2. This work was partially supported by the Italian Association for Cancer Research, AIRC, (IG# 12869) and by CIBIO start-up funds.

Author contributions

SZ carried out the experiments, analyzed the microarray data and cowrote the manuscript. TT contributed to microarray data analysis. CP participated in validation experiments and draft correction. YC participated in the coordination of the study. AB conceived the study, and participated in its design. AI conceived the study, participated in its coordination and cowrote the manuscript. All authors read and approved the final manuscript.

1. Levine aJ, Hu W, Feng Z. The P53 pathway: what questions remain to be explored? *Cell Death Differ* 2006; **13**: 1027–1036.
2. Lion M, Bisio A, Tebaldi T, De Sanctis V, Menendez D, Resnick MA *et al.* Interaction between p53 and estradiol pathways in transcriptional responses to chemotherapeutics. *Cell Cycle* 2013; **12**: 1211–1224.
3. Sonenberg N, Hinnebusch AG. Regulation of translation initiation in eukaryotes: mechanisms and biological targets. *Cell* 2009; **136**: 731–745.
4. Hinnebusch AG, Lorsch JR. The mechanism of eukaryotic translation initiation: new insights and challenges. *Cold Spring Harb Perspect Biol* 2012; **4**: a011544.
5. Dever TE, Green R. The elongation, termination, and recycling phases of translation in eukaryotes. *Cold Spring Harb Perspect Biol* 2012; **4**: a013706.
6. Glisovic T, Bachorik JL, Yong J, Dreyfuss G. RNA-binding proteins and post-transcriptional gene regulation. *FEBS Lett* 2008; **582**: 1977–1986.
7. He L, Hannon GJ. MicroRNAs: small RNAs with a big role in gene regulation. *Nat Rev Genet* 2004; **5**: 522–531.
8. Provenzani A, Fronza R, Loreni F, Pascale A, Amadio M, Quattrone A. Global alterations in mRNA polysomal recruitment in a cell model of colorectal cancer progression to metastasis. *Carcinogenesis* 2006; **27**: 1323–1333.
9. Tebaldi T, Re A, Viero G, Pegoretti I, Passerini A, Blanzieri E *et al.* Widespread uncoupling between transcriptome and translatome variations after a stimulus in mammalian cells. *BMC Genomics* 2012; **13**: 220.
10. Le MTN, Teh C, Shyh-Chang N, Xie H, Zhou B, Korzh V *et al.* MicroRNA-125b is a novel negative regulator of p53. *Genes Dev* 2009 862–876.

11. Chen J, Kastan MB. 5′-3′-UTR interactions regulate p53 mRNA translation and provide a target for modulating p53 induction after DNA damage. *Genes Dev* 2010; **24**: 2146–2156.
12. Freeman Ja, Espinosa JM. The impact of post-transcriptional regulation in the p53 network. *Brief Funct Genomics* 2013; **12**: 46–57.
13. Scoumanne A, Cho SJ, Zhang J, Chen X. The cyclin-dependent kinase inhibitor p21 is regulated by RNA-binding protein PCBP4 via mRNA stability. *Nucleic Acids Res* 2011; **39**: 213–224.
14. Wang W, Furneaux H, Cheng H, Caldwell MC, Hutter D, Liu Y *et al.* HuR regulates p21 mRNA stabilization by UV light. *Mol Cell Biol* 2000; **20**: 760–769.
15. Ghosh M, Aguila HL, Michaud J, Ai Y, Wu MT, Hemmes A *et al.* Essential role of the RNA-binding protein HuR in progenitor cell survival in mice. *J Clin Invest* 2009; **119**: 3530–3543.
16. Suzuki HI, Yamagata K, Sugimoto K, Iwamoto T, Kato S, Miyazono K. Modulation of microRNA processing by p53. *Nature* 2009; **460**: 529–533.
17. Zhang J, Cho SJ, Chen X. RNPC1, an RNA-binding protein and a target of the p53 family, regulates p63 expression through mRNA stability. *Proc Natl Acad Sci USA* 2010; **107**: 1–6. www.pnas.org/cgi/doi/10.1073/pnas.0912594107.
18. Rahman-roblick R, Roblick UJ, Hellman U, Conrotto P, Liu T, Becker S *et al.* p53 targets identified by protein expression profiling. *Proc Natl Acad Sci USA* 2007; **104**: 5401–5406.
19. Arava Y. Isolation of polysomal RNA for microarray analysis. *Methods Mol Biol* 2003; **224**: 79–87.
20. Brummelkamp TR, Bernards R, Agami R. A system for stable expression of short interfering RNAs in mammalian cells. *Science* 2002; **296**: 550–553.
21. Melamed D, Eliyahu E, Arava Y, Bähler J. Exploring translation regulation by global analysis of ribosomal association. *Methods* 2009; **48**: 301–305.
22. Ek P, Pettersson G, Ek B, Gong F, Li JP, Zetterqvist O. Identification and characterization of a mammalian 14-kDa phosphohistidine phosphatase. *Eur J Biochem* 2002; **269**: 5016–5023.
23. Peterson D, Lee J, Lei XC, Forrest WF, Davis DP, Jackson PK *et al.* A chemosensitization screen identifies TP53RK, a kinase that restrains apoptosis after mitotic stress. *Cancer Res* 2010; **70**: 6325–6335.
24. Riley T, Sontag E, Chen P, Levine A. Transcriptional control of human p53-regulated genes. *Nat Rev Mol Cell Biol* 2008; **9**: 402–412.
25. Andrysik Z, Kim J, Tan AC, Espinosa JM. A genetic screen identifies TCF3/E2A and TRIAP1 as pathway-specific regulators of the cellular response to p53 activation. *Cell Rep* 2013; **3**: 1346–1354.
26. Sax JK, El-Deiry WS. Identification and characterization of the cytoplasmic protein TRAF4 as a p53-regulated proapoptotic gene. *J Biol Chem* 2003; **278**: 36435–36444.
27. Salvador JM, Brown-Clay JD, Fornace AJ. Gadd45 in stress signaling, cell cycle control, and apoptosis. *Adv Exp Med Biol* 2013; **793**: 1–19.
28. Nikulenkov F, Spinnler C, Li H, Tonelli C, Shi Y, Turunen M *et al.* Insights into p53 transcriptional function via genome-wide chromatin occupancy and gene expression analysis. *Cell Death Differ* 2012; **19**: 1992–2002.
29. Xu K, Chen Z, Qin C, Song X. miR-7 inhibits colorectal cancer cell proliferation and induces apoptosis by targeting XRCC2. *Onco Targets Ther* 2014; **7**: 325–332.
30. Fregoso OI, Das S, Akerman M, Krainer AR. Splicing-factor oncoprotein SRSF1 stabilizes p53 via RPL5 and induces cellular senescence. *Mol Cell* 2013; **50**: 56–66.
31. Tian B, Liu J, Liu B, Dong Y, Liu J, Song Y *et al.* p53 suppresses lung resistance-related protein expression through Y-box binding protein 1 in the MCF-7 breast tumor cell line. *J Cell Physiol* 2011; **226**: 3433–3441.
32. Thoreen CC, Chantranupong L, Keys HR, Wang T, Gray NS, Sabatini DM. A unifying model for mTORC1-mediated regulation of mRNA translation. *Nature* 2012; **485**: 109–113.
33. Feng Z. p53 regulation of the IGF-1/AKT/mTOR pathways and the endosomal compartment. *Cold Spring Harb Perspect Biol* 2010; **2**: a001057.
34. Zhu X, Li Y, Shen H, Li H, Long L, Hui L *et al.* miR-137 restoration sensitizes multidrug-resistant MCF-7/ADM cells to anticancer agents by targeting YB-1. *Acta Biochim Biophys Sin (Shanghai)* 2013; **45**: 80–86.
35. Helwak A, Kudla G, Dudnakova T, Tollervey D. Mapping the human miRNA interactome by CLASH reveals frequent noncanonical binding. *Cell* 2013; **153**: 654–665.
36. Das S, Anczuków O, Akerman M, Krainer AR. Oncogenic splicing factor SRSF1 is a critical transcriptional target of MYC. *Cell Rep* 2012; **1**: 110–117.
37. Lasham A, Samuel W, Cao H, Patel R, Mehta R, Stern JL *et al.* YB-1, the E2F pathway, and regulation of tumor cell growth. *J Natl Cancer Inst* 2012; **104**: 133–146.
38. Muñoz Ú, Puche JE, Hannivoort R, Lang UE, Cohen-Naftaly M, Friedman SL. Hepatocyte growth factor enhances alternative splicing of the Kruppel-like factor 6 (KLF6) tumor suppressor to promote growth through SRSF1. *Mol Cancer Res* 2012; **10**: 1216–1227.
39. Weidensdorfer D, Stöhr N, Baude A, Lederer M, Köhn M, Schierhorn A *et al.* Control of c-myc mRNA stability by IGF2BP1-associated cytoplasmic RNPs. *RNA* 2009; **15**: 104–115.
40. Bugaut A, Balasubramanian S. 5′-UTR RNA G-quadruplexes: translation regulation and targeting. *Nucleic Acids Res* 2012; **40**: 4727–4741.
41. Pichon X, Wilson LA, Stoneley M, Bastide A, King HA, Somers J *et al.* RNA binding protein/RNA element interactions and the control of translation. *Curr Protein Pept Sci* 2012; **13**: 294–304.
42. Dassi E, Re A, Leo S, Tebaldi T, Pasini L, Peroni D *et al.* AURA 2: empowering discovery of post-transcriptional networks. *Translation* 2014; **2**: e27738.
43. Menendez D, Nguyen TA, Freudenberg JM, Mathew VJ, Anderson CW, Jothi R *et al.* Diverse stresses dramatically alter genome-wide p53 binding and transactivation landscape in human cancer cells. *Nucleic Acids Res* 2013; **41**: 7286–7301.
44. Nicholson J, Neelagandan K, Huart AS, Ball K, Molloy MP, Hupp T. An iTRAQ proteomics screen reveals the effects of the MDM2 binding ligand nutlin-3 on cellular proteostasis. *J Proteome Res* 2012; **11**: 5464–5478.
45. Mazan-Mamczarz K, Hagner PR, Dai B, Wood WH, Zhang Y, Becker KG *et al.* Identification of transformation-related pathways in a breast epithelial cell model using a ribonomics approach. *Cancer Res* 2008; **68**: 7730–7735.
46. Fernández-Miranda G, Méndez R. The CPEB-family of proteins, translational control in senescence and cancer. *Ageing Res Rev* 2012; **11**: 460–472.
47. Novoa I, Gallego J, Ferreira PG, Mendez R. Mitotic cell-cycle progression is regulated by CPEB1 and CPEB4-dependent translational control. *Nat Cell Biol* 2010; **12**: 447–456.
48. Fuller-Pace FV, Nicol SM. DEAD-box RNA helicases as transcription cofactors. *Methods Enzymol* 2012; **511**: 347–367.
49. Das S, Fregoso OI, Krainer AR. A new path to oncogene-induced senescence: at the crossroads of splicing and translation. *Cell Cycle* 2013; **12**: 1477–1479.
50. Leão M, Gomes S, Soares J, Bessa C, Maciel C, Ciribilli Y *et al.* Novel simplified yeast-based assays of regulators of p53-MDMX interaction and p53 transcriptional activity. *FEBS J* 2013; **280**: 6498–6507.
51. Marcel V, Ghayad SE, Belin S, Therizols G, Morel AP, Solano-Gonzàlez E *et al.* p53 acts as a safeguard of translational control by regulating fibrillarin and rRNA methylation in cancer. *Cancer Cell* 2013; **24**: 318–330.
52. Loayza-Puch F, Drost J, Rooijers K, Lopes R, Elkon R, Agami R. p53 induces transcriptional and translational programs to suppress cell proliferation and growth. *Genome Biol* 2013; **14**: R32.
53. Bisio A, Nasti S, Jordan JJ, Gargiulo S, Pastorino L, Provenzani A *et al.* Functional analysis of CDKN2A/p16INK4a 5′-UTR variants predisposing to melanoma. *Hum Mol Genet* 2010; **19**: 1479–1491.
54. Tebaldi T, Dessi E, Kostoska G, Viero G, Quattrone A. tRanslatome: an R/Bioconductor package to portrait translational control. *Bioinformatics* 2014; **30**: 289–291.
55. Huang DW, Sherman BT, Lempicki RA. Systematic and integrative analysis of large gene lists using DAVID bioinformatics resources. *Nat Protoc* 2009; **4**: 44–57.
56. Castello A, Fischer B, Eichelbaum K, Horos R, Beckmann BM, Strein C *et al.* Insights into RNA biology from an Atlas of mammalian mRNA-binding proteins. *Cell* 2012; **149**: 1393–1406.
57. Baltz AG, Munschauer M, Schwanhäusser B, Vasile A, Murakawa Y, Schueler M *et al.* The mRNA-bound proteome and its global occupancy profile on protein-coding transcripts. *Mol Cell* 2012; **46**: 674–690.
58. Bustin SA, Benes V, Garson JA, Hellemans J, Huggett J, Kubista M *et al.* The MIQE guidelines: minimum information for publication of quantitative real-time PCR experiments. *Clin Chem* 2009; **55**: 611–622.
59. Thoreen CC, Kang SA, Chang JW, Liu Q, Zhang J, Gao Y *et al.* An ATP-competitive mammalian target of rapamycin inhibitor reveals rapamycin-resistant functions of mTORC1. *J Biol Chem* 2009; **284**: 8023–8032.
60. Denti MA, Rosa A, Sthandier O, De Angelis FG, Bozzoni I. A new vector, based on the PolII promoter of the U1 snRNA gene, for the expression of siRNAs in mammalian cells. *Mol Ther* 2004; **10**: 191–199.
61. Ciribilli Y, Monti P, Bisio A, Nguyen HT, Ethayathulla AS, Ramos A *et al.* Transactivation specificity is conserved among p53 family proteins and depends on a response element sequence code. *Nucleic Acids Res* 2013; **41**: 8637–8653.

Supplementary Information accompanies this paper on Cell Death and Differentiation website (http://www.nature.com/cdd)

Cooperative interactions between p53 and NFκB enhance cell plasticity

Alessandra Bisio[1], Judit Zámborszky[1,3], Sara Zaccara[1], Mattia Lion[1,4], Toma Tebaldi[2], Vasundhara Sharma[1], Ivan Raimondi[1], Federica Alessandrini[1], Yari Ciribilli[1], Alberto Inga[1]

[1]Laboratory of Transcriptional Networks, Centre for Integrative Biology, CIBIO, University of Trento, Trento, 38123, Italy

[2]Laboratory of Translational Genomics, Centre for Integrative Biology, CIBIO, University of Trento, Trento, 38123, Italy

[3]Institute of Enzymology, Research Centre for Natural Sciences, Budapest, Hungary

[4]Department of Genetics, Massachusetts General Hospital, Boston, MA, USA

correspondence to:
Yari Ciribilli, **e-mail:** ciribilli@science.unitn.it
Alberto Inga, **e-mail:** inga@science.unitn.it

Keywords: p53, NFkB, chemotherapy, doxorubicin, TNFα, EMT, synergy, breast cancer

Received: June 25, 2014 ***Accepted:*** October 01, 2014 ***Published:*** October 21, 2014

ABSTRACT

The p53 and NFκB sequence-specific transcription factors play crucial roles in cell proliferation and survival with critical, even if typically opposite, effects on cancer progression. To investigate a possible crosstalk between p53 and NFκB driven by chemotherapy-induced responses in the context of an inflammatory microenvironment, we performed a proof of concept study using MCF7 cells. Transcriptome analyses upon single or combined treatments with doxorubicin (Doxo, 1.5μM) and the NFκB inducer TNF-alpha (TNFα, 5ng/ml) revealed 432 up-regulated (log_2 FC> 2), and 390 repressed genes (log_2 FC< -2) for the Doxo+TNFα treatment. 239 up-regulated and 161 repressed genes were synergistically regulated by the double treatment. Annotation and pathway analyses of Doxo+TNFα selectively up-regulated genes indicated strong enrichment for cell migration terms. A panel of genes was examined by qPCR coupled to p53 activation by Doxo, 5-Fluoruracil and Nutlin-3a, or to p53 or NFκB inhibition. Transcriptome data were confirmed for 12 of 15 selected genes and seven (PLK3, LAMP3, ETV7, UNC5B, NTN1, DUSP5, SNAI1) were synergistically up-regulated after Doxo+TNFα and dependent both on p53 and NFκB. Migration assays consistently showed an increase in motility for MCF7 cells upon Doxo+TNFα. A signature of 29 Doxo+TNFα highly synergistic genes exhibited prognostic value for luminal breast cancer patients, with adverse outcome correlating with higher relative expression. We propose that the crosstalk between p53 and NFκB can lead to the activation of specific gene expression programs that may impact on cancer phenotypes and potentially modify the efficacy of cancer therapy.

INTRODUCTION

Cancer cells are continuously exposed to a number of signaling cues that reflect the distinct nature of the microenvironment at primary tumor site, metastastic lesions and potentially also during circulation in the blood stream [1–4]. Therapeutic intervention strategies can result in acute changes in microenvironment signaling, acting also through non-transformed cellular components resident at the primary tumor site [3, 5]. Cellular responses to changes in the microenvironment requires coordinated activation of sequence-specific transcription factors [6], among which NFκB and p53 have a prominent role and often opposing functions [7].

The p53 tumor suppressor gene is activated in response to a large number of cellular stress signals, including genotoxic stress, carbon and oxygen deficiencies, excessive proliferation signals [8, 9]. There are >150 established p53 target genes that link p53 to many different biological outcomes [10–14].

The NFκB family of sequence-specific transcription factors consists of essential regulators of immune, inflammatory, proliferative and apoptotic responses [15], and their activation generally results in the onset of pro-survival signals [16]. The most common form of the NFκB complexes is the p50/RELA (p65) heterodimer. p53 and NFκB activation occurs simultaneously in response to diverse stress conditions, including genotoxic stress and NFκB proteins are frequently de-regulated in cancer, resulting in constitutive activation [17]. Competition between p53 and NFκB for a common limiting cofactor such as p300 can result in mutual inhibition [17, 18]. However, examples of positive interactions have also been reported. For example, it was shown that p65 can induce the p53 target gene p21 by direct binding to its promoter [19] and participates in p53-dependent apoptosis [20]. Several human Toll-like receptors (TLRs), whose signaling leads to NFκB activation [21], were identified as direct p53 target genes both in cancer cells and primary cells [22] and it was demonstrated that p53 and NFκB can cooperate in the activation of pro-inflammatory genes in primary human monocytes and macrophages [23].

To investigate more globally the transcriptional crosstalk between p53 and NFκB we performed a proof of concept study using breast cancer-derived MCF7 cells treated with Doxorubicin, Tumor Necrosis Factor alpha (TNFα) and a combination of the two compounds (Doxo+TNFα). Our results demonstrated a synergistic interaction between p53 and NFκB transcription factors, which can lead to the reprogramming of cell fate and enhanced migratory potential. Seven genes (PLK3, LAMP3, ETV7, UNC5B, NTN1, DUSP5, SNAI1) were established as synergistically up-regulated after Doxo+TNFα and dependent both on p53 and NFκB. A 29-gene signature of highly synergistic genes up-regulated by Doxo+TNFα appeared to have prognostic value in a cohort of luminal breast cancer patients [24].

RESULTS

Striking transcriptome changes upon the combination of Doxorubicin and TNFα treatment of MCF7 cells

We first investigated the potential crosstalk between Doxorubicin (Doxo) and TNFα treatment using gene reporter assays in the human breast adenocarcinoma-derived MCF7 cells (Figure S1A). p53-dependent responsiveness of the P21 and MDM2 promoter plasmid constructs was observed following Doxo treatment and confirmed by p53 silencing. The transactivation of the P21 and MDM2 constructs was reduced upon addition of TNFα to Doxo, suggesting possible inhibition of p53 activity by NFκB. Mutual inhibition of the p53 and p65/RELA proteins has been previously shown on p21 [17], while both inhibition and cooperation were reported at the BAX gene [18, 20]. However, this effect was not observed at the level of the endogenous P21 and MDM2 genes (Figure S1B), which showed similar level of activation in response to either Doxo alone or Doxo+TNFα. An NFκB reporter construct was responsive to both Doxo and TNFα as single treatments and showed a strong increase following the double treatment that was unaffected by p53 silencing. On the contrary, the endogenous TNFα and MCP1 NFκB target genes were weakly responsive to Doxo alone, highly induced by TNFα treatment, and showed intermediate induction levels upon double treatment. Hence, canonical p53 or NFκB target genes did not exhibit synergistic transcriptional responses to the combined treatment with doxorubicin and TNFα.

Next we performed a genome-wide transcriptome analysis after Doxo, TNFα, or the combination of the two compounds using the Agilent 4 × 44k array and single color labeling. Differentially expressed genes (DEGs) were selected based on rank product test, setting a threshold of 0.05 on the percentage of false positives (pfp) and a threshold of 2 on the absolute log2 fold changes. The double treatment more than doubled the number of DEGs (Figure 1). The vast majority of DEGs resulting from the single treatments were also differentially expressed in the double treatment. Gene Ontology (GO) as well as pathway and upstream regulators analyses (DAVID, http://david.abcc.ncifcrf.gov/; IPA, http://www.ingenuity.com/) confirmed activation of p53 signaling upon Doxo treatment as most significant pathway, and apoptosis induction as the most significantly enriched GO terms among up-regulated DEGs (Figure 1A-C). TNFα treatment also resulted in gene annotation terms consistent with NFκB activation, such as regulation of T cell activation. The gene annotation of DEGs resulting from the double treatment was enriched for terms typical of the two single treatments (*e.g.* T cell activation and apoptosis regulation among the up-regulated DEGs). TP53 as an upstream regulator was less significant in the double treatment compared to the Doxo single treatment, while p65/RELA, NFKBIA, IRF7 and STAT1 appeared to be even more enriched in the double treatment compared to TNFα single treatment (Figure 1B). The double treatment not only led to a higher number of DEGs, but resulted in quantitative differences in gene expression levels compared to the single treatments. We applied a rigorous filter and identified 212 repressed, 361 induced DEGs that were synergistically regulated by the double treatment Doxo+TNFα (see Methods) (Figure 1D). Notably, this subgroup of up-regulated DEGs was enriched for cell migration GO biological process along with the expected canonical terms for p53 and NFκB. Collectively, our systematic analysis indicates a vast network of genes that can be mutually affected by combined activation of p53- and NFκB-dependent responses.

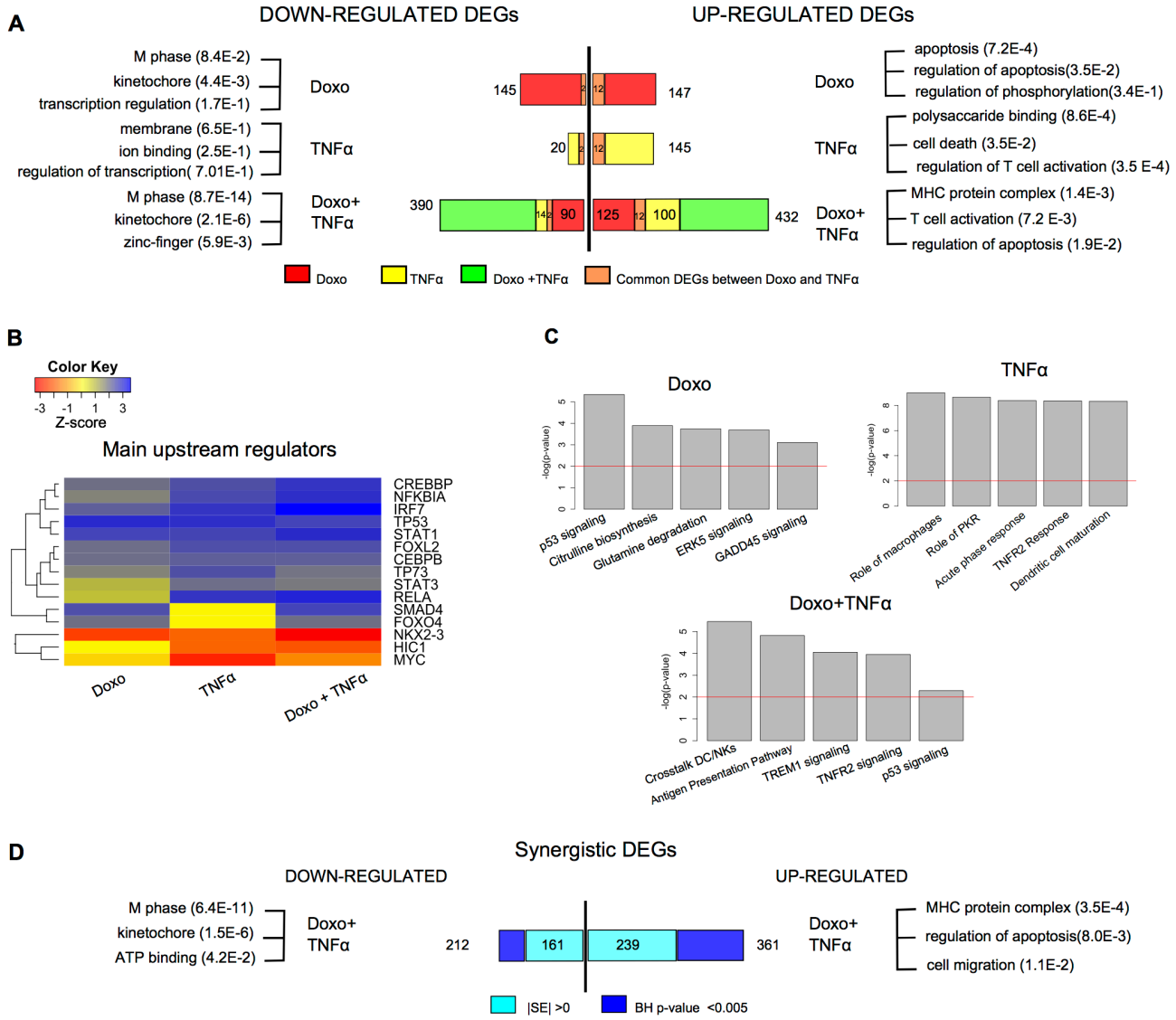

Figure 1: A vast array of genes responds selectively to Doxorubicin and TNFα in MCF7 cells. **(A)** Number of DEGs identified after single or combined treatment (see Methods for statistical filters). Most significant gene ontology terms of down- or up-regulated DEGs, according to DAVID (http://david.abcc.ncifcrf.gov). **(B)** Predicted upstream regulators of the DEGs for the indicated treatments, according to IPA (IPA, http://www.ingenuity.com). The color code reflects the enrichment or depletion of the listed transcription factors targeting the DEGs from the array analysis. **(C)** Statistically relevant pathways predicted to be modulated in response to the indicated treatments according to IPA. **(D)** Number of DEGs that are synergistically regulated by the double treatment according to two different statistical filters (see Materials and Methods). The most significant gene ontology terms are also indicated.

Doxorubicin + TNFα transcriptional synergy identifies new direct p53 and NFκB target genes

We selected fifteen genes for validation experiments based on (a) statistical analysis of synergistic up-regulated DEGs, (b) prior knowledge on direct regulation by either p53 or NFκB, (c) availability of ChIP-seq data for both transcription factors, and (d) gene functions in relation to cancer biology. The selected list contains genes encoding players of the control of various cellular processes, *e.g.* cell proliferation (PLK3, DUSP5, PLAU, GBX2, ETV7, EDN2), apoptosis (TNFRSF10B, UNC5B), inflammation (LAMP3, EGR2), development (GBX2, SOX9, NPPC, FOXC1) and cell migration (SNAI1, PLAU, UNC5B, NTN1, EDN2).

For twelve of the 15 genes we confirmed a synergistic response to the Doxo+TNFα treatment by qPCR (Figure 2A). Most of them were independently reported as putative targets of either p53, p65 or both according to published ChIP-seq data (for p65, http://genome.ucsc.edu/ENCODE) [14, 25]. A potential direct contribution of NFκB on the observed gene expression

changes was evaluates using the small molecule inhibitor BAY 11–7082 (BAY) used as single agent or in combination with Doxo or/and TNFα (Figure 2B). Eight of the twelve validated synergistic DEGs were tested and for five of them BAY markedly inhibited the effect of Doxo+TNFα, or of TNFα alone. TNFα treatment led to higher levels of nuclear p65, while Doxo alone or in the combined treatment did not significantly impact p65 nuclear protein levels. BAY treatment led to a slight reduction of p65 nuclear levels, which was paralleled by an increase in the cytoplasm (Figure 2C). p53 protein levels were induced to similar levels by the different treatment combinations (Figure S2).

The five genes that showed more convincing p65 dependence on the synergistic response to Doxo+TNFα (PLK3, NTN1, UNC5B, ETV7, LAMP3) were investigated more deeply to establish a direct role of wild type p53 in their transcription. MCF7 cells were treated with the chemotherapeutic agent 5-Fluorouracil (5FU) or with the MDM2 inhibitor Nutlin-3a, alone or in combination with TNFα. Both p53-inducing molecules were at least additive with TNFα in the responsiveness of the five genes (Figure 2D). Although the magnitude of the synergistic response was higher with Doxo, the fact that three different p53-activating treatments led to up-regulation of these five genes strongly suggested a direct role of p53. We next employed an MCF7 clone with stable knock-down of p53 and the HCT116 $p53^{-/-}$ cell line, to further establish p53-dependence of the five genes expression upon Doxo treatment. Matched MCF7 vector and HCT116 $p53^{+/+}$ were used as a comparison (Figure 2E, F). Invariably, Doxo responsiveness was strongly reduced in the p53-defective cells. Previous reports in the literature demonstrated or suggested p53-dependent regulation of PLK3, NTN1 and UNC5B. Our results confirm those findings and establish, for the first time, the possibility of synergistic regulation by NFκB. PLK3, a polo-like kinase, is an important regulator of the cell cycle and it is involved in the control of hypoxia signaling pathway [26]. NTN1 is ligand for both DCC1 and UNC5B receptors whose signaling can potentially modulate p53 activity, impacting on the decision between cell survival and cell death [27]. LAMP3 is a lysosomal membrane associated protein important in dendritic cells and potentially involved in tumor invasion [28], while ETV7 is a transcription factor associated to cell proliferation and tumorigenesis [29].

Given the lack of definitive evidence for LAMP3 and ETV7 being direct p53 targets and since our finding of synergistic responsiveness, we examined p53 and

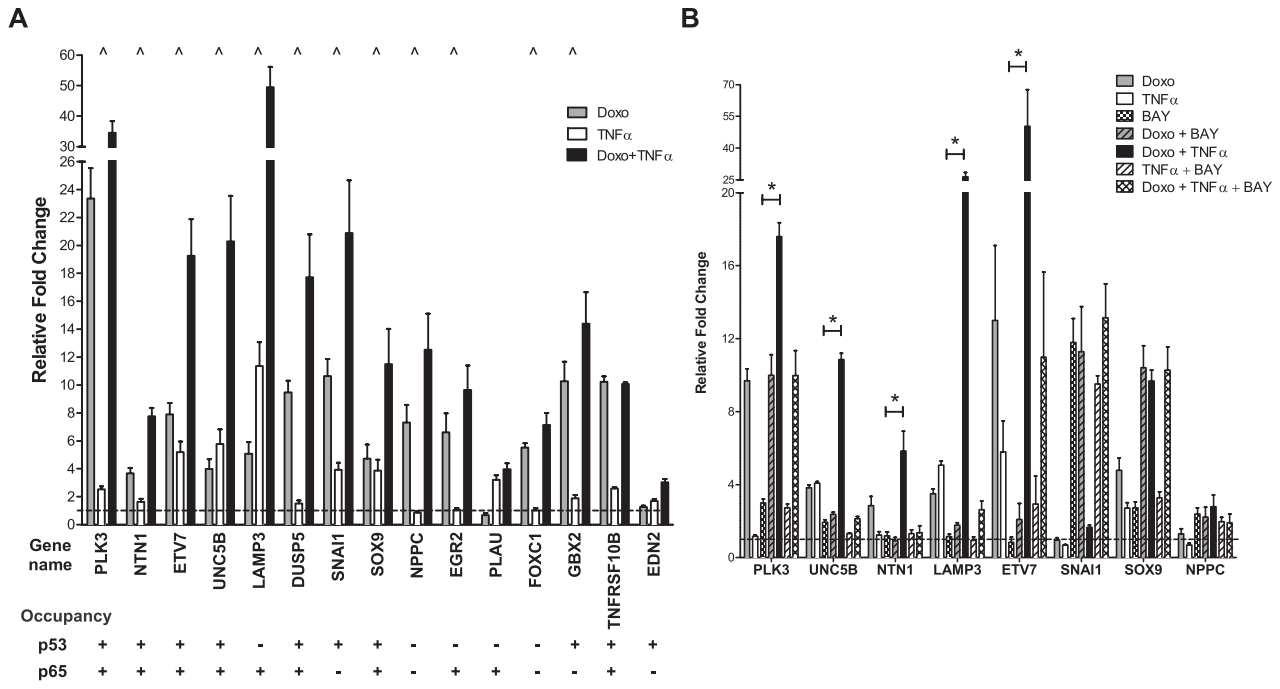

Figure 2: p53- and p65-dependent up-regulation of selected synergistic DEGs. (A) Twelve out of fifteen selected synergistic DEGs were validated by qPCR. Plotted are the average fold change relative to the mock condition and three reference genes (GAPDH, B2M, ACTB) and the standard deviations of three biological replicates. "^" marks genes responding in synergistic manner to the double treatment. p53 and p65 occupancy data from available ChIP-seq datasets are summarized below each gene name. **(B)** Impact of the NFκB inhibitor BAY 11-7082 on the synergistic gene expression response plotted as in panel A. "*" Significant inhibition of by BAY when combined to Doxo + TNFα (t-test, $p<0.01$). NPPC and SNAI1 were also tested but their expression levels were not affected by BAY treatment.

(*Continued*)

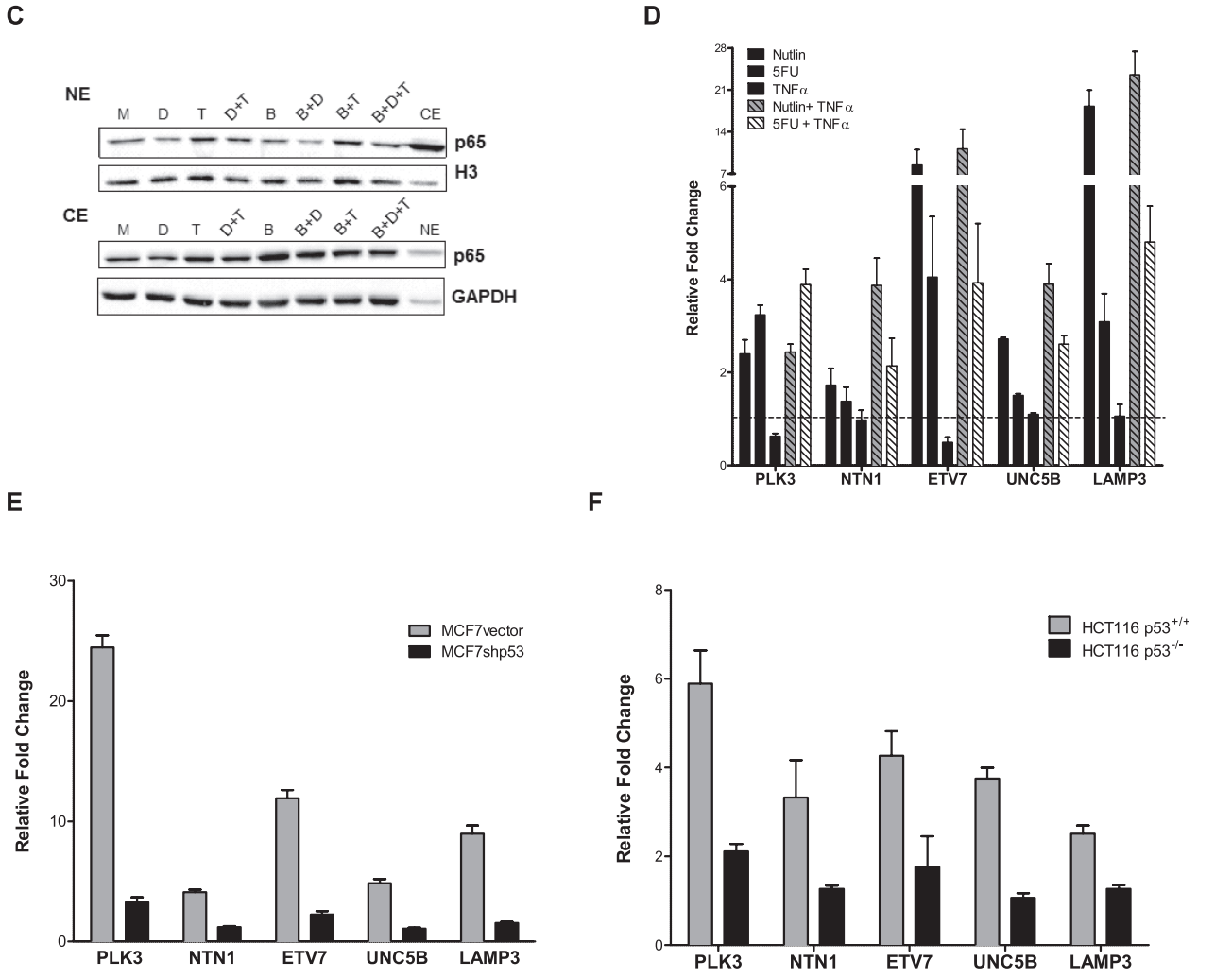

Figure 2: (C) p65 nuclear (NE) and cytoplasmic (CE) relative protein levels under the different treatments used in panel B. M = mock; D = Doxo; T = TNFα; B = BAY. Proteins were fractionated as described in Materials and Methods. GAPDH and histone 3 (H3) served as controls for cytoplasmic and nuclear fraction respectively. As controls, a cytoplasmic mock fraction sample (CE) is loaded together with the nuclear proteins and vice versa a nuclear mock sample (NE) in included in the cytoplasmic blot. **(D)** 5-fluorouracil and Nutlin-3a induced expression of 5 selected DEGs alone or in combination with TNFα. Results were obtained and are plotted as in A. **(E), (F)** The relative expression of the 5 selected genes shown in panel C was tested in doxorubicin treated matched cell lines differing for p53 status (MCF7 vector and shp53, D; HCT116 $p53^{+/+}$ and $p53^{-/-}$, E).

p65 occupancy in MCF7 cells treated with Doxo or TNFα (Figure 3). p53 occupancy was detected both for ETV7 and LAMP3 as well as for the positive control P21, in Doxo treated cells. For ETV7 p53 occupancy appeared to increase also after TNFα treatment. P21 was the only target for which p53 appeared to be bound also in the mock condition, a result consistent with previous data [30]. p53 occupancy levels were not distinguishable between Doxo and Doxo+TNFα treatment.

Both LAMP3 and ETV7 exhibited p65 occupancy in TNFα treated cells, although to a lower extent compared to the positive control MCP1. For the three promoter regions, occupancy was increased also by Doxo treatment alone, but no additive effect of the double treatment was apparent, except for a trend with LAMP3. On the contrary lower occupancy at MCP1 was detected in double treated cells. This latter result is consistent with the MCP1 mRNA expression changes (Figure S1B).

Hence, we identified genes whose expression is co-regulated by Doxo and TNFα. The gene expression studies conducted with different p53-activating molecules, the use of cells lines with different p53 status, and the chromatin immune-precipitation studies collectively established a direct role for p53 and p65 on the transcriptional regulation of PLK3, NTN1, ETV7, UNC5B and LAMP3. However, we did not find a direct correlation between occupancy levels at predicted promoter binding sites and gene expression changes.

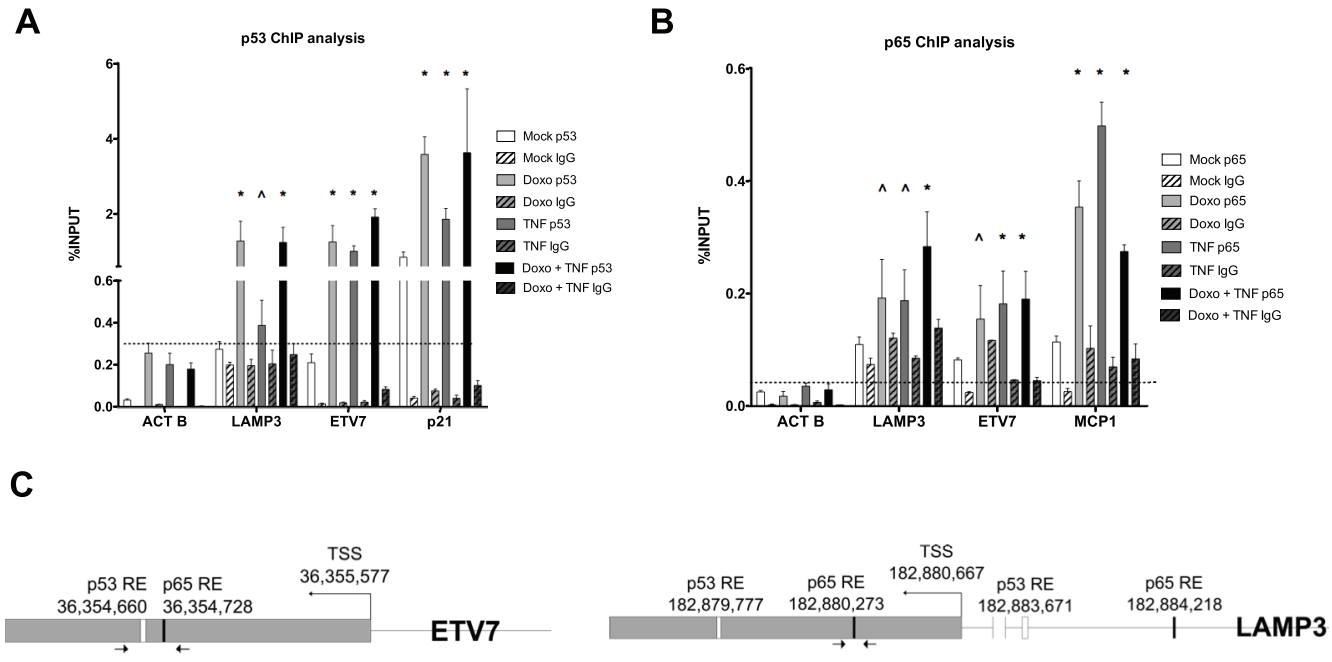

Figure 3: Occupancy analysis establishes ETV7 and LAMP3 as direct p65 and/or p53 target genes. (A) Relative quantification of immune-precipitated gene fractions by qPCR from MCF7 cells subjected to Doxo or TNFα single treatments and to the double treatment. The antibodies used for the immune-precipitations are listed. P21 was used as positive control, while ACTB was used as a negative control. Plotted are the average percentages relative to input signals. Error bars represent the standard errors of at least three biological replicates. **(B)** as in A, but probing p65 occupancy. MCP1 was used as positive control. The IgG antibody controls were anti-mouse (A) or anti-rabbit (B) to match the specific primary antibodies. **(C)** The position of the primers used for the qPCR and the location of predicted p53 and p65 binding sites in the ETV7 and LAMP3 genes are depicted.

Doxorubicin + TNFα treatment enhances the migration potential of MCF7 cells

Both the gene ontology enrichments of synergistic DEGs and the known function of the fifteen genes chosen for validation suggested the possible activation of gene expression programs influencing cell motility, epithelial mesenchymal transition (EMT) or even stem-like phenotypes. Projected to an *in vivo* context, the crosstalk of signals present in an inflammatory microenvironment could have a negative impact on the efficacy of chemotherapy, possibly by enhancing tumor cell plasticity. To begin exploring this hypothesis, we investigated migration and invasion potential of MCF7 cells treated with Doxo, TNFα or both. Three different experimental approaches consisting in real-time cell migration analysis (Figure 4A), transwell migration test (Figure 4B) and wound healing assay (Figure 4D) consistently showed higher migration potential of double-treated MCF7 cells, while the invasion phenotype was unaffected by all three types of treatment (Figure 4C).

Several studies suggest that EMT not only enhances the motility and invasiveness of cancer cells, but also provides additional aggressive features such as stemness and therapeutic resistance [31]. Indeed, several of the 15 synergistic DEGs we validated are directly or indirectly associated with acquisition of stem-like phenotypes in normal or cancer cells, particularly SNAI1 [32, 33], SOX9 [34] and GBX2 [35]. Different lines of evidence indicate that breast cancer stem cells (BCSCs) display increased cell motility, invasion, and overexpress genes that promote metastasis [36] and can be traced by $CD44^{+}/CD24^{-/low}$ surface marker expression [37]. We asked if the Doxo+TNFα treatment could enhance the stem-like subpopulation of the MCF7 cell line (Figure 4E). FACS analysis showed that the $CD44^{+}/CD24^{-}$ subpopulation virtually disappeared after all treatments. Therefore, the higher motility observed upon double treatment cannot be directly related to the expression of these surface markers, hence to putative stem-like features.

Prognostic value of Doxorubicin + TNFα synergistic DEGs

Since luminal type breast cancer, of which MCF7 is considered as a model, frequently retains wild type p53 and NFκB responsiveness, we asked if Doxo+TNFα synergistic DEGs could be endowed with prognostic significance. Up-regulated DEGs were further filtered by selecting genes that were strongly responsive to the double treatment but minimally responsive to the single ones (see Materials and Methods). A signature list of

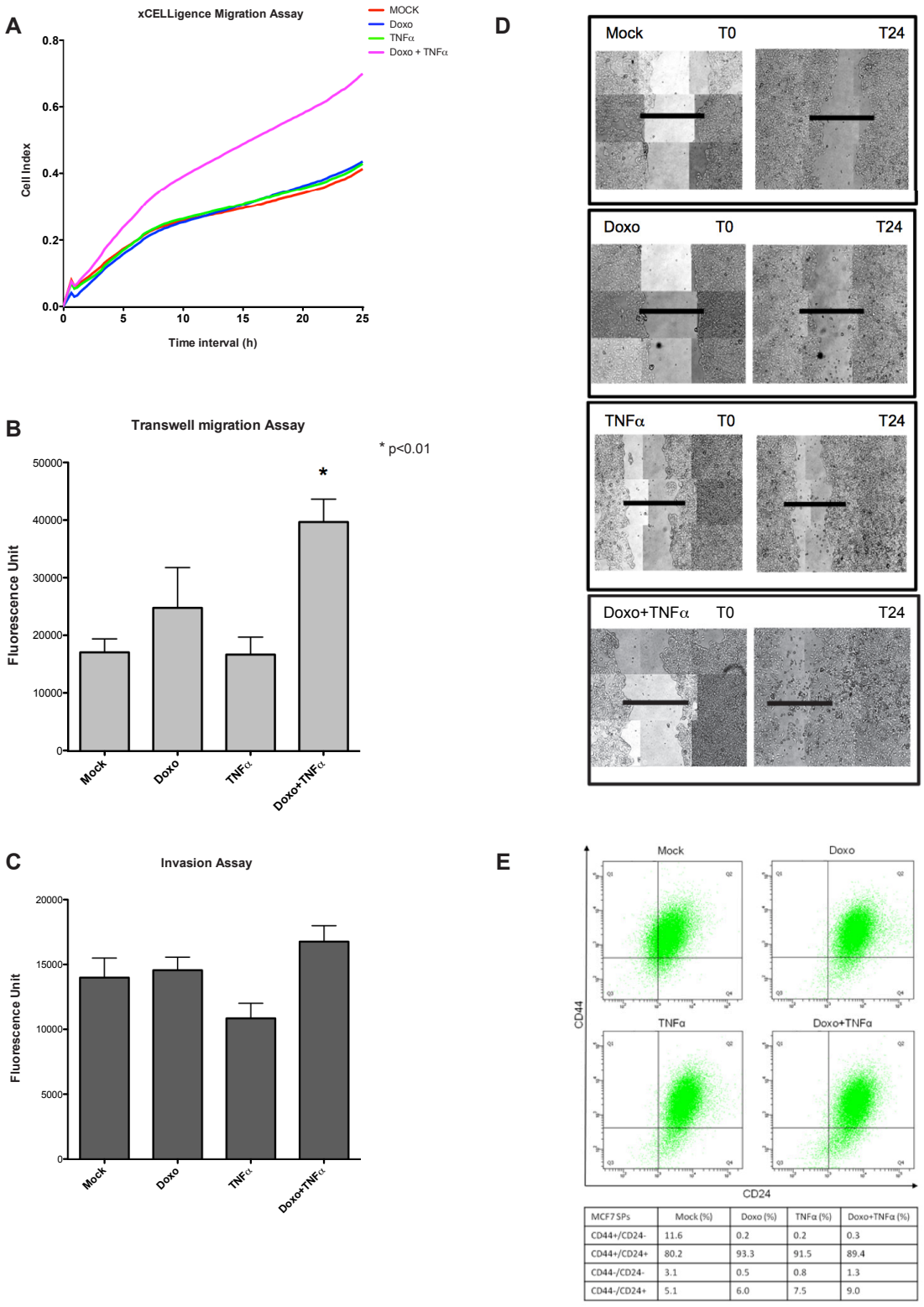

MCF7 SPs	Mock (%)	Doxo (%)	TNFα (%)	Doxo+TNFα (%)
CD44+/CD24-	11.6	0.2	0.2	0.3
CD44+/CD24+	80.2	93.3	91.5	89.4
CD44-/CD24-	3.1	0.5	0.8	1.3
CD44-/CD24+	5.1	6.0	7.5	9.0

Figure 4: Doxo+TNFα leads to enhanced MCF7 motility but ablates the stem-like side population. **(A)** Real-time migration assays examined by xCELLigence. Plotted are the average results of four biological repeats. Cell Index is proportional to the number of cells migrating through a hole in the culture plate. The treatments relative to the different curves are indicated. **(B)** Relative transwell migration values quantified by a fluorescence readout (see Materials and Methods). Average and standard deviation of triplicate biological replicates are presented. The applied treatments are listed on the x-axis. **(C)** As for B, but measuring the invasion potential of MCF7. **(D)** Images of a wound healing assay obtained at T0 or T24. Composite (3×3) images were acquired using an automated Zeiss microscope and the AxioVision3.1 software. **(E)** Cell sorting results based on intensity of CD44 and CD24 surface markers on 30000 cells. Q1 individuates the $CD44^{+}/CD24^{-(low)}$ cells, considered as stem-like. The percentages in the four quadrants after the various treatments are presented in the table.

29 genes (DT29) was generated (Figure 5A) and used to interrogate clinical data using the KM plotter tool [38]. Interestingly, breast cancer patients with luminal type A diagnosis who underwent chemotherapy and exhibited higher relative expression of DT29 genes showed poorer prognosis (Figure 5B). The same was true for luminal A patients with lymph node infiltration or luminal A grade 2 (Figure 5C, D).

Analysis of Doxorubicin and TNFα crosstalk in lung cancer-derived and HUVEC cells

We extended our analysis to another pair of cancer cell lines that differ for p53 status. A549 (p53 wild type) and H1299 (p53 null) lung cancer derived cells were treated with Doxo or/and TNFα or/and BAY. Expression of PLK3, NTN1, ETV7, UNC5B and LAMP3 was measured by qPCR (Figure 6A-E). The impact of the various treatments on p65 nuclear and cytoplasmic, p53 and p21 protein levels was also evaluated (Figure 6F, 6G). In the p53 null H1299 cells the relative expression changes of all the genes was invariably much lower compared to A549 cells. However, NTN1 was weakly TNFα inducible and ETV7 was weakly Doxo+TNFα responsive. Instead in A459 cells NTN1, ETV7 and LAMP3 were synergistically up-regulated by Doxo+TNFα, while PLK3 and UNC5B were additive. The magnitude of induction upon Doxo was often one order of magnitude higher compared to TNFα alone. Transient transfection assays with the κB luciferase reporter construct were performed using different concentrations of TNFα or BAY (Figure S3). Based on the results, 10ng/ml TNFα and/or 20μM BAY were chosen for the qPCR experiments, although the reduction of TNFα-induced reporter activity was modest, albeit significant. At the endogenous gene level in A549 cells we did not observe the inhibitory effect of BAY on either TNFα-induced changes or Doxo+TNFα, with the possible exception of UNC5B (Figure 6A-E). However, BAY treatment reduced the Doxo responsiveness of these genes, which might be dependent on its effect on the activation of NFκB by endogenous production of TNFα. In the p53 wild type A549 cells, p53 and p21 protein levels were induced by Doxo and not affected by the treatment with TNFα. Total p65 levels were unaffected by all treatments in both cell lines (Figure 6F). Nuclear p65 protein levels were increased in response to TNFα or

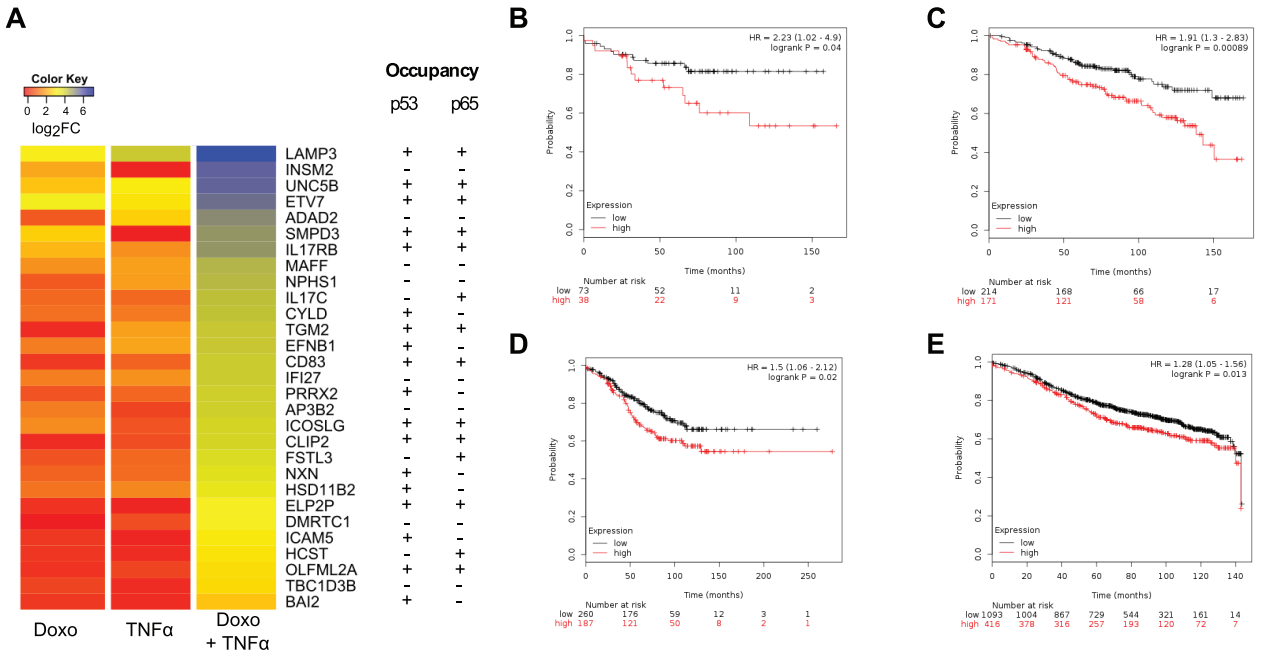

Figure 5: Prognostic significance of a 29-gene list of synergistic Doxo+TNFα DEGs. (A) Top list of 29 genes (DT-29) exhibiting minimal responsiveness to Doxo or TNFα as single agents, but strong synergy upon combined treatment. A heat map view of the gene expression results is presented (see Materials Methods for statistical filters). Occupancy of both for p65 and p53 in the vicinity of the transcription start sites of these genes has been summarized from ChIP-seq data available in the literature. **(B-E)** Kaplan-Meier plots stratifying a breast cancer patient cohort based on the relative expression of the DT-29 gene list and relapse free survival. Graphs were generated with the KM-plotter tool (ref). Patients' numbers are listed below the graph. Hazardous Ratio and the statistical analysis is reported for selected patients subgroups: **(B)** luminal A patients who underwent chemotherapy treatment (n = 111); **(C)** luminal A patients with a Grade 2 cancer at diagnosis (n = 385); **(D)** luminal A patients with lymph node infiltration at diagnosis (n = 447) and **(E)** the entire cohort of luminal A patients (n = 1509). Patients with a diagnosis of Luminal A breast cancer subtype were selected as the p53 status is not available in KM plotter, but this subgroup of breast cancer is expected to be strongly enriched for cases retaining wild type p53 protein.

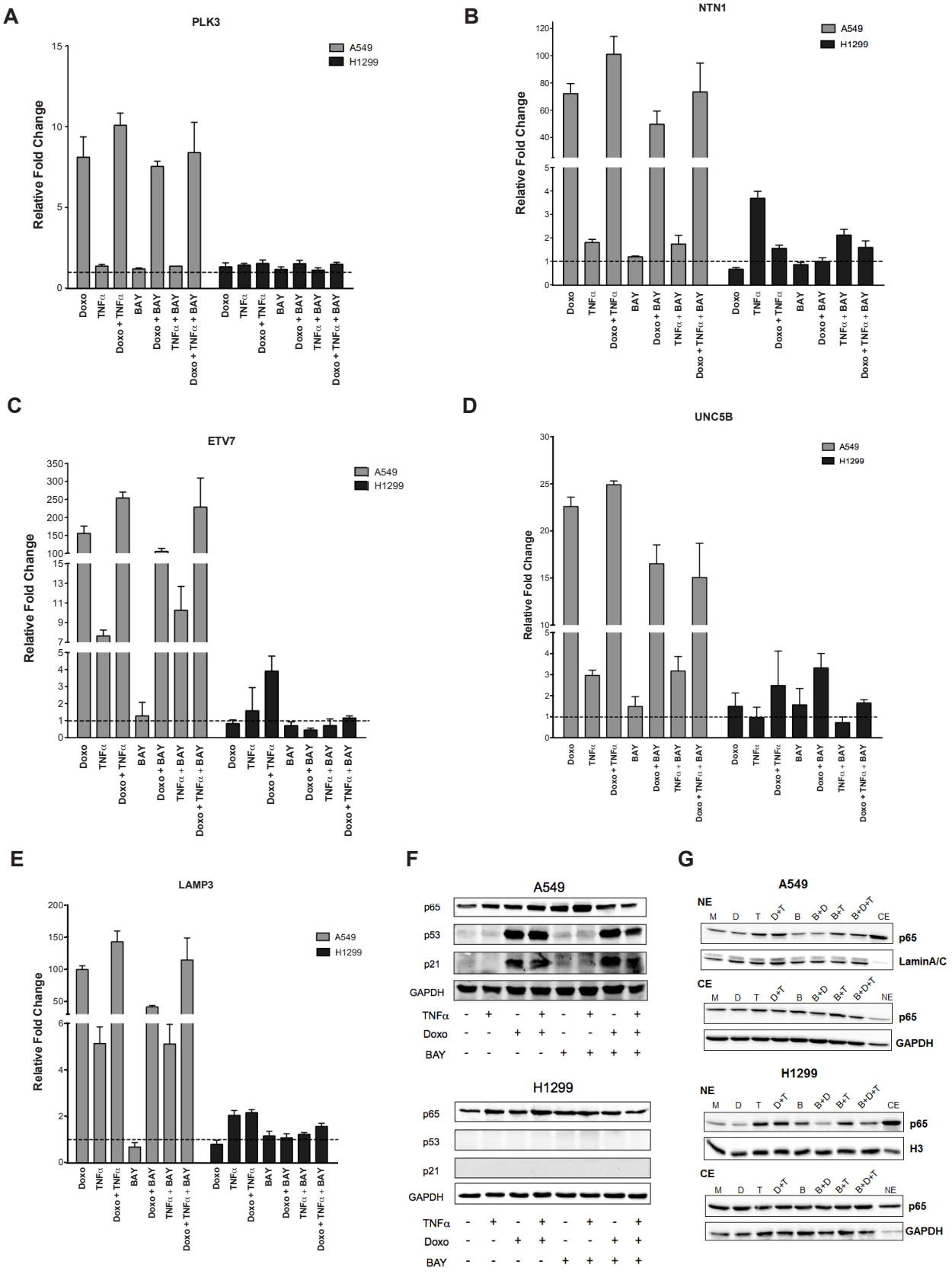

Figure 6: PLK3, NTN1, ETV7, UNC5B and LAMP3 responsiveness in lung cancer cell lines. **(A-E)** Relative fold change expression of the indicated genes and after the listed treatments in A549 (p53 wild type) and H1299 (p53 null) cells, measured by qPCR. Average and standard deviations of three biological replicates are presented. **(F)** Western blot of total p65, p53 and the p53 target p21. GAPDH was used as loading control. **(G)** Western blot of nuclear and cytoplasmic protein fractions were performed as for Figure 2C.

Doxo+TNFα in both A549 and H1299 cells (Figure 6G). Interestingly, BAY treatment alone or in combination led to a reduction in p65 nuclear accumulation (Figure 6G).

HUVEC primary cells were also subjected to Doxo and TNFα single or double treatment and the expression of the same panel of five genes was tested by qPCR (Figure S4). Results among biological repeats varied, but in the majority of tests, all genes with the exception of LAMP3 were Doxo responsive; NTN1 and ETV7 were also TNFα responsive. No synergistic up-regulation by the double treatment could be consistently established. p53 and p65 protein levels confirmed i) the activation of p53, with a similar level of p53 protein in the double treatment, and ii) the p65 proficiency of this cell line.

DISCUSSION

Wild type p53 functions are intricately related to multiple tumor suppressor pathways, primarily acting in cell autonomous manner to restrain cell proliferation and including cell death and senescence in response to genotoxic and many other types of cellular stresses [8, 9]. Furthermore, p53 also contributes to modulate the microenvironment in a non-cell autonomous manner [39]. p53 has also been linked to inhibition of EMT, for example through an indirect stimulation of E-cadherin expression [40]. At the same time, paracrine signaling in mice triggered by Doxorubicin were found to stimulate EMT and metastatic potential of cancer cells, in part through NFκB activation [3]. Many studies have highlighted the potential contribution of NFκB-induced signaling in the acquisition of cancer cell traits conducive to chemoresistance and higher metastasis risk [2] [41]. While, the canonical functions of p53 and NFκB are consistent with the co-occurrence of p53 inactivation and NFκB hyper-activation that is frequent in cancer [7], recent studies provided examples of positive cooperation between p53 and NFκB that would occur in specific cell types, such as antigen presenting cells or macrophages, and contribute to physiological responses, such as for example in the process of innate immunity and inflammation [12, 22, 23, 42].

Here we modeled the impact of a first line chemotherapeutic drug leading to genotoxic stress and p53 activation, using exposure to the immune cytokine and NFκB activator molecule TNFα as a variable, mimicking the effect of an inflammatory microenvironment. We used transcriptome analysis as primary endpoint and uncovered a vast network of differentially expressed genes that selectively responds to combined treatment with Doxorubicin and TNFα. Furthermore, genes that were synergistically up-regulated by both treatments appeared to endow cells with higher motility potential *in vitro*. Analyses of the annotated gene functions related to the aforementioned genes also revealed the possibility of an induced epithelial mesenchymal transition upon combination of the treatments. For example, SNAI1 appeared to be regulated in more than additive manner by the double treatment, as well as LAMP3, a lysosomal protein previously associated with metastasis risk [28, 43]. Multiple cytokines and secreted factors, including IL6, IL17, IL15 and its receptor, S100A8 and S100A9, CXCL12 and several Serpins were also identified as synergistic DEGs (Table S1). The presence of S100A8, S100A9 and CXCL12 among synergistic DEGs raises the possibility that, unlike the case of the triple negative cell line MDA-MB-231 for which S100A8-mediated signaling appeared to require heterotypic cell interactions [3] contributing to metastasis potential, in MCF7 cells this signaling could become homotypic or even autocrine. A marked difference in secreted factors and associated signaling among MDA and MCF7 cells was elegantly shown in recent studies [4].

A direct contribution of p65/RELA and p53 in the observed gene expression changes elicited by Doxorubicin and TNFα was inferred for some of the synergistic DEGs by modulating pharmacologically or genetically p65 or p53 activities. However, we cannot exclude at this stage a (Doxo+TNFα)-dependent, but p53- or NFκB- independent gene expression changes. For example, NFkB can functionally interact with AP-1 [44–46] or ER [47], which in turn can modulate p53-dependent responses [48] [49] [50].

Among the most synergistic genes, 29 appear to be prognostic in luminal A breast cancer patients who underwent chemotherapy, where their higher expression correlated with adverse outcome. The majority of luminal A breast cancers are wild type for p53 [51], although data is not available to stratify patients for p53 status in the KM plotter tool [24]. Based on available ChIP-seq data [14, 25, 52, 53], 20 of these 29 genes are putative targets of either p53 or p65 and 10 of them are putative targets of both factors (Figure 5). This result raises the possibility of an unexpected negative outcome of chemotherapy in the context of an inflammatory microenvironment. The prognostic significance of this gene signature needs in-depth evaluation in independent patients cohorts. If confirmed, the results would further support the value of combining treatments activating p53 and repressing NFκB [7].

Given that the crosstalk between Doxorubicin and TNFα and the interplay between p53 and NFκB would occur in cells residing or infiltrating the tumor microenvironment, the ultimate *in vivo* outcome of these functional interactions may vary and cannot be directly predicted from our study using a pure culture of MCF7 cells *in vitro*. Here we have explored Doxo+TNFα impact on HUVEC cells and also on a p53 wild type lung adenocarcinoma-derived cancer cell line. Although limited by the number of genes tested, the results suggest that a positive crosstalk between Doxorubicin and TNFα can be a general characteristic of different cell types and is

at least in part p53-dependent, based on the results with a p53 null lung cancer cell line. Furthermore, while we have addressed here the functional interactions between two small molecules, cells are constantly exposed to a complex milieu of signaling factors. However, both p53 and NFκB are master regulators, often contributing a dominant trait in gene expression changes to their target genes. Nuclear receptors, including Estrogen Receptors (ERs) can also modulate NFκB as well as p53 functions [54–56] and have critical roles in breast cancer etiology. We also explored the impact of ER function in the transcriptional programs responding to Doxorubicin and TNFα exposure, using estrogen-depleted culture conditions and adding 17β-estradiol (10^{-9}M, E2) as variable (Table S2 and GSE 24065). However, the combination of E2 to Doxo and TNFα resulted only in 15 and 11 selective up- and down-regulated DEGs, respectively (Table S3). A hierarchical cluster analysis of all the treatments confirmed graphically the large difference between TNFα- and Doxo-induced transcriptomes and also the significant impact of TNFα when combined to Doxo, while E2 had a minor effect both in the combination with Doxo and with Doxo + TNFα (Figure S5).

With this study we established an example of positive cooperation between p53 and NFκB, in the context of the responses of an epithelial cancer cell to standard chemotherapy but in the presence of active signaling by a pleiotropic inflammatory cytokine, such as TNFα. A signature gene of the consequent transcriptional reprogramming appears to be prognostic in breast cancer patients. Associated gene functions indicate the potential acquisition of enhanced cell plasticity and motility and provide a rationale to investigating mechanisms resulting in acquired chemoresistance, particularly for luminal A breast cancer, but potentially with general implication for p53 wild type tumors of different tissue types, and for overcoming such resistance by targeting NFκB. The unexpected positive crosstalk between p53 and NFκB emerging from our and other very recent studies [23] may represent an evolutionary consequence of anti-viral and infection responses towards which NFκB is an established master regulator [57], but the p53 and p73 family member are emerging as important/critical contributors [42, 58, 59].

MATERIALS AND METHODS

Cell lines and culture conditions

MCF7 (p53 wild type, expressing p65 and positive for ERs) and HUVEC (Human Umbilical Vein Endothelial Cells) cells were obtained from ICLC (Genoa, Italy), while A549 from ATCC (Manassas, VA, USA). H1299 cells were a gift of Dr. Resnick's laboratory (NIEHS, NIH, RTP, NC, USA); HCT116 $p53^{+/+}$ and $p53^{-/-}$ of Dr. Vogelstein's (John Hopkins Kimmel Cancer Center, Baltimore, MD, USA). MCF7-shp53 or control MCF7-vector cells were provided by Dr. Agami (Netherlands Cancer Institute, Amsterdam, The Netherlands). Cells were cultured in DMEM or RPMI media supplemented with 10% FBS, or Medium 199 (Lonza Milan, Italy) supplemented with 50 units/ml Low Serum Growth Supplements (Life Technologies, Milan, Italy) in the case of HUVEC cells that were also cultured on 0.1% gelatin pre-coated plastics. Media were supplemented by 2mM L-Glutamine and 1XPenicillin/Streptomycin mixture (Pen/Strep), and Puromycin (0.5 μg/mL) in the case of MCF7-shp53 and –vector cells. When appropriate, cells were maintained in DMEM without Phenol Red (Lonza) supplemented with Charcoal/Dextran treated FBS (Hyclone, GE Healthcare, South Logan, UT, USA).

Drug treatments

Doxorubicin (Doxo, 1.5 μM), 5-Fluorouracil (5FU, 375 μM), Nutlin-3a (10 μM) were used to stabilize p53 protein. When needed TNFα (5ng/ml in MCF7 and 10ng/ml in H1299, A549 and HUVEC cells –based on dose-response tests with gene reporter assays) or BAY11-7082 (10μM or 20μM in H1299 and A549) were added to the culture medium. All compounds were from Sigma-Aldrich (Milan, Italy).

Microarray experiment and data analysis

Total RNA was extracted from 4 biological replicates using the Agilent Total RNA Isolation Mini Kit (Agilent Technologies, Santa Clara, CA, USA). Samples with RNA Integrity Number (RIN) above 9 (Agilent 2100 BioAnalyzer) were processed. Details are provided with the Gene Expression Omnibus (GEO) (www.ncbi.nlm.nih.gov/geo) submission (GSE24065) and in [56]. The output of Feature Extraction (Agilent standard protocol GE1_107_Sep09) was analyzed with the R software for statistical computing and the Bioconductor library of biostatistical packages. Probes with low signals were removed in order to filter out the unexpressed genes and keep only probes with acceptable signals in most of the replicates. Signal intensities across arrays were normalized by quantile normalization. Signal intensities from probes associated with the same gene were averaged. This procedure resulted in quantitative signals for 14095 HGNC genes. To identify potential target genes of Doxorubicin and TNFα, we compared the signals after the double treatment (Doxo+TNFα) and the two single treatments relative to the untreated control (mock). DEGs were selected applying a statistical test based on rank products implemented in RankProd Bioconductor package, setting a threshold of 0.05 on the percentage of false positives (pfp) and a threshold of 2 on the absolute log2 fold changes [60]. Every treatment was compared to the mock condition (Table S1, S2 and Figure S5).

To select genes with synergistic effect, i.e. genes whose expression variations were more than additive in the double treatment with respect to single treatments, a further comparison between the double treatment samples and all the remaining samples (single treatments and control samples) was performed (double treatment vs all). Synergistic DEGs were selected applying an additional pfp filter (pfp<0.005) derived from this comparison, to the list of DEGs resulting from the "double treatment vs mock" comparison. A more stringent criterion was obtained by calculating the synergistic effect (SE) of the double treatment as the observed difference between the fold change of the double treatment and the sum of the fold changes of the single treatments (SE=log2 FC double treatment – (log2 FC Doxorubicin + log2 FC TNFα). We filtered genes with SE>0 for up-regulated DEGs, SE<0 for down-regulated genes (Figure 1). To select genes where the up-regulation contribution of each single treatment was low respect to the up-regulation of the double treatment, the ratio of the single/double treatments was calculated, applying a 0.25 filter on them (FC Doxorubicin/FC double treatment <0.25 and FC TNFα/ FC double treatment <0.25) (see Table S1, S2).

RNA isolation and quantitative qPCR

Total RNA was extracted using Qiagen RNeasy Kit (Qiagen). cDNA was converted from 1 µg of RNA using M-MuLV reverse transcriptase and RevertAid cDNA Synthesis kit (ThermoFisher, Milan, Italy). qPCR was performed on a Bio-Rad CFX384 (Bio-Rad, Milan, Italy). TaqMan gene expression assays (Applied Biosystems, Life Technologies) and Probe MasterMix (Kapa Biosystems, Resnova, Rome, Italy) were used starting with 25ng of cDNA as previously described [56, 61]. GAPDH, B2M or ACTB served as reference genes.

Western blot

Protein extraction and immunodetections were performed as previously described [62], using ECL Select detection reagent (GE Healthcare) and anti-p53 (DO-1) anti-RelA/p65 (C-20) anti- p21 (C19), anti-GAPDH (6C5) (Santa Cruz Biotechnology, Heidelberg, Germany). When appropriate, nuclear and cytoplasmic fractionation was performed. MCF7, A549 and H1299 cell lines were seeded on 100mm Petri dishes and treated at 80% confluence with Doxo, TNFα, BAY or the combination of the drugs for 16 hours. Cells were harvested and cytoplasmic and nuclear proteins were extracted using NE-PER Nuclear and Cytoplasmic Extraction Kit (Pierce, ThermoFisher Scientific), following the instructions provided by the manufacturer. 20 µg of nuclear and cytoplasmic extracts were loaded on a 12% poly-acrylamide gel and transferred to nitrocellulose membranes. Antibodies used for detection were: anti-Histone H3 (clone #: ab1791, AbCam, Milan, Italy) and anti-Lamin A/C (clone #: 2032, Cell Signaling, Milan, Italy) used as nuclear loading control, and anti-GAPDH used as cytoplasmic loading control.

Chromatin immunoprecipitation assay

We used previously described protocols [63, 64]. The following antibodies were used: anti-p53 (DO-1), anti-p65 (C-20) and IgG (sc-2025 or sc-2027) (Santa Cruz Biotechnology). ChIP-qPCR experiments were performed using Sybr MasterMix (Kapa Biosystems) and 2 µl of enriched DNA. Results were analyzed by the comparative Ct method (ΔCt) and normalized as % of input. Regions in the promoter of GAPDH or ACTB and p21 or MCP1 genes served as negative and positive controls, respectively. Primers were selected using Primer 3 (http://primer3.ut.ee/).

Migration and wound healing assays

The migration potential of MCF7 cells was monitored by a real-time technique using the xCELLigence Instrument (Acea Biosciences, Euroclone) and CIM-16 plates, following manufacturer's instructions. Prior to the analysis, cells were grown in estrogen-free medium for two days and left untreated (mock) or treated with Doxo, TNFα or the combination. 16 hours after the treatments, cells were detached and added to the top chamber in serum-free medium. Migration was detected every 10 minutes for 24 hours. We used 0.5% and 5% FBS as chemo-attractant. Migration and Invasion were also measured by QCM™ Fluor 24-Well Cell Migration and Cell Invasion kits (Merck-Millipore, Milan, Italy), according to manufacturer's instructions. For wound healing, cells were seeded in 12-well plates and treated with Doxo, TNFα or the combination. After 16 hours a scratch was introduced using a 10 µl pipette tip. Images of the same field were acquired immediately (T0) and after 24 hours (T24) using an automated Zeiss microscope and the AxioVision3.1 software in multidimensional mode with mosaic (3x3) acquisition.

Flow cytometry

MCF7 cells, seeded and treated as described above, were washed with PBS and harvested by 0.05% trypsin/0.025% EDTA. The cells were washed again with PBS containing 2% FBS before being subjected to antibody binding, a combination of fluorochrome-conjugated monoclonal antibodies against human CD44 (APC) and CD24 (FITC) or their respective isotype controls (BD Biosciences, Milan, Italy) and incubated on ice in the dark for 30 minutes. Cells were then washed twice with PBS/2% FBS and resuspended in PBS. Flow cytometry analysis was conducted using a FACSCanto II instrument (BD Biosciences).

ACKNOWLEDGEMENTS

We thank Dr. Valentina Adami (CIBIO High-throughput screening facility), Dr. Isabella Pesce (CIBIO Cell Separation facility), Ms. Sonia Leonardelli, Mr. Dennis Pedri for technical support. This work was supported by the Italian Association for Cancer Research, AIRC (IG grant # 12869 to AI). IR is supported by a Fellowship from the Pezcoller Foundation.

Competing interests

The authors declare no conflict of interest.

REFERENCES

1. Hanahan D, Weinberg RA. Hallmarks of cancer: the next generation. Cell. 2011; 144:646–674.
2. Labelle M, Begum S, Hynes RO. Direct signaling between platelets and cancer cells induces an epithelial-mesenchymal-like transition and promotes metastasis. Cancer Cell. 2011; 20:576–590.
3. Acharyya S, Oskarsson T, Vanharanta S, Malladi S, Kim J, Morris PG, Manova-Todorova K, Leversha M, Hogg N, Seshan VE, Norton L, Brogi E, Massague J. A CXCL1 paracrine network links cancer chemoresistance and metastasis. Cell. 2012; 150:165–178.
4. Kuznetsov HS, Marsh T, Markens BA, Castano Z, Greene-Colozzi A, Hay SA, Brown VE, Richardson AL, Signoretti S, Battinelli EM, Mc Allister SS. Identification of luminal breast cancers that establish a tumor-supportive macroenvironment defined by proangiogenic platelets and bone marrow-derived cells. Cancer Discov. 2012; 2: 1150–1165.
5. Cooke VG, Le Bleu VS, Keskin D, Khan Z, O'Connell JT, Teng Y, Duncan MB, Xie L, Maeda G, Vong S, Sugimoto H, Rocha RM, Damascena A, Brentani RR, Kalluri R. Pericyte depletion results in hypoxia-associated epithelial-to-mesenchymal transition and metastasis mediated by met signaling pathway. Cancer Cell. 2012; 21:66–81.
6. Darnell JE Jr. Transcription factors as targets for cancer therapy. Nat Rev Cancer. 2002; 2:740–749.
7. Dey A, Tergaonkar V, Lane DP. Double-edged swords as cancer therapeutics: simultaneously targeting p53 and NF-kappaB pathways. Nat Rev Drug Discov. 2008; 7: 1031–1040.
8. Vogelstein B, Lane D, Levine AJ. Surfing the p53 network. Nature. 2000; 408:307–310.
9. Vousden KH, Prives C. Blinded by the Light: The Growing Complexity of p53. Cell. 2009; 137:413–431.
10. Espinosa JM. Mechanisms of regulatory diversity within the p53 transcriptional network. Oncogene. 2008; 27: 4013–4023.
11. Riley T, Sontag E, Chen P, Levine A. Transcriptional control of human p53-regulated genes. Nat Rev Mol Cell Biol. 2008; 9:402–412.
12. Vousden KH. Outcomes of p53 activation--spoilt for choice. J Cell Sci. 2006; 119(Pt 24):5015–5020.
13. Menendez D, Inga A, Resnick MA. The expanding universe of p53 targets. Nat Rev Cancer. 2009; 9:724–737.
14. Nikulenkov F, Spinnler C, Li H, Tonelli C, Shi Y, Turunen M, Kivioja T, Ignatiev I, Kel A, Taipale J, Selivanova G. Insights into p53 transcriptional function via genome-wide chromatin occupancy and gene expression analysis. Cell Death Differ. 2012.
15. Karin M. Nuclear factor-kappaB in cancer development and progression. Nature. 2006; 441:431–436.
16. Chen LF, Greene WC. Shaping the nuclear action of NF-kappaB. Nat Rev Mol Cell Biol. 2004; 5:392–401.
17. Webster GA, Perkins ND. Transcriptional cross talk between NF-kappaB and p53. Mol Cell Biol. 1999; 19:3485–3495.
18. Kawauchi K, Araki K, Tobiume K, Tanaka N. Activated p53 induces NF-kappaB DNA binding but suppresses its transcriptional activation. Biochem Biophys Res Commun. 2008; 372:137–141.
19. Ma S, Tang J, Feng J, Xu Y, Yu X, Deng Q, Lu Y. Induction of p21 by p65 in p53 null cells treated with Doxorubicin. Biochim Biophys Acta. 2008; 1783:935–940.
20. Ryan KM, Ernst MK, Rice NR, Vousden KH. Role of NF-kappaB in p53-mediated programmed cell death. Nature. 2000; 404:892–897.
21. Kawai T, Akira S. Signaling to NF-kappaB by Toll-like receptors. Trends in molecular medicine. 2007; 13:460–469.
22. Menendez D, Shatz M, Azzam K, Garantziotis S, Fessler MB, Resnick MA. The Toll-like receptor gene family is integrated into human DNA damage and p53 networks. PLoS Genet. 2011; 7:e1001360.
23. Lowe JM, Menendez D, Bushel PR, Shatz M, Kirk EL, Troester MA, Garantziotis S, Fessler MB, Resnick MA. p53 and NF-kappaB Coregulate Proinflammatory Gene Responses in Human Macrophages. Cancer Res. 2014; 74:2182–2192.
24. Gyorffy B, Lanczky A, Eklund AC, Denkert C, Budczies J, Li Q, Szallasi Z. An online survival analysis tool to rapidly assess the effect of 22,277 genes on breast cancer prognosis using microarray data of 1,809 patients. Breast Cancer Res Treat. 2010; 123:725–731.
25. Menendez D, Nguyen TA, Freudenberg JM, Mathew VJ, Anderson CW, Jothi R, Resnick MA. Diverse stresses dramatically alter genome-wide p53 binding and transactivation landscape in human cancer cells. Nucleic Acids Res. 2013; 41:7286–7301.
26. Xu D, Yao Y, Lu L, Costa M, Dai W. Plk3 functions as an essential component of the hypoxia regulatory pathway by direct phosphorylation of HIF-1alpha. J Biol Chem. 2010; 285:38944–38950.

27. Arakawa H. Netrin-1 and its receptors in tumorigenesis. Nat Rev Cancer. 2004; 4:978–987.
28. Nagelkerke A, Bussink J, Mujcic H, Wouters BG, Lehmann S, Sweep FC, Span PN. Hypoxia stimulates migration of breast cancer cells via the PERK/ATF4/LAMP3-arm of the unfolded protein response. Breast Cancer Res. 2013; 15:R2.
29. Cardone M, Kandilci A, Carella C, Nilsson JA, Brennan JA, Sirma S, Ozbek U, Boyd K, Cleveland JL, Grosveld GC. The novel ETS factor TEL2 cooperates with Myc in B lymphomagenesis. Mol Cell Biol. 2005; 25:2395–2405.
30. Espinosa JM, Verdun RE, Emerson BM. 2003; p53 functions through stress- and promoter-specific recruitment of transcription initiation components before and after DNA damage. Mol Cell. :1015–1027.
31. Gupta PB, Chaffer CL, Weinberg RA. Cancer stem cells: mirage or reality? Nat Med. 2009; 15:1010–1012.
32. Lim S, Becker A, Zimmer A, Lu J, Buettner R, Kirfel J. SNAI1-mediated epithelial-mesenchymal transition confers chemoresistance and cellular plasticity by regulating genes involved in cell death and stem cell maintenance. PLoS One. 2013; 8:e66558.
33. Deep G, Jain AK, Ramteke A, Ting H, Vijendra KC, Gangar SC, Agarwal C, Agarwal R. SNAI1 is critical for the aggressiveness of prostate cancer cells with low E-cadherin. Molecular cancer. 2014; 13:37.
34. Sun L, Mathews LA, Cabarcas SM, Zhang X, Yang A, Zhang Y, Young MR, Klarmann KD, Keller JR, Farrar WL. Epigenetic regulation of SOX9 by the NF-kappaB signaling pathway in pancreatic cancer stem cells. Stem cells. 2013; 31:1454–1466.
35. Tai CI, Ying QL. Gbx2, a LIF/Stat3 target, promotes reprogramming to and retention of the pluripotent ground state. J Cell Sci. 2013; 126(Pt 5):1093–1098.
36. Shipitsin M, Campbell LL, Argani P, Weremowicz S, Bloushtain-Qimron N, Yao J, Nikolskaya T, Serebryiskaya T, Beroukhim R, Hu M, Halushka MK, Sukumar S, Parker LM, Anderson KS, Harris LN, Garber JE, et al. Molecular definition of breast tumor heterogeneity. Cancer Cell. 2007; 11:259–273.
37. Al-Hajj M, Wicha MS, Benito-Hernandez A, Morrison SJ, Clarke MF. Prospective identification of tumorigenic breast cancer cells. Proc Natl Acad Sci U S A. 2003; 100: 3983–3988.
38. Gyorffy B, Lanczky A, Szallasi Z. Implementing an online tool for genome-wide validation of survival-associated biomarkers in ovarian-cancer using microarray data from 1287 patients. Endocrine-related cancer. 2012; 19: 197–208.
39. Lujambio A, Akkari L, Simon J, Grace D, Tschaharganeh DF, Bolden JE, Zhao Z, Thapar V, Joyce JA, Krizhanovsky V, Lowe SW. Non-cell-autonomous tumor suppression by p53. Cell. 2013; 153:449–460.
40. Muller PA, Vousden KH, Norman JC. p53 and its mutants in tumor cell migration and invasion. J Cell Biol. 2011; 192:209–218.
41. Dalmases A, Gonzalez I, Menendez S, Arpi O, Corominas JM, Servitja S, Tusquets I, Chamizo C, Rincon R, Espinosa L, Bigas A, Eroles P, Furriol J, Lluch A, Rovira A, Albanell J, et al. Deficiency in p53 is required for doxorubicin induced transcriptional activation of NF-small ka, CyrillicB target genes in human breast cancer. Oncotarget. 2014; 5:196–210.
42. Wang B, Niu D, Lai L, Ren EC. p53 increases MHC class I expression by upregulating the endoplasmic reticulum aminopeptidase ERAP1. Nat Commun. 2013; 4:2359.
43. Kanao H, Enomoto T, Kimura T, Fujita M, Nakashima R, Ueda Y, Ueno Y, Miyatake T, Yoshizaki T, Buzard GS, Tanigami A, Yoshino K, Murata Y. Overexpression of LAMP3/TSC403/DC-LAMP promotes metastasis in uterine cervical cancer. Cancer Res. 2005; 65:8640–8645.
44. Fujioka S, Niu J, Schmidt C, Sclabas GM, Peng B, Uwagawa T, Li Z, Evans DB, Abbruzzese JL, Chiao PJ. NF-kappaB and AP-1 connection: mechanism of NF-kappaB-dependent regulation of AP-1 activity. Mol Cell Biol. 2004; 24:7806–7819.
45. Redhu NS, Saleh A, Halayko AJ, Ali AS, Gounni AS. Essential role of NF-kappaB and AP-1 transcription factors in TNF-alpha-induced TSLP expression in human airway smooth muscle cells. American journal of physiology Lung cellular and molecular physiology. 2011; 300:L479–485.
46. Westwick JK, Weitzel C, Minden A, Karin M, Brenner DA. Tumor necrosis factor alpha stimulates AP-1 activity through prolonged activation of the c-Jun kinase. J Biol Chem. 1994; 269:26396–26401.
47. Sas L, Lardon F, Vermeulen PB, Hauspy J, Van Dam P, Pauwels P, Dirix LY, Van Laere SJ. The interaction between ER and NFkappaB in resistance to endocrine therapy. Breast Cancer Res. 2012; 14:212.
48. Shaulian E, Karin M. AP-1 in cell proliferation and survival. Oncogene. 2001; 20:2390–2400.
49. Sayeed A, Konduri SD, Liu W, Bansal S, Li F, Das GM. Estrogen receptor alpha inhibits p53-mediated transcriptional repression: implications for the regulation of apoptosis. Cancer Res. 2007; 67:7746–7755.
50. Lion M, Bisio A, Tebaldi T, De Sanctis V, Menendez D, Resnick MA, Ciribilli Y, Inga A. Interaction between p53 and estradiol pathways in transcriptional responses to chemotherapeutics. Cell Cycle. 2013; 12:1211–1224.
51. Cancer Genome Atlas N: Comprehensive molecular portraits of human breast tumours. Nature. 2012; 490:61–70.
52. Consortium EP. A user's guide to the encyclopedia of DNA elements (ENCODE). PLoS biology. 2011; 9:e1001046.

53. Wang B, Niu D, Lam TH, Xiao Z, Ren EC. Mapping the p53 transcriptome universe using p53 natural polymorphs. Cell Death Differ. 2014; 21:521–532.

54. Quaedackers ME, van den Brink CE, van der Saag PT, Tertoolen LG. Direct interaction between estrogen receptor alpha and NF-kappaB in the nucleus of living cells. Molecular and cellular endocrinology. 2007; 273:42–50.

55. Thomas C, Gustafsson JA. The different roles of ER subtypes in cancer biology and therapy. Nat Rev Cancer. 2011; 11:597–608.

56. Lion M, Bisio A, Tebaldi T, De Sanctis V V, Menendez D, Resnick MA, Ciribilli Y, Inga A. Interaction between p53 and estradiol pathways in transcriptional responses to chemotherapeutics. Cell Cycle. 2013; 12.

57. Vallabhapurapu S, Karin M. Regulation and function of NF-kappaB transcription factors in the immune system. Annual review of immunology. 2009; 27:693–733.

58. Yang A, Walker N, Bronson R, Kaghad M, Oosterwegel M, Bonnin J, Vagner C, Bonnet H, Dikkes P, Sharpe A, Mc Keon F, Caput D. p73-deficient mice have neurological, pheromonal and inflammatory defects but lack spontaneous tumours. Nature. 2000; 404:99–103.

59. Menendez D, Shatz M, Resnick MA. Interactions between the tumor suppressor p53 and immune responses. Curr Opin Oncol. 2013; 25:85–92.

60. Breitling R, Armengaud P, Amtmann A, Herzyk P. Rank products: a simple, yet powerful, new method to detect differentially regulated genes in replicated microarray experiments. FEBS Lett. 2004; 5733:83–92.

61. Raimondi I, Ciribilli Y, Monti P, Bisio A, Pollegioni L, Fronza G, Inga A, Campomenosi P. P53 family members modulate the expression of PRODH, but not PRODH2, via intronic p53 response elements. PLoS One. 2013; 8:e69152.

62. Ciribilli Y, Monti P, Bisio A, Nguyen HT, Ethayathulla AS, Ramos A, Foggetti G, Menichini P, Menendez D, Resnick MA, Viadiu H, Fronza G, Inga A. Transactivation specificity is conserved among p53 family proteins and depends on a response element sequence code. Nucleic Acids Res. 2013; 41:8637–8653.

63. Ciribilli Y, Andreotti V, Menendez D, Langen JS, Schoenfelder G, Resnick MA, Inga A. The coordinated p53 and estrogen receptor cis-regulation at an FLT1 promoter SNP is specific to genotoxic stress and estrogenic compound. PLoS One. 2010; 5:e10236.

64. Bisio A, De Sanctis V V, Del Vescovo V, Denti MA, Jegga AG, Inga A, Ciribilli Y. Identification of new p53 target microRNAs by bioinformatics and functional analysis. BMC Cancer. 2013; 13:552.

Tebaldi et al. BMC Genomics _####################_
DOI 10.1186/s12864-015-1643-9

BMC Genomics

RESEARCH ARTICLE Open Access

Whole-genome cartography of p53 response elements ranked on transactivation potential

Toma Tebaldi*†, Sara Zaccara†, Federica Alessandrini, Alessandra Bisio, Yari Ciribilli and Alberto Inga*

Abstract

Background: Many recent studies using ChIP-seq approaches cross-referenced to trascriptome data and also to potentially unbiased *in vitro* DNA binding selection experiments are detailing with increasing precision the p53-directed gene regulatory network that, nevertheless, is still expanding. However, most experiments have been conducted in established cell lines subjected to specific p53-inducing stimuli, both factors potentially biasing the results.

Results: We developed *p53retriever*, a pattern search algorithm that maps p53 response elements (REs) and ranks them according to predicted transactivation potentials in five classes. Besides canonical, full site REs, we developed specific pattern searches for non-canonical half sites and 3/4 sites and show that they can mediate p53-dependent responsiveness of associated coding sequences. Using ENCODE data, we also mapped p53 REs in about 44,000 distant enhancers and identified a 16-fold enrichment for high activity REs within those sites in the comparison with genomic regions near transcriptional start sites (TSS). Predictions from our pattern search were cross-referenced to ChIP-seq, ChIP-exo, expression, and various literature data sources. Based on the mapping of predicted functional REs near TSS, we examined expression changes of thirteen genes as a function of different p53-inducing conditions, providing further evidence for PDE2A, GAS6, E2F7, APOBEC3H, KCTD1, TRIM32DICER, HRAS, KITLG and TGFA p53-dependent regulation, while MAP2K3, DNAJA1 and potentially YAP1 were identified as new direct p53 target genes.

Conclusions: We provide a comprehensive annotation of canonical and non-canonical p53 REs in the human genome, ranked on predicted transactivation potential. We also establish or corroborate direct p53 transcriptional control of thirteen genes. The entire list of identified and functionally classified p53 REs near all UCSC-annotated genes and within ENCODE mapped enhancer elements is provided. Our approach is distinct from, and complementary to, existing methods designed to identify p53 responsive elements. *p53retriever* is available as an R package at: http://tomateba.github.io/p53retriever.

Keywords: p53, Response element, Transactivation potential, Distal enhancer

Background

The p53 tumor suppressor is certainly one of the most studied sequence-specific transcription factor to date. Yet, much has still to be learned to fully describe its transcriptional regulatory network, both in terms of the crosstalk with other transcription factors and in terms of the entire spectrum of regulated transcriptional target genes, that can be both up-regulated or down-regulated [1–6].

Recently, several genome-scale techniques such as ChIP-on-chip, ChIP-seq, and, more recently, ChIP-exo, have provided us with different and largely non-overlapping maps of p53 bound sites in the human genome in response to specific stimuli [7–17]. Correlation between occupancy data and modulation of transcription levels of nearby genes helped identifying additional direct p53 target genes, of which >200 have been established [2, 15]. Furthermore, new methodologies are refining the potential to map the p53 network taking also into account the kinetics of transcriptional initiation [18, 19]. It is worth noting that, to date, most experiments have been developed in cancer-derived cell lines that may represent an adapted environment potentially biasing a comprehensive annotation of physiological p53 target sites [7, 20]. To this respect, the impact of specific p53-inducing stimuli and the differentiation/

* Correspondence: t.tebaldi@unitn.it; alberto.inga@unitn.it
†Equal contributors
Centre for Integrative Biology (CIBIO), University of Trento, via delle Regole 101, 38123 Mattarello, TN, Italy

tissue context of the cell have not been systematically investigated [4, 7, 8, 21, 22].

Considerable attention has been given to the sequence and structural features of p53 binding sites that provide for p53 recruitment to target sites [2, 5, 6]. It is now more clear that the loose definition of p53 response element (RE) [23] that has been used for many years comprises a wide range of DNA binding affinity, occupancy rates and transactivation potentials measured by various types of assays, and that specific differences in the definition of p53 REs are evident between purely *in vitro* biochemical assays and *in vivo* occupancy measurements [24–28] .

The canonical p53 consensus found in many identified binding sites of mostly up-regulated p53 target genes consists of two copies of the palindromic half-site RRRCWWGYYY separated by a spacer of 0–13 bp, in which R = purine, W = A or T and Y = pyrimidine. Theoretically, each p53 monomer binds five nucleotides – i.e., one monomer binds the I° quarter site $R_1R_2R_3C_1$ W_1 and the second monomer the II° quarter site $W_2G_1Y_1Y_2Y_3$-. As reviewed previously, the rather degenerate p53 consensus sequence, reflects the established observation that in virtually all cases of validated p53 REs, an optimal consensus site is not found, because of mismatches, in some cases resulting in partial binding sites, referred to as non-canonical REs [5, 24, 29]. This has raised the hypothesis of a selection pressure to limit the intrinsic potential of p53 proteins to target binding sites, thereby allowing for modulation of p53-induced transcriptional changes by signal transduction pathways affecting p53 protein amount, DNA binding potential, quaternary structures and/or availability of multiple trans-factors [30–36]. For example, p53 REs with lower DNA binding affinity appear to be more frequent in target genes involved in apoptosis [28]. Consistent with this hypothesis, optimized p53 REs have been recently studied in experimental models and *in vitro* for their kinetic and thermodynamic interactions with p53 as well as transactivation potential and shown to provide for high level of p53-mediated transactivation even at low p53 protein levels [25].

Functional assays in a defined experimental setting provided by the yeast *S. cerevisiae* has been extensively used to characterize the transactivation potential of p53 RE in isogenic conditions and exploit variable expression of p53 under an inducible promoter to yield a matrix of transactivation results, to some extent comparable in precision to that of a biochemical assay in a test tube [5, 24, 26, 28, 37–41]. Further, high correlation was reported between results in yeast and transactivation or occupancy data in cancer cell lines [24, 27]. For example, experiments in this model system led to identify functionally active half-site and 3/4 site (3Q) p53 REs, a group of REs collectively considered as non-canonical that were then mapped and validated also in human cells [7].

Here we have combined all the data obtained so far with the yeast-based p53 transactivation assay and developed an algorithm, p53retriever, to scan DNA sequences, identify p53 REs and classify them based on predicted transactivation potential into five broad categories. As unique features, this algorithm takes into account cooperative interactions between groups of mismatches in two p53 dimers and scores also non-canonical REs.

Specifically we used this approach to map functional p53 REs in the proximity of all annotated coding genes, searched for high affinity p53 REs in the entire genome, and mapped functional p53 REs within ENCODE-defined distant enhancer regions. The predictive power of mapping p53 REs with high functional score near transcription start sites (TSS) was validated for a panel of 13 genes, using cell lines differing for p53 status, two p53-inducing stimuli and measuring relative expression by qPCR at three time points. APOBEC3H, E2F7, GAS6, TRIM32, PDE2A, KCTD1, DICER, MAP2K3, DNAJA1, HRAS, KITLG, TGFA and potentially YAP1 were confirmed or identified as p53 target genes.

Results and discussion

Development and implementation of p53retriever, a pattern search code that identifies canonical and non-canonical p53 REs based on predictions from transactivation assays

In general, the degree of p53 binding depends on various factors including the state of the p53 protein, its cofactors, and the sequence composition of the p53-RE [5, 32]. Because easier to predict than the p53 state, computational algorithms were developed to explore p53 binding through sequence motif analysis. The majority of these algorithms, such as p53MH [42], do not directly consider the response element (RE) potential to drive p53-dependent transactivation. On the contrary, p53retriever is based on a set of manually curated rules, derived from a compendium of p53 transactivation data obtained using a yeast-based assay [24, 26, 37, 43, 44].

REs are scored from five (= highly functional REs activity) to one (= unlikely functional REs) (Fig. 1a). The **F1** grade represents the inferred transactivation potential rather than being an indication of the percent similarity to the canonical p53 consensus sequence. For full site p53 REs the grade considers a severe negative impact of a spacer between the two half sites larger than two nucleotides (Fig. 1c). Variable p53-RE spacer lengths are known to affect transactivation capacity. Only two previous studies tried to incorporate the spacer length as one of the relevant features [11, 45], calculating a penalty score directly proportional to spacer length. Also in our algorithm, based on previous results, we attribute high

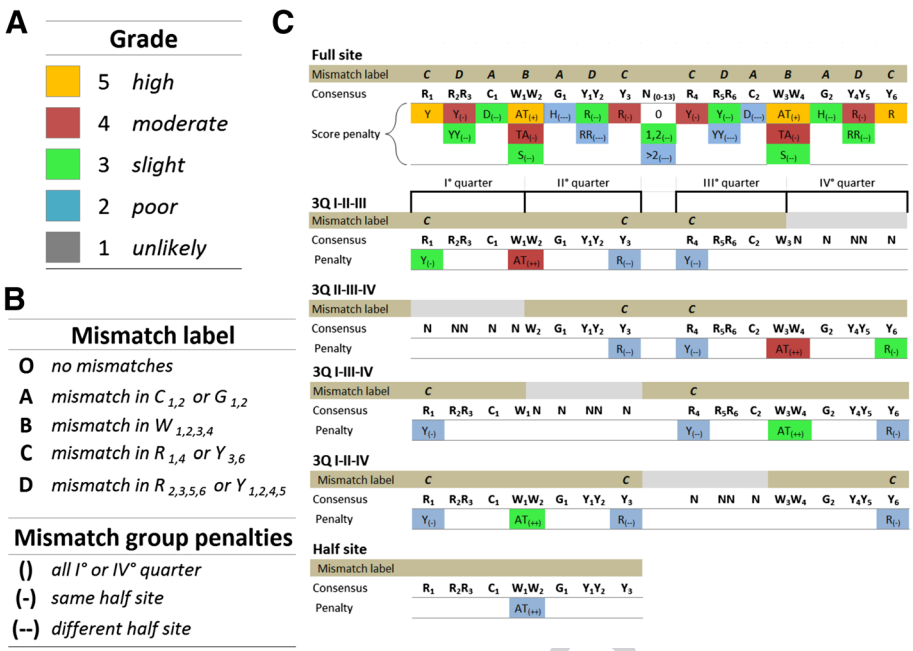

Fig. 1 Summary of RE sequence features and associated grades in p53retriever. **a** Grade: classification of REs reflecting associated functional scores. The color code matching the 5 different grades will be maintained in all figures. **b** Mismatch label: classification of mismatches in different positions. High penalties are given to mismatches located in the core consensus sequence (label A and B), lower penalties are given when mismatches are gradually distant from the core (label C and D). Label O is given to a site without mismatches. Mismatches group penalties: different penalties are attributed to groups of mismatches according to how they are scattered or grouped along the site. **c** Schematic representation of the main rules on which p53retriever search algorithm is based. The full list of rules is listed in Additional file 1. The p53 consensus sequence is presented, grouping dinucleotide motifs that were revealed to provide a specific impact on transactivation potentials, based on our previous studies (see text for details) [28]. Penalties are indicated by an increment in the number of the "-" symbol and a color code broadly matching the grade scale. Single mismatches are more penalized when affecting a base in the internal portion of the RE, as indicated. On the contrary, the AT motif at the center of the CWWG core is a positive feature, particularly in the case of non-canonical REs (3Q = 3Q sites and half sites)

negative impact to spacers longer than two nucleotides (Fig. 1c). Indeed, REs with a long spacer length are also confirmed to be rarely bound by p53 *in vivo* [7, 14, 46, 47]. Many of the computational approaches for identifying putative p53-REs define how similar that putative binding site is to the consensus, but do not consider the local context of single mismatches within the RE. In our approach mismatches from consensus are also weighted depending on their position within the RE 20-mer sequence, given the finding that mismatches in the quarter sites at the interface between the two half sites have a more severe impact likely due to cooperative interactions among two p53 dimers [28] (Fig. 1b). In addition, interaction effects between groups of mismatches are also considered. In general, any combination of mismatches is penalized in a different way according to their location, considering that p53 is functionally active as a tetramer, that each p53 monomer interacts with a 5 nt motif (quarter site) and that the p53 tetramer is thought to be assembled as a dimer of dimers [48]. If groups of mismatches are localized in the same "quarter" of the RE, the score is less penalized than if the same mismatches were scattered in different quarters (Fig. 1b). Importantly, non-canonical REs consisting of 3Q sites and ½ sites [5, 7] are considered functional p53 REs with specific pattern searches. A graphical view of these features presented as "penalty matrix" summarizes the main features of our pattern search (Fig. 1c). The complete list of the rules used to attribute the functional score is presented (Additional file 1). The p53retriever pattern search algorithm, together with functions to better visualize search results, has been implemented as an R package and is available for download at: http://tomateba.github.io/p53retriever.

Distribution of identified p53 response elements around human promoters

We applied p53 retriever to the set of sequences in the human genome placed around annotated transcriptional start sites (TSS), selecting a window from -10 kb to 10 kb. The entire list of identified REs, chromosomal coordinates, official gene name, distance from TSS and RE sequence features resulting in the given grade, is available in Additional file 2.

The distribution of identified p53 REs grouped based on the functional score, shows a very large preponderance of "grade 1" REs, that are considered as unlikely functional (Fig. 2a). Also, the distribution of RE scores is highly skewed, with only 0.05 % of REs obtaining the highest grade, supporting the hypothesis of a selecting pressure to reduce p53 binding affinity and provide plasticity in the modulation of p53-mediated stress responses *in vivo* [4, 28]. Very recent analyses confirmed that p53 REs that are more highly conserved in evolution are relatively weak p53 RE sites displaying lower levels of occupancy compared to higher affinity REs that exhibit low evolutionary conservation [47]. Grade five sequences either lack entirely mismatches, or contain two or fewer mismatches in the external positions (R1,Y6/R4,Y3, see Fig. 1c), and contain the positive AT motif in the CWWG core. The vast majority of REs that can be considered functional are in the grade two category. Predicted to be poorly responsive on their own, these REs could participate in the regulation of gene expression conditional to other features, such as the local sequence context of promoter architecture. Included in the grade two category are ~30 % of all half sites mapped (Fig. 2a). A unique feature of our search tool is the specific pattern search for non-canonical 3Q sites. Interestingly, even though mismatches in the two internal quarter sites have an higher impact on p53 transactivation for 3Q sites compared to full sites, and thus result in a final lower grade, many 3Q sites obtained a grade higher than 2. Hence, a great number (13,744) of p53 REs are predicted to be functional even though the entire motif is not present. This observation strongly supports recent reports suggesting that p53 REs match the consensus in one half site, with the two central quarter sites being somehow less variable [14]. It is also consistent with the recent report of the frequent identification of p53 half-sites among p53 ChIP-seq peaks lacking full sites [47].

We compared the results obtained searching within human promoters with what we would expect by chance, by applying p53retriever to sets of scrambled sequences obtained by local permutations of real promoter sequences (see Methods and Supplementary Additional file 3: Table S1). Local permutations allowed us to preserve the local GC content of promoter regions, showing

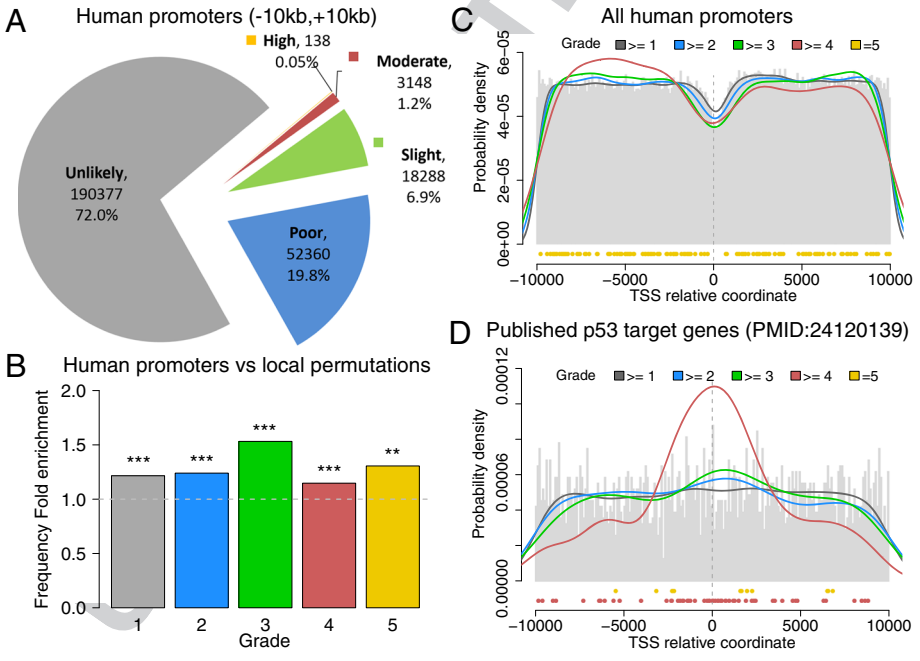

Fig. 2 analysis of p53 REs found in human promoters. **a** Pie chart displaying the distribution of grades associated to REs found in all human promoters. **b** Comparison between the frequencies of REs found in human promoters, and the frequencies of REs found in scrambled promoter sequences after applying local permutations (to preserve the local GC content). The comparison is shown for each grade. The ratio is 1 if the frequency is the same, > 1 if the frequency is higher in real promoters, <1 if the frequency is higher in scrambled promoters. All enrichments are significant, the binomial test p-value is 4.84E-04 for grade 5 (**), <1E-15 for all the other grades (***). **c** p53 occupancy metaprofile, based on the position of REs in all human promoters, centered on the TSS position. The grey histogram displays the probability distribution of all REs independently from the grade. Colored lines represent the density distribution of REs with higher grades (the grade threshold corresponding to each color is displayed in the legend). The specific positions of grade 5 REs are dotted in yellow under the histogram. **d** p53 occupancy metaprofile, based on the position of REs in the human promoters of 228 p53 target genes, published in [15]. The color scheme is the same as in panel C. The specific positions of grade 4 and 5 REs are dotted under the histogram (in yellow for grade 5, red for grade 4)

in fact an increase in GC content around the TSS (see Additional file 3: Figure S1). From this analysis we could determine that the frequency of REs in the global set of human promoters is slightly but significantly higher than the frequency of REs in scrambled sequences (Fig. 2b). This soft enrichment is plausible, given that we are considering all known human TSS and not specific populations of genes. Grade five and three are the most enriched class of REs when comparing the frequency of each grade (Fig. 2b).

Mapping all the REs considering their position with respect to the TSS, we obtained an occupancy metaprofile of p53 REs, displayed in Fig. 2c. This occupancy profile reveals a general decrease of REs in the region proximal to TSS (from -2 kb to +2 kb). This decrease affects all REs, independently from the grade, and appears to be a consequence of the local increase in GC content, since we observed the same effect in scrambled sequences when applying local permutations (Additional file 3: Figure S2). Overall the REs reduction (approximately of ¼.) could be interpreted as a selection against a high density of active p53 REs from promoter regions of non-target genes that is limited to about 2 kbs from TSS. This reduction is driven by the general increase in GC content around the TSS, which more globally is instrumental in the interplay between chromatin conformation and transcription processes. On the other hand, when restricting our analysis to the promoter region of known p53 targets, we found an entirely different landscape. Fig. 2d displays the promoter occupancy metaprofile of REs identified by p53retriever in a group of 189 HGNC genes listed as targets of p53 in literature and collected in [15, 45]. Interestingly, this profile shows the highest probability density in the region closer to the TSS, especially for functional REs with grade four and five (red line in Fig. 2d). Indeed, recent data reported a prevalence of p53 REs nearby the TSS of known target genes [16, 47].

Comparison with other p53 binding site datasets and search tools

>To further verify if p53retriever recognized already established p53 binding sites, we compared our approach with lists of p53 target genes and REs previously reported. The detailed results of all comparisons are contained in Additional file 4.

First, we used our method to score 81 REs sequences that are consistently bound by p53 according to seven different ChIP-seq datasets, reported in [15]. All these sequences were picked by p53retriever as potentially functional. Interestingly, excluding one sequence, all p53 REs from this list obtained a grade greater than one with the majority being of grade 5, confirming that our tool can discriminate functional and well-known REs (Fig. 3a).

Next, we applied p53retriever on p53 REs obtained by Chip-exo analysis [14], providing near-nucleotide resolution of p53 bound sites in response to a variety of genotoxic stresses. (Fig. 3b). While 28 % of sites were not classified, the majority of bound sequences from ChIP-exo obtained a grade greater than 1, with a predominance of grade four and five, (Fig. 3b, left panel). Interestingly, we saw a clear correlation between higher relative occupancy and higher RE grade (Fig. 3b, right panel). Looking in more detail to the "no grade" group, we noticed that all non-scored sequences differed from the canonical RE site for features which are highly penalized by our algorithm, like a number of mismatches higher than three scattered on three different quarter sites. Nevertheless, we could show that these not-scored sequences are mostly characterized by low occupancy values (white boxplot in Fig. 3b right panel, Wilcoxon rank sum test p-value=1.29E-09). Consistently, when considering the subset of regions increasingly bound by p53 after all the stimuli used in [14], the percentage of "no grade" drops to 17.6 % (Additional file 3: Figure S3).

We also extended the comparison to a Chip-seq dataset, reported in [17] (Fig. 3c) and obtained an overall similar distribution of RE grades. The percentage of regions with "no grade" is 22.8 %.

Next, we extended the comparisons to other lists of REs, starting from two small collections of reported p53 REs, based on heterogeneous experimental approaches [2, 15, 45]. Only a minority of those REs obtained the highest grade, and the proportion of sequences not scored as potentially functional was approximately 40 % (Additional file 3: Figure S4). It has to be said that the REs reported in those lists are not guaranteed to be the ones actually or solely responsible for the responsiveness of the associated genes to p53.

Even though total mRNA levels are an indirect measurement of p53 transcriptional activity, they reflect the transcriptome status upon p53 activation. Thus, we did an additional comparison using microarray data obtained after p53 activation upon Doxorubicin treatment of MCF7 cells [49]. The majority of differentially expressed, up-regulated genes turned out to have a p53 binding sites with grade three (Fig. 3d), and exhibited a specific enrichment of REs with grade >3 near the TSS (Additional file 3: Figure S5). Similar comparisons were done with lists of p53 target genes in curated databases such as TRANSFAC and IPA. Again, the majority of these genes have a RE of grade three predicted by p53retriever in their promoter region (Fig. 3d). Using Ingenuity Pathway analysis (IPA), grade five and grade four human promoters revealed a strong p53 pathway signature (Additional file 5).

Finally, we compared p53retriever results with the standard PWM approach, using two PWMs provided by

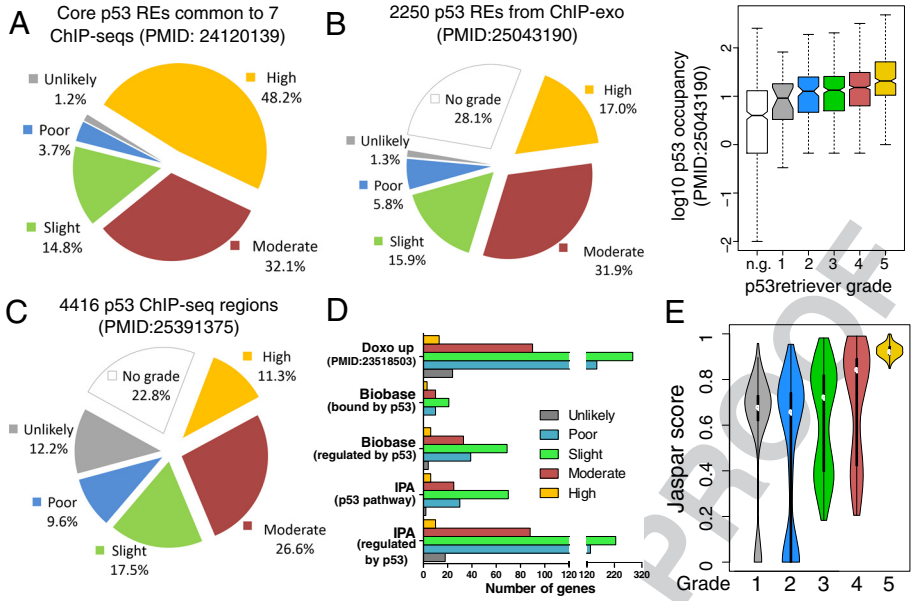

Fig. 3 comparison of p53retriever with other p53 binding site datasets and tools. **a** Pie chart displaying p53retriever classification on a list of 81 regions commonly identified by 7 different ChIP-seq experiments [15]. **b** Left panel: pie chart displaying p53retriever classification on a list of 2250 regions identified by ChIP-exo [14]. Right panel: boxplot displaying for each grade assigned by p53retriever to ChIP-exo sequences, the distribution of the corresponding ChIP-exo occupancies, measured in [14]. n.g. = no grade given by p53retriever. **c** Pie chart displaying p53retriever classification on a list of 4416 regions identified by ChIP-seq in [17]. **d** p53 target gene lists from curated databases (Biobase and IPA) or from expression datasets (Doxo up: genes up-regulated upon doxorubicin treatment) were compared to the list of p53 promoter REs obtained with p53retriever. Presented in the bar graph are the predicted p53 REs grouped by the maximum functional grade identified by p53retriever in their promoter. **e** Comparison between p53 REs identified in human promoters by p53retriever, and the corresponding score given by Jaspar p53 PWM (MA0106.2), based on ChIPseq data. REs are divided in 5 groups along the horizontal axis, corresponding to the grade assigned by p53retriever. For each group, the distribution of the scores given by Jaspar PWM is represented as a violin plot, i.e., a box plot with a rotated kernel density plot on each side. Jaspar scores range from 0 (the RE is not identified) to 1 (the RE is optimal)

the JASPAR database (see Methods). All REs identified by p53retriever in the set of human promoters were scored in parallel with both JASPAR PWMs: the comparison with the JASPAR PWM derived from ChIPseq data is shown in Fig. 3e. Although there is a high agreement on REs with the maximum grade, very close to the optimal p53 consensus, the comparison shows divergences between the two methods for the lower grades. For example, a considerable population of REs assigned to grade four by p53retriever receives very low scores from JASPAR. This is likely due to the presence of ¾ sites that are over-penalized by the PWM approach. On the other hand, many REs with low grades are highly scored by JASPAR, that doesn't penalize groups of scattered mismatches. Apart from grade 1, we can observe a linear trend between the two scoring systems if we look at the median values of the boxplots displayed in Fig. 3e, so we can conclude that the two approaches are distinct and complementary. On the other hand, the second JASPAR matrix, based on SELEX data, gives misleading results, since even optimal REs (grade 5) receive low scores (Additional file 3: Figure S6).

High grade p53 REs are enriched in distant enhancers

Recent functional genomics approaches, particularly resulting from the ENCODE initiative, have revealed that transcription is rather pervasive, that enhancer sequence can be very distant, at least in terms of primary sequence, from genes, and that active enhancers can be mapped based on specific histone code marks [50, 51]. Hence, we exploited this rich body of available information to map p53 REs in distal enhancer sites, using DNAse hypersensitive sites tracks. We filtered out sites overlapping with promoter regions defined in the previous sections, and considered a population of 43,787 distal regions, whose length distribution is displayed in Fig. 4a. p53retriever was run on this set of regions, and the complete results are provided in Additional file 6. The grade distribution of REs found in distal DNAse regions is displayed in Fig. 4b. The frequency of REs in these regions is significantly higher than the frequency found in human promoters and also in random sequences (Fig. 4c and Additional file 3: Figure S7). The overall fold enrichment is 3.54, but this trend grows proportionally to the grade of the REs, reaching a peak with

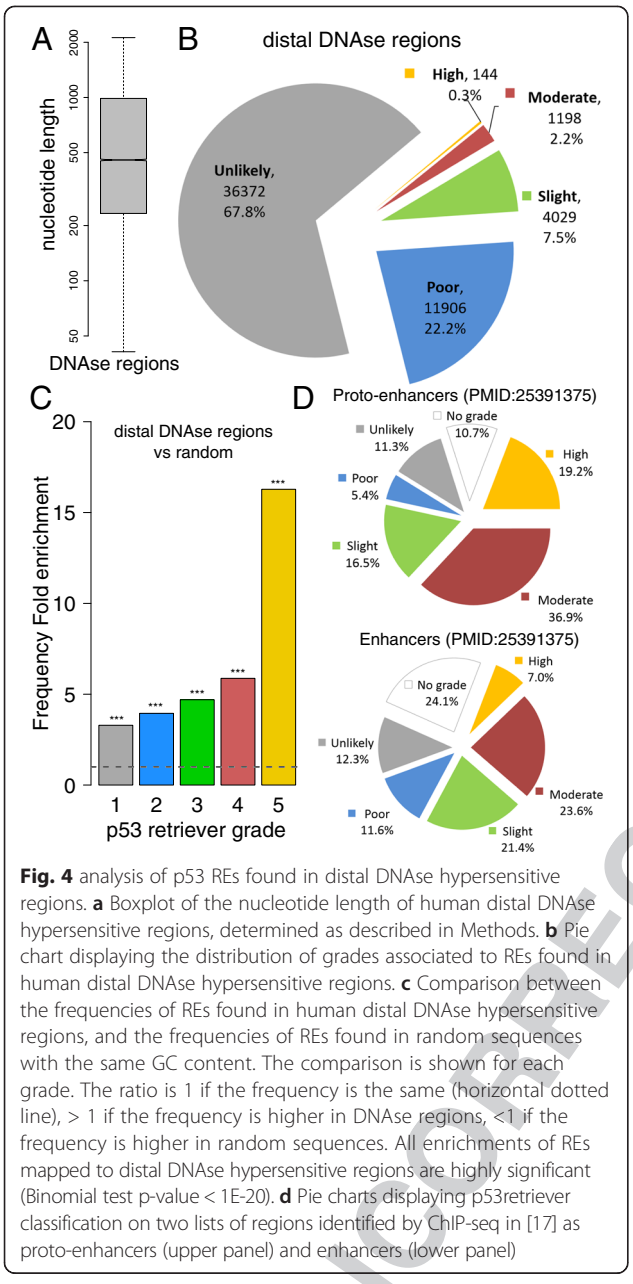

Fig. 4 analysis of p53 REs found in distal DNAse hypersensitive regions. **a** Boxplot of the nucleotide length of human distal DNAse hypersensitive regions, determined as described in Methods. **b** Pie chart displaying the distribution of grades associated to REs found in human distal DNAse hypersensitive regions. **c** Comparison between the frequencies of REs found in human distal DNAse hypersensitive regions, and the frequencies of REs found in random sequences with the same GC content. The comparison is shown for each grade. The ratio is 1 if the frequency is the same (horizontal dotted line), > 1 if the frequency is higher in DNAse regions, <1 if the frequency is higher in random sequences. All enrichments of REs mapped to distal DNAse hypersensitive regions are highly significant (Binomial test p-value < 1E-20). **d** Pie charts displaying p53retriever classification on two lists of regions identified by ChIP-seq in [17] as proto-enhancers (upper panel) and enhancers (lower panel)

grade 5. In fact, 144 high grade REs are found within DNAse hypersensitive sites (Fig. 4b), more than in the entire human promoter dataset. The fold enrichment of grade five REs is 16.3 (Fig. 4c). Presently, it is undetermined if this enrichment for high quality binding sites reflects a common trend for sequence-specific transcription factors or a distinct feature of p53 family proteins. Consistent with our results, higher levels of p53 occupancy in distal enhancers compared to promoters was very recently reported based on ChIP-seq analysis of lymphoblastoid cell lines treated with doxorubicin [47]. Additionally, Chip-seq analysis reported in [17] allowed us to expand the study of p53 REs in enhancers regions. In fact that paper provided p53 bound regions classified as enhancers based on ENCODE annotation or as proto-enhancers, where p53 could act as pioneer transcription factor. Interestingly, this latter group showed an enrichment for high scoring (grade four and grade five) p53 REs according to p53retriever and a lower proportion of sequences with no grade (Fig. 4d, top panel).

New direct p53 target genes identified based on the p53 RE functional search tool

High-activity, or non-canonical p53 REs predicted to be moderately active were mapped by our tools near the TSS of genes that are not completely established or novel putative direct p53 target genes. To infer the predictive power of the pattern search on p53-dependent transcriptional changes, 13 genes were selected and their expression were tested followed by qPCR in cell lines differing for p53 status (MCF7, two derivative clone so called MCF7 vector and MCF7shp53, HCT $p53^{+/+}$ and HCT $p53^{-/-}$) and at different time points (8, 16, 24 h) after p53 activation by two different treatments, i.e., Doxorubicin -a genotoxic chemotherapeutic drug- and Nutlin-3A -an MDM2 inhibitor- (Fig. 5a) (Additional file 7). Results support p53-dependent up-regulation for most genes. The p53-dependency is confirmed by the absence of induction in HCT $p53^{-/-}$ and MCF7shp53 cell lines, despite the different p53 status between the two cells lines (a p53-null and a partial knockdown cell line, respectively). In some cases, the increase in gene expression compared to the mock condition was time-dependent. Differences in these kinetic features were apparent between the two treatments applied. E2F7 was inducible by doxorubicin at different time points, while after Nutlin-3A treatment an early up-regulation was followed by repression, which appeared to be p53-dependent. GAS6 and KCTD1 had a similar trend especially in MCF7 cells. Differences were noted between MCF7 and the MCF7-vector derivative clone in the magnitude or the kinetics of relative expression changes (*e.g.*, PDE2A, APOBEC3H, KCTD1, DNAJA1, DICER). Nine of the thirteen candidates (PDE2A, GAS6, E2F7, APOBEC3H, KCTD1, TRIM32, TGFA, KITLG, HRAS) were selected among the list of genes having both a predicted binding sites in our algorithm output with a grade higher or equal to 2, and a reported p53 binding sites on ChIPseq datasets [7, 8]. For all of them except TRIM32, total mRNA levels are also reported as upregulated after Doxorubicin treatment by microarray data [49]. Although the induction is not directly proportional to the grade, we confirmed p53 dependent induction by qPCR for all of them in time/cell line dependent manner. Even though TRIM32 is not upregulated after Doxorubicin treatment in all the tested cell lines, it is upregulated upon Nutlin-3A treatment, confirming ChIP-seq data. Besides

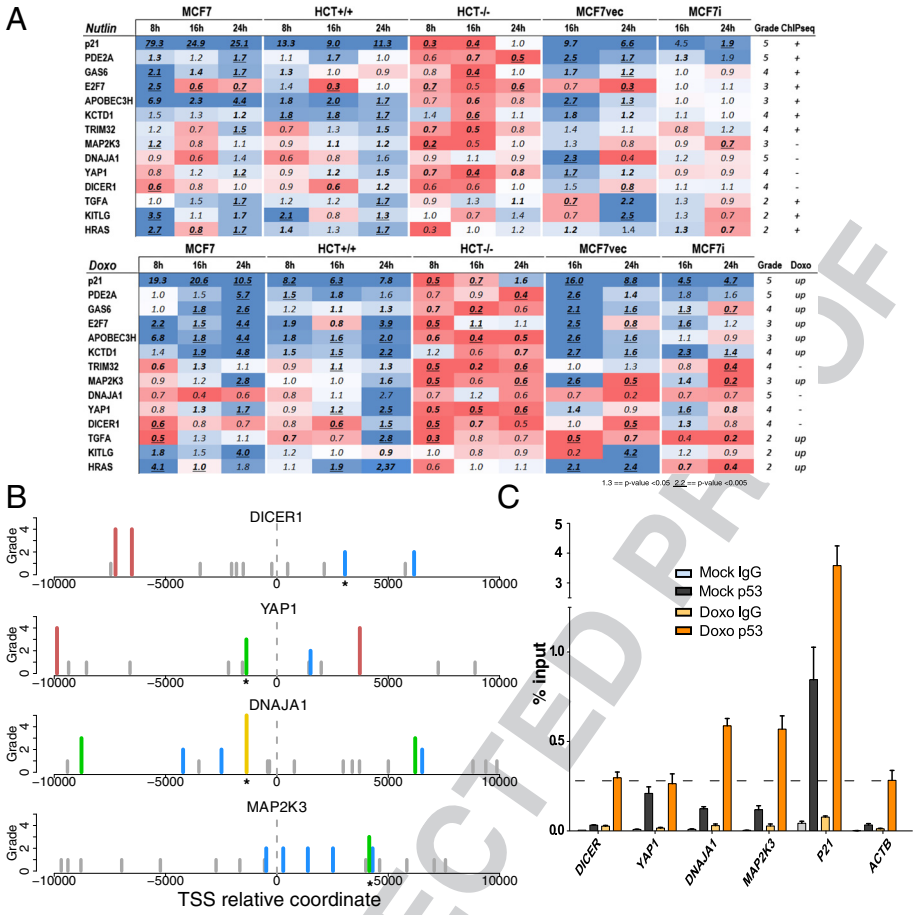

Fig 5 p53-responsiveness of target genes associated with predicted functional REs. **a** qPCR results of 13 selected genes. Fold of changes values (ΔΔCq) upon each treatment are presented as a heatmap Upper part shows mRNAs level after Nutlin-3A treatment while the lower shows the same after Doxo treatment. Expression levels were tested in different cell lines (MCF7, HCT +/+, HCT −/−, MCF7 vector and MCF7 shp53) and at different time points (8, 16 and 24 h) (Details are presented in Suppl. File7). For each gene, the "Grade" column presents the binding site grade reported by our algorithm. "ChIPseq" column shows the presence (+) or absence (–) of reported p53 binding sites [8]. "Doxo" column presents mRNA levels obtained by microarray data [49]. **b** Positional representation of p53 binding sites in TSS proximity for DICER, YAP1, DNAJA1, MAP2K3. Bar height is proportional to the binding site grade. Grade 5 is yellow, grade 4 is red, grade 3 is green, grade 2 is blue and grade 1 is grey. **c** p53 occupancy on the promoter of DICER, YAP1, DNAJA1 and MAP2K3 comparing Mock and Doxo condition in MCF7 cells. P21, well-known p53 direct target, is a positive control. ACTB is used as a reference. Sites validated by ChIP are indicated by a * symbol in Figure 5b

their p53 binding sites, these candidates were selected because of their reported involvement in cell-cycle control e tumor progression (PDE2A, E2F7, GAS6, TRIM32, HRAS, KITLG and TGFA), in transcription (KCTD1), and DNA editing (APOBEC3H) (see Supplementary Text in Additional file 3).

For the remaining four genes, whose REs are displayed in Fig. 5b, we performed a chromatin-immunoprecipitation experiment in MCF7 cells treated with Doxorubicin for 16 h. Weak p53 occupancy was observed by qPCR at DNAJA1 and MAP2K3 loci after doxorubicin treatment, while a region containing a predicted grade 3 category p53 RE in the YAP1 gene showed evidence for p53 occupancy in the mock condition. Our results did not support direct p53 binding to the DICER promoter, consistent with a previous study [52] (Fig. 5c).

Overall, we propose DNAJA1, MAP2K3 and potentially YAP1 as new direct p53 target genes, although the level of transactivation was relatively low.

DNAJA1 can act as a co-chaperone of Hsc70 that was previously associated to radioresistance phenotype in wild type p53 glioblastoma cells treated with farnesyltransferase inhibitors [53]. Recently, overexpression of DNAJA1 was associated with a reduction of pancreatic cancer cell survival and with c-Jun repression [54].

MAP2K3 participates in the MAP kinase cascade and can phosphorylate p38. This protein was identified as a senescence-promoting factor in human breast epithelial

cells [55]. However, it has also been associated to tumor invasion potential and to be regulated at transcriptional level by NFY, NFkB and gain-of-function mutant p53 [56].

The Yes-associated protein 1 (YAP1) is a transcriptional regulator involved in the Hippo signaling pathway. Evidences support both an oncogenic and a tumor suppressor role for YAP1, linked to ABL1-induced apoptosis [57]. YAP1 protein was found capable to bind the p53 promoter and a positive feedback loop was proposed based on the finding that p53 can bind the YAP promoter [58]. In part consistent with this view we found p53-dependent YAP1 gene up-regulation both after doxorubicin and Nutlin-3A treatment.

Conclusions

Several previous tools were developed to identify bona fide p53 response elements, starting with pioneering *in vitro* selection experiments that led to the initial and still accepted definition of the consensus p53 RE [11, 42, 45, 59, 60]. The majority of these tools were based on position weight matrices derived from results of *in vitro* approaches, namely competitive gel shift assays and SELEX, more recently integrated with results obtained from Chromatin immunoprecipitation experiments. A systematic effort to quantify changes in DNA binding affinity (dissociation constants) using fluorescence anisotropy titration led to the development of a p53 binding site predictor algorithm [60]. This tool was also used to search genome wide for high affinity p53 REs and to map naturally occurring single nucleotide polymorphisms (SNPs) that can impact on the DNA binding affinity of p53. The functional relevance of SNPs within p53 REs has been established in several reports [15, 24, 27, 44, 61].

All position weight matrix approaches assume additive contributions of the individual positions within the RE sequence, and except for [45] and [11], all tools do not specifically weigh the impact of spacers between half site decameric RE motifs in the 0-13 nt range. This spacer length was in fact considered neutral in the initial *in vitro* experiments [23]. However, DNA binding assays where RE sequence are embedded in longer DNA molecules, competitive binding experiments in microfluidics, Chromatin Immunoprecipitation assays, yeast- and mammalian-cell based transactivation assays all indicate that even a single nucleotide spacer between p53 RE half sites can reduce transactivation potential [5, 24, 27, 44]. In fact, when the spacer is longer than 2–3 nt the two decameric half sites no longer show cooperative interactions [24, 28, 62], although when the distance in primary sequence approach one helical pass, transactivation potential appears to increase beyond additivity [24], yet remaining much lower compared to the absence of a spacer. The negative impact of spacer is even more dramatic for TAp73 [62] and TAp63 proteins, but not for ΔNp63 [63], suggesting that the structure as well as the sequence of DNA binding sites can lead to conformational changes in the quaternary tetrameric structure of p53 family proteins, and that intrinsic differences exist in the oligomerization state of these proteins [64].

We have coded in p53retriever sequence and structural features of p53 REs impacting on transactivation potential that were revealed in the past several years using our yeast-based transactivation assay [5, 26, 28, 63, 65, 66]. The resulting algorithm has several distinctive features compared to previous tools, particularly for scoring interactions among groups of mismatches, non-canonical 3Q sites and half sites p53 REs, weighting the impact of consensus mismatches considering their position within the full site RE sequence, i.e., giving higher penalty to mismatches in the two internal quarter sites, and weighs consensus sequence variations within dinucleotide motifs in the core and flanking regions [28] (Fig. 1, Additional file 1). Possible interactions between nearby half site p53 REs or clusters of full site and 3Q sites are currently not considered by our algorithm.

We mapped and ranked functional REs near TSS for all annotated transcripts in UCSC (Additional file 2). Further, we exploited ENCODE data and provide a cartography of ranked p53 REs within distant DNAse hypersensitive sites, considered as distant enhancers (Additional file 6). In these regions we found a significant 16-fold enrichment of high grade REs with respect to the basal frequency expected by chance or observed in promoter regions. An enrichment for high grade REs was also found among proto-enhancer sequences bound by p53 identified by ChIP-seq [17]. It is worth noting that our results represent a projection from all DNAse hypersensitive sites, irrespective of the specific tissues in which they are active. Tissue variability may influence which REs are selectively bound. An additional layer of complexity is represented by the known interplay between different transcription factors. This important aspect is not included in our analysis that is focused on p53 alone.

Although the data on which the algorithm is construed are the outcome of transactivation assays measured from chromatinized promoter-reporter construct, the isogenic nature of the yeast-based functional assays, minimizes most variables potentially impacting on transactivation by p53; at the same time distinct chromatin features of the natural context of the REs' location *in vivo* may certainly influence the associated gene transcriptional responsiveness to p53. Hence the yeast-based results might be more similar to ChIP-seq and ChIP-exo results, albeit with a more quantitative power.

Undoubtedly different ChIP-seq experiments do not agree with each other and there is limited overlap among the results obtained with different cell lines or

using different treatments to activate p53. While global differences in occupancy could be related to differences in accessibility between different tissue-derived cells or to distinct p53 post-translational modifications or cofactors activated by different treatments, it was interesting to find that the list of p53 bound sites that are common to multiple ChIP-experiments were highly enriched for high scoring (grade four and grade five) REs and none of them failed to be classified by our tool (Fig. 3a). Instead, when examining individual ChIP-seq or even, although to a lower extent, ChIP-exo data, 20 % to 30 % of p53 bound fragments did not contain a motif scored by p53retriever. While those sites may represent examples of p53 proteins tethered to DNA by protein interactions, the manual inspection of "no grade" sites from the ChIP-exo datasets showed that the majority of these sites resemble p53 response elements but contain several (three or more) "core" mismatches scattered on three different quarter sites. These multiple mismatched REs are not presently scored by p53retriever, but would probably result in weak responsiveness. Consistently, the majority of no grade ChIP-exo REs showed lower occupancies (Fig. 3b right panel).

Finally, we decided to validate a few of the predictions from the pattern search, particularly for non-canonical 3Q sites using cell lines as a model.13 genes with mapped functional REs were chosen. Overall, despite our algorithm doesn't consider the system complexity of transcriptional regulation in living cells and the response variability upon each different p53 stimulus, results support p53-dependent transactivation for the majority of them. Based on the combined qPCR and ChIP results we conclude that DNAJA1, MAP2K3, and potentially YAP1 can be considered new direct p53 target sites, linking p53 to yet additional potential biological outcomes. Furthermore, our data further establish the very recent findings of PDE2A, GAS6, E2F7, APOBEC3H, KCTD1, TRIM32, HRAS, KITLG and TGFA as p53 target genes.

Methods

Implementation of pattern search rules in p53retriever

We implemented the set of manually curated rules (Additional file 1) in an R package called p53retriever. p53retriever source and binary files are available on Github, at (http://tomateba.github.io/p53retriever/). p53retriever contains a main function that identifies potential REs. This function needs as input an arbitrary DNA sequence, and returns a table containing information about the identified REs, such as position, sequence, spacer length, mismatch label and grade. The format of the output is similar to Additional file 6. Many functions are also provided in order to graphically display the results. The package is documented with usage examples, and fully integrated with other CRAN and Bioconductor packages. In particular, p53retriever depends only on the previous installation of the Bioconductor Biostrings package.

Human promoters dataset

Human promoter sequences were extracted from the UCSC database (http://genome.ucsc.edu/) considering, for each transcript with a distinct TSS, the 20 kB region surrounding the transcription binding site (genome build GRCh37/hg19). The final dataset consists of 23,541 promoter sequences, associated to distinct UCSC identifiers and corresponding to 18,355 HGNC genes.

Human distal DNase regions dataset

Encode DNase-seq regulatory regions (genome build GRCh37/hg19) were obtained from the following cell lines: Gm12878, H1hesc, Helas3, Hepg2, Hmec, Hsmm, Hsmmt, Huvec, K562, Monocd14, Nha, Nhdfad, Nhek, Nhlf, Osteobl, Hsmmfshd, Lncap, Nb4, Nt2d1,Panc1. The consensus was defined as the merge of all the regions that were present in at least two cell lines. Only distal regions, with more than 10 kb from the nearest annotated TSS, were kept in the dataset, in order to avoid overlap with promoter regions. The final dataset consists of 43,787 regions, with a mean length of 673.3 bases.

Simulations with random sequences

Sets of scrambled promoter sequences were generated by local permutations (bin size = 500 nt) of human promoter sequences (−10 kb, +10 kb from TSS). This allowed to preserve the local GC content in the random model; p53 REs were then identified and classified with p53retriever. The random simulation was run ten times, and the results were compared to REs identified in real human promoters.

Set of random sequences were generated, with the same number and the same GC content (44 %) of human DNA sequences; p53 REs were then identified and classified with p53retriever. The random simulation was run ten times, and the results were compared to REs identified in human distal DNase regions promoters.

Pathway analysis of DEGs

All pathways analyses were performed using IPA (www.ingenuity.com). Only direct interactions were considered in the setting parameters.

Comparison with other datasets

Several lists of p53 targets, identified by their HGNC symbol, were extracted from online databases such as Biobase TRANSFAC (http://www.biobase-international.-com/product/transcription-factor-binding-sites) and IPA, or from previous publications, referenced in the main text.

These lists were used to select populations of genes among our dataset of human promoters, and analyze the grade of the REs identified by p53retriever (as shown in Fig. 2d).

Several sets of p53 RE sequences or p53 bound regions were taken from previous publications, referenced in the main text. p53retriever was run directly on these sequences (as shown in Fig. 3a, b, c).

Comparison with JASPAR PWMs

Two PWMs for p53 were downloaded from the JASPAR database (http://jaspar.genereg.net/). One PWM, MA0106.1, is built on SELEX data, while the second, MA0106.2, is built on ChIPseq data. The original values of the dowloaded PWMs were based on nucleotide frequencies and therefore more similar to Positional Frequency Matrices. These frequency values were transformed in log2 probability ratio values with the PWM function implemented in the Bioconductor Biostring package, using a multinomial model with a Dirichlet conjugate prior to calculate the estimated probability of base b at position i. The final score of a match ranges from 0 to 1. All REs identified by p53retriever in the set of human promoters were scored with JASPAR PWMs: the comparison with MA0106.2 is shown in Fig. 3d, while the comparison with MA0106.1 is shown in Additional file 3: Figure S2.

Cell lines and culture conditions

The human breast adenocarcinoma-derived MCF7 cell line (p53 wild type) was obtained from the InterLab Cell Line Collection bank, ICLC (Genoa, Italy) while the colon adenocarcinoma HCT116 ($p53^{+/+}$) cell line and its $p53^{-/-}$ derivative were a gift from B. Vogelstein (The Johns Hopkins Kimmel Cancer Center, Baltimore, Maryland,USA). MCF7 cells stably expressing an shRNA targeting p53 (MCF7shp53) or control cells (MCF7vector) were kindly provided by Dr. Agami (ref.). Cells were normally maintained in DMEM or RPMI (BioWhittaker, Lonza, Milan, Italy) supplemented with 10 % FCS, antibiotics (100 units/ml penicillin plus 100 mg/ml streptomycin) and 2 mM glutamine. Puromycin (Sigma-Aldrich, Milan, Italy) was used to maintain the selection, at 0.5 μg/mL as final concentration.

RNA extraction

Cells were seeded into 6-well plates and allowed to reach 70-80 % of confluence before treating with 1.5 μM Doxorubicin or 10 Mm Nutlin-3A. Doxorubicin was purchased from Sigma-Aldrich (Milan, Italy) while Nutlin-3A was obtained from Alexis Biochemicals (Enzo Life Science, Exeter, UK). After 8 h, 16 h or 24 h of treatment cells were harvested and total RNA was extracted using RNeasy Mini Kit (Qiagen, Milan, Italy) according to the manufacturer's instructions. In-column DNAse treatment (RNase-Free DNase Set, Qiagen, Hilden, Germany) was performed to remove DNA contamination during the extraction. Purity of RNAs (A260/A280 value of 1.8–2.1) and concentration were measured using the Nanodrop spectrophotometer.

qPCR

cDNA was generated starting from 1 μg of RNA by using the RevertAidTM First Strand cDNA Synthesis Kit (Fermentas, Milan, Italy) in 20 μL as final volume following manufacturer's instructions. Primers were designed by Primer-BLAST performing in silico analysis as well as standard curves to define assay specificity and efficiency (Additional file 7). All qPCR assays were performed on CFX Touch Real-Time PCR Detection System (Bio-rad, Milan, Italy) in a 384-well plate format. Optimal primer concentrations (200nM-400nM) were determined by identifying conditions resulting in the lowest C_q combined with absence of primer dimer formation. Reaction volumes were set at 10 μl. SYBR Green assays contained 5X KAPA SYBR FAST qPCR Mastermix (Kapa Biosystems, Resnova, Rome, Italy), 400 nM each primer (MWG, Operon, Ebersberg, Germany) and 25 ng of cDNA. Initial thermal cycling conditions were 1 cycle of 95 °C for 3 mins, followed by 40 cycles of 95 °C for 30 s, 60 °C for 20 s, 72 °C for 60 s. At the end a melt curve analysis was performed. Post-run relative mRNA quantification was obtained using the comparative C_q method ($\Delta\Delta C_q$), where glyceraldehyde 3-phosphate dehydrogenase (GAPDH) and β-2microglobulin (B2M) served as reference genes.

ChIP assays

MCF7 cells were cultured in complete medium in a 150-mm Petri dishs and when reaching 70/80 % confluence were treated for 16 h with Doxo. The procedure for crosslinking, sonication, IP and analysis followed a previously described protocol (Lion, 2012). Antibodies used for ChIP assays were: p53 (DO-1) and IgG (sc-2025 or sc-2027) (Santa Cruz Biotechnology®) (Millipore). ChIP analysis was performed with the comparative Cq method (ΔΔCq) and normalized as % of input, using β-actin gene as negative control and p21 as positive control for p53 enrichment.

Availability of supporting data

The data sets supporting the results of this article are included within the article and its additional files. p53retriever source and binary files are available on Github, at (http://tomateba.github.io/p53retriever/).

Additional files

Additional file 1: Complete list of the rules used to attribute the functional score in the pattern search algorithm.

Additional file 2: Complete list of identified REs within human propoter regions (−10 kb, 10 kb from TSS). The list contains chromosomal coordinates, official gene name, distance from TSS and RE sequence features resulting in the given functional grade.

Additional file 3: Figures S1–S7, Table S1 and Supplementary Information.

Additional file 4: Comparison between p53retriever classification and lists of published p53 bound regions.

Additional file 5: Gene lists from data curated Ingenuity Pathway (TP53 Canonical Pathway) were compared to prediction and functional ranking of p53 REs. The RE grade is stated in the name of the various worksheets. A) Grade four and grade five. B) All grade 3, 4, and 5.

Additional file 6: Complete list of identified REs within ENCODE distal DNAse regions. The list contains chromosomal coordinates and RE sequence features resulting in the assigned functional grade.

Additional file 7: qPCR data summarized in Figure 5. For each gene, time point and treatment time, the average fold change of three biological repeats is presented along with the Standard Deviation. The results obtained with different cell lines are presented in different worksheets

Abbreviations

RE: Response element; TSS: Transcription start site; 3Q: 3/4 binding site.

Competing interests

The authors declare that they have no competing interests.
The authors declare that none of the work required ethical approval.

Authors' contributions

TT: implemented the tool and performed computational experiments. SZ, AB, YC, AI: curated the pattern search rules. SZ, FA: performed biological experiments. AI, TT, SZ: designed the study. TT, SZ, FA, AB, YC, AI: analyzed the data. TT, SZ, AI: wrote the manuscript. All authors read and approved the final manuscript.

Acknowledgements

We thank Dr. Francesca Demichelis and Alessandro Romanel for providing human DNAse hypersensitive regions from ENCODE data. We thank Dr. Paola Monti, Mattia Lion and Ivan Raimondi, for critical discussion. This work was partially supported by the Italian Association for Cancer Research, AIRC (IG grant 12869 to AI).

Received: 10 October 2014 Accepted: 20 May 2015

References

1. Lane D, Levine A. p53 Research: The Past Thirty Years and the Next Thirty Years. Cold Spring Harb Perspect Biol. 2010;2(12):a000893.
2. Riley T, Sontag E, Chen P, Levine A. Transcriptional control of human p53-regulated genes. Nat Rev Mol Cell Biol. 2008;9:402–12.
3. Beckerman R, Prives C. Transcriptional regulation by p53. Cold Spring Harb Perspect Biol. 2010;2(8):a000935.
4. Sullivan KD, Gallant-Behm CL, Henry RE, Fraikin JL, Espinosa JM. The p53 circuit board. Biochim Biophys Acta. 2012;1825(2):229–44.
5. Menendez D, Inga A, Resnick MA. The expanding universe of p53 targets. Nature Rev Cancer. 2009;9:724–37.
6. Wang B, Xiao Z, Ren EC. Redefining the p53 response element. Proc Natl Acad Sci U S A. 2009;106(34):14373–8.
7. Menendez D, Nguyen TA, Freudenberg JM, Mathew VJ, Anderson CW, Jothi R, et al. Diverse stresses dramatically alter genome-wide p53 binding and transactivation landscape in human cancer cells. Nucleic Acids Res. 2013;41(15):7286–301.
8. Nikulenkov F, Spinnler C, Li H, Tonelli C, Shi Y, Turunen M, et al. Insights into p53 transcriptional function via genome-wide chromatin occupancy and gene expression analysis. Cell Death Differ. 2012;19(12):1992–2002.
9. Wang B, Niu D, Lam TH, Xiao Z, Ren EC. Mapping the p53 transcriptome universe using p53 natural polymorphs. Cell Death Differ. 2014;21(4):521–32.
10. Wang B, Niu D, Lai L, Ren EC. p53 increases MHC class I expression by upregulating the endoplasmic reticulum aminopeptidase ERAP1. Nat Commun. 2013;4:2359.
11. Smeenk L, van Heeringen SJ, Koeppel M, van Driel MA, Bartels SJ, Akkers RC, et al. Characterization of genome-wide p53-binding sites upon stress response. Nucleic Acids Res. 2008;36:3639–54.
12. Hearnes JM, Mays DJ, Schavolt KL, Tang L, Jiang X, Pietenpol JA. Chromatin immunoprecipitation-based screen to identify functional genomic binding sites for sequence-specific transactivators. Mol Cell Biol. 2005;25(22):10148–58.
13. Wei CL, Wu Q, Vega VB, Chiu KP, Ng P, Zhang T, et al. A global map of p53 transcription-factor binding sites in the human genome. Cell. 2006;124(1):207–19.
14. Chang GS, Chen XA, Park B, Rhee HS, Li P, Han KH, et al. A Comprehensive and High-Resolution Genome-wide Response of p53 to Stress. Cell Reports. 2014;8(2):514–27.
15. Zeron-Medina J, Wang X, Repapi E, Campbell MR, Su D, Castro-Giner F, et al. A polymorphic p53 response element in KIT ligand influences cancer risk and has undergone natural selection. Cell. 2013;155(2):410–22.
16. Allen MA, Andrysik Z, Dengler VL, Mellert HS, Guarnieri A, Freeman JA, et al. Global analysis of p53-regulated transcription identifies its direct targets and unexpected regulatory mechanisms. eLife. 2014;3, e02200.
17. Sammons MA, Zhu J, Drake AM, Berger SL. TP53 engagement with the genome occurs in distinct local chromatin environments via pioneer factor activity. Genome Res. 2015;25(2):179–88.
18. Gomes NP, Espinosa JM. Gene-specific repression of the p53 target gene PUMA via intragenic CTCF-Cohesin binding. Genes Dev. 2010;24(10):1022–34.
19. Melo CA, Leveille N, Agami R. eRNAs reach the heart of transcription. Cell Res. 2013;23(10):1151–2.
20. Shaked H, Shiff I, Kott-Gutkowski M, Siegfried Z, Haupt Y, Simon I. Chromatin immunoprecipitation-on-chip reveals stress-dependent p53 occupancy in primary normal cells but not in established cell lines. Cancer Res. 2008;68(23):9671–7.
21. Kaeser MD, Iggo RD. Promoter-specific p53-dependent histone acetylation following DNA damage. Oncogene. 2004;23(22):4007–13.
22. Vousden KH. Outcomes of p53 activation–spoilt for choice. J Cell Sci. 2006;119:5015–20.
23. El-Deiry WS, Kern SE, Pietenpol JA, Kinzler KW, Vogelstein B. Definition of a consensus binding site for p53. Nat Genet. 1992;1(1):45–9.
24. Jordan JJ, Menendez D, Inga A, Nourredine M, Bell D, Resnick MA. Noncanonical DNA motifs as transactivation targets by wild type and mutant p53. PLoS Genet. 2008;4(6), e1000104.
25. Jordan JJ, Menendez D, Sharav J, Beno I, Rosenthal K, Resnick MA, et al. Low-level p53 expression changes transactivation rules and reveals superactivating sequences. Proc Natl Acad Sci U S A. 2012;109(36):14387–92.
26. Inga A, Storici F, Darden TA, Resnick MA. Differential transactivation by the p53 transcription factor is highly dependent on p53 level and promoter target sequence. Mol Cell Biol. 2002;22(24):8612–25.
27. Noureddine MA, Menendez D, Campbell MR, Bandele OJ, Horvath MM, Wang X, et al. Probing the functional impact of sequence variation on p53-DNA interactions using a novel microsphere assay for protein-DNA binding with human cell extracts. PLoS Genet. 2009;5(5), e1000462.
28. Ciribilli Y, Monti P, Bisio A, Nguyen HT, Ethayathulla AS, Ramos A, et al. Transactivation specificity is conserved among p53 family proteins and depends on a response element sequence code. Nucleic Acids Res 2013.
29. Menendez D, Inga A, Snipe J, Krysiak O, Schonfelder G, Resnick MA. A single-nucleotide polymorphism in a half-binding site creates p53 and estrogen receptor control of vascular endothelial growth factor receptor 1. Mol Cell Biol. 2007;27(7):2590–600.
30. Wieczorek AM, Waterman JL, Waterman MJ, Halazonetis TD. Structure-based rescue of common tumor-derived p53 mutants. Nat Med. 1996;2(10):1143–6.
31. Donner AJ, Szostek S, Hoover JM, Espinosa JM. CDK8 is a stimulus-specific positive coregulator of p53 target genes. Mol Cell. 2007;27(1):121–33.
32. Espinosa JM. Mechanisms of regulatory diversity within the p53 transcriptional network. Oncogene. 2008;27:4013–23.

33. Samuels-Lev Y, O'Connor DJ, Bergamaschi D, Trigiante G, Hsieh JK, Zhong S, et al. ASPP proteins specifically stimulate the apoptotic function of p53. Mol Cell. 2001;8:781–94.
34. Schlereth K, Beinoraviciute-Kellner R, Zeitlinger MK, Bretz AC, Sauer M, Charles JP, et al. DNA binding cooperativity of p53 modulates the decision between cell-cycle arrest and apoptosis. Mol Cell. 2010;38(3):356–68.
35. Timofeev O, Schlereth K, Wanzel M, Braun A, Nieswandt B, Pagenstecher A, et al. p53 DNA binding cooperativity is essential for apoptosis and tumor suppression in vivo. Cell Reports. 2013;3(5):1512–25.
36. Anderson CW, Appella E. Signaling to the p53 Tumor Suppressor through Pathways Activated by Genotoxic and Non-Genotoxic Stresses. In: Handbook of cell signaling. Edited by Dennis RABaEA, vol. Second edition: Elsevier; 2009: part III, section C.
37. Jegga AG, Inga A, Menendez D, Aronow BJ, Resnick MA. Functional evolution of the p53 regulatory network through its target response elements. Proc Natl Acad Sci U S A. 2008;105(3):944–9.
38. Raimondi I, Ciribilli Y, Monti P, Bisio A, Pollegioni L, Fronza G, et al. P53 family members modulate the expression of PRODH, but not PRODH2, via intronic p53 response elements. PLoS One. 2013;8(7), e69152.
39. Flaman JM, Frebourg T, Moreau V, Charbonnier F, Martin C, Chappuis P, et al. A simple p53 functional assay for screening cell lines, blood, and tumors. Proc Natl Acad Sci U S A. 1995;92(9):3963–7.
40. Kato S, Han SY, Liu W, Otsuka K, Shibata H, Kanamaru R, et al. Understanding the function-structure and function-mutation relationships of p53 tumor suppressor protein by high-resolution missense mutation analysis. Proc Natl Acad Sci U S A. 2003;100(14):8424–9.
41. Shiraishi K, Kato S, Han SY, Liu W, Otsuka K, Sakayori M, et al. Isolation of temperature-sensitive p53 mutations from a comprehensive missense mutation library. J Biol Chem. 2004;279(1):348–55.
42. Hoh J, Jin S, Parrado T, Edington J, Levine AJ, Ott J. The p53MH algorithm and its application in detecting p53-responsive genes. Proc Natl Acad Sci U S A. 2002;99(13):8467–72.
43. Menendez D, Inga A, Resnick MA. Estrogen receptor acting in cis enhances WT and mutant p53 transactivation at canonical and noncanonical p53 target sequences. Proc Natl Acad Sci U S A. 2010;107(4):1500–5.
44. Tomso DJ, Inga A, Menendez D, Pittman GS, Campbell MR, Storici F, et al. Functionally distinct polymorphic sequences in the human genome that are targets for p53 transactivation. Proc Natl Acad Sci U S A. 2005;102(18):6431–6.
45. Gowrisankar S, Jegga AG. Regression based predictor for p53 transactivation. BMC Bioinformatics. 2009;10:215.
46. Jolma A, Yan J, Whitington T, Toivonen J, Nitta KR, Rastas P, et al. DNA-binding specificities of human transcription factors. Cell. 2013;152(1–2):327–39.
47. Su D, Wang X, Campbell MR, Song L, Safi A, Crawford GE, et al. Interactions of Chromatin Context, Binding Site Sequence Content, and Sequence Evolution in Stress-Induced p53 Occupancy and Transactivation. PLoS Genet. 2015;11(1), e1004885.
48. Nicholls CD, McLure KG, Shields MA, Lee PW. Biogenesis of p53 involves cotranslational dimerization of monomers and posttranslational dimerization of dimers. Implications on the dominant negative effect. J Biol Chem. 2002;277(15):12937–45.
49. Lion M, Bisio A, Tebaldi T, De Sanctis V, Menendez D, Resnick MA, et al. Interaction between p53 and estradiol pathways in transcriptional responses to chemotherapeutics. Cell Cycle. 2013;12(8):1211–24.
50. Kaneshiro K, Tsutsumi S, Tsuji S, Shirahige K, Aburatani H. An integrated map of p53-binding sites and histone modification in the human ENCODE regions. Genomics. 2007;89(2):178–88.
51. Consortium EP. An integrated encyclopedia of DNA elements in the human genome. Nature. 2012;489(7414):57–74.
52. Su X, Chakravarti D, Cho MS, Liu L, Gi YJ, Lin YL, et al. TAp63 suppresses metastasis through coordinate regulation of Dicer and miRNAs. Nature. 2010;467(7318):986–90.
53. Wang CC, Liao YP, Mischel PS, Iwamoto KS, Cacalano NA, McBride WH. HDJ-2 as a target for radiosensitization of glioblastoma multiforme cells by the farnesyltransferase inhibitor R115777 and the role of the p53/p21 pathway. Cancer Res. 2006;66(13):6756–62.
54. Stark JL, Mehla K, Chaika N, Acton TB, Xiao R, Singh PK, et al. Structure and function of human DnaJ homologue subfamily a member 1 (DNAJA1) and its relationship to pancreatic cancer. Biochemistry. 2014;53(8):1360–72.
55. Jia M, Souchelnytskyi N, Hellman U, O'Hare M, Jat PS, Souchelnytskyi S. Proteome profiling of immortalization-to-senescence transition of human breast epithelial cells identified MAP2K3 as a senescence-promoting protein which is downregulated in human breast cancer. Proteomics Clin Appl. 2010;4(10–11):816–28.
56. Gurtner A, Starace G, Norelli G, Piaggio G, Sacchi A, Bossi G. Mutant p53-induced up-regulation of mitogen-activated protein kinase kinase 3 contributes to gain of function. J Biol Chem. 2010;285(19):14160–9.
57. Cottini F, Hideshima T, Xu C, Sattler M, Dori M, Agnelli L, et al. Rescue of Hippo coactivator YAP1 triggers DNA damage-induced apoptosis in hematological cancers. Nat Med. 2014;20(6):599–606.
58. Bai N, Zhang C, Liang N, Zhang Z, Chang A, Yin J, et al. Yes-associated protein (YAP) increases chemosensitivity of hepatocellular carcinoma cells by modulation of p53. Cancer Biol Ther. 2013;14(6):511–20.
59. Ma B, Pan Y, Zheng J, Levine AJ, Nussinov R. Sequence analysis of p53 response-elements suggests multiple binding modes of the p53 tetramer to DNA targets. Nucleic Acids Res. 2007;35(9):2986–3001.
60. Veprintsev DB, Fersht AR. Algorithm for prediction of tumour suppressor p53 affinity for binding sites in DNA. Nucleic Acids Res. 2008;36:1589–98.
61. Resnick MA, Tomso D, Inga A, Menendez D, Bell D. Functional diversity in the gene network controlled by the master regulator p53 in humans. Cell Cycle. 2005;4(8):1026–9.
62. Ethayathulla AS, Tse PW, Monti P, Nguyen S, Inga A, Fronza G, et al. Structure of p73 DNA-binding domain tetramer modulates p73 transactivation, Proceedings of the National Academy of Sciences of the United States of America. 2012.
63. Monti P, Ciribilli Y, Bisio A, Foggetti G, Raimondi I, Campomenosi P, et al. DN-P63alpha and TA-P63alpha exhibit intrinsic differences in transactivation specificities that depend on distinct features of DNA target sites. Oncotarget. 2014;5(8):2116–30.
64. Luh LM, Kehrloesser S, Deutsch GB, Gebel J, Coutandin D, Schafer B, et al. Analysis of the oligomeric state and transactivation potential of TAp73alpha. Cell Death Differ. 2013;20(8):1008–16.
65. Campomenosi P, Monti P, Aprile A, Abbondandolo A, Frebourg T, Gold B, et al. p53 mutants can often transactivate promoters containing a p21 but not Bax or PIG3 responsive elements. Oncogene. 2001;20(27):3573–9.
66. Resnick MA, Inga A. Functional mutants of the sequence-specific transcription factor p53 and implications for master genes of diversity. Proc Natl Acad Sci U S A. 2003;100(17):9934–9. Epub 2003 Aug 9938.

Acknowledgements

I would like to express my extreme gratitude to prof. Alberto Inga. During these years, his passion and dedication for science has inspired and enriched my growth as a student and a young researcher. I learned more and more during countless meetings discussing results, deciding what to do next, writing papers and … during hundreds of Skype calls! Despite lessons and bench work, he always found time to support and encourage me… even when results were negative! I thank him for his patience during these three years (since I'm not a very patient student!!). Above all, I acknowledge profoundly his capacity to believe in me as a young researcher.

I gratefully acknowledge Prof. Joaquin Espinosa for hosting me in his lab for eight months of my PhD. I will never forget our incredible lab meetings discussing about science! His charisma and eloquence have made me realize how brilliantly presenting science is as important as doing good science.

I also would like to thank A.I.R.C. (Associazione Italiana per la Ricerca sul Cancro) for its financial support granted through the PhD fellowship of this last year.

Moreover, I would like to acknowledge people which contributed every single day making our lab such an enjoyable place: to Ale, who guided me in culturing cells for the first time, to Ivan, for our crazy discussions about science and life, to Toma, who suggested me to download R for the first time, to Yari, the "problem solving" master of the lab, to Federica, my colleague of the cell culture room, to Vasu and her yeast strains, to all lab colleagues which decide the music playlist of the day (Nicola e Lisa), to Annalisa for RIP suggestions, to Laura and Sonia for their help with Western Blots! A thank also to PhD colleagues and friends which started this adventure with me: Chiara, Antonio, Micaela, Angela and Gaia.
At the same time, I would like to thank all members of the Espinosa lab; special thanks to all women for our running times, our "jumba" juice breaks… to Hestia for being more than just a wonderful lab colleague but such an adorable friend, to Matt for helping me with that absurd Ion Torrent Proton machine.

Finally, for their support and love I would like to express my gratitude to Erik and my family for being a source of strength and encouragement during these three years.